



**AGNICO EAGLE**

---

***In-Pit Tailings Disposal Study for the  
Meliadine Extension***

Prepared by:  
Ardent Innovation Inc.  
737 Edgebank Place NW  
Calgary, AB, T3A 4S2  
and  
Lorax Environmental Services Ltd.  
2289 Burrard St.  
Vancouver, BC, V6J 3H9

Prepared for:  
Agnico Eagle Mines Limited  
Nunavut Office  
11600 rue Louis-Bisson  
Mirabel, Québec, Canada J7N 1G9

Project No. A667-1  
16 December 2022



**ARDENT**  
INNOVATION INC.  
GEOSCIENCE AND ENGINEERING SOLUTIONS



**LORAX**  
ENVIRONMENTAL

## ***Executive Summary***

---



**AGNICO EAGLE**

## ***Executive Summary***

---

Agnico Eagle is proposing an extension (referred to as the Meliadine Extension) to the Approved Meliadine Mine located approximately 25 kilometers north of Rankin Inlet, and 80 kilometers southwest of Chesterfield Inlet in the Kivalliq region of Nunavut. The Meliadine Extension proposes to include underground mining and associated saline water management infrastructures at the Pump, F zone, and Discovery deposits; this saline water will be managed and discharged to Itivia Harbour seasonally through the waterline. There are no changes proposed to the Rankin Inlet facilities for the Meliadine Extension. The current life of mine includes operations to 2032. Through the Meliadine Extension, the life of the mine would be extended by an additional 11 years until 2043, closure will occur from 2044 to 2050, and post-closure from 2051 to 2060.

This report presents a pre-feasibility level thermal and groundwater evaluation of in-pit tailings disposal for the Meliadine Extension. The outcomes of this study are intended to inform an alternatives assessment for an application of a Final Environmental Impact Statement (FEIS) Addendum to the Nunavut Impact Review Board (NIRB). This study has been completed by Ardent Innovation Inc. (Ardent) and Lorax Environmental Services Ltd. (Lorax) on behalf of Agnico Eagle Mines Ltd. (Agnico Eagle).

Agnico Eagle identified six open pits as potential candidates for in-pit slurry tailings storage: Wesmeg 01 (WES01), Wesmeg 04 (WES04), Wesmeg 05 (WES05), Wesmeg North 01 (WN01), Pump 01 (PUM01) and Pump 03 (PUM03). The pits range in depth from 32 m to 120 m below ground surface (bgs). WES04 and WES05 have no associated underground workings; PUM03 is underlain by a single level of stopes; and WES01, WN01 and PUM01 have more extensive underground workings. All pits except WN01 are in permafrost while WN01 is in an existing open talik underlying lake B5.

The thermal analysis was comprised of two phases of numerical modelling. Thermal parameters used in this analysis were consistent with previous thermal analyses conducted by others. A baseline model, devoid of waterbodies, was calibrated to a deep temperature profile measured on an instrument completed well away from water bodies in the Meliadine project area. The first phase of thermal modelling focussed on establishing the relationship between waterbody areal footprint size on the long-term talik depth beneath the waterbody at the Meliadine Project; the sensitivity of this relationship to the waterbody temperature was also explored. Note that an in-pit tailings capped with water behaves like other waterbodies from a thermal perspective in cases where the maximum ice depth does not reach the bottom of the water column because the water temperature there remains at or above freezing throughout the winter. Both two-dimensional (2D) axisymmetric and 2D

cross-section planar model domain geometries were assessed to consider circular- and elongated-shaped water bodies, respectively.

The thermal modelling showed that for mean annual waterbody temperatures of +4°C and +1°C, open taliks form in the long-term under circular waterbodies when the waterbody radius exceeds 240 m and 325 m, respectively (diameters of 480 m and 750 m, respectively). For elongate waterbodies under these same temperature conditions, open taliks form when the waterbody half-width across its short axis is about 120 m and 185 m, respectively (full widths of 240 m and 370 m, respectively). In these analyses, delineation of the talik boundaries was based on the freezing point of freshwater (*i.e.*, 0°C). If the freezing point is lower than 0°C, as will occur for saline water, then this can significantly decrease the minimum size of the waterbody under which an open talik will develop as evidenced by subsurface temperature distributions shown later in this report.

The second phase of thermal modelling explored timeframes for talik development beneath prototypical open pits at the Meliadine Project where in-pit tailings disposal may occur. For this, WES05 and WN01 were chosen as they were considered representative of the range of pits at the Meliadine Project which have generally circular or elongated areal footprints, respectively. The numerical analyses assessed the sensitivity of talik development (or talik depletion) below pits with in-pit tailings deposition to particularly sensitive physical parameters, specifically, mean annual tailings temperature (and the associated latent heat contained in the tailings post-closure) and long-term tailings cover type. The main findings from simulations on WES05, which are generally applicable and informative for all other generally circular and slightly elongated pits permafrost in the Meliadine area, are summarized as follows:

- Deposition of relatively warm in-pit tailings (+1°C) in WES05 that are water-covered after pit closure caused an open talik (based on a -3.4°C freezing temperature, which corresponds to a bedrock groundwater TDS concentration of 60,000 mg/L) to develop about 62 years after pit closure. In this document, pit closure is the time after the in-pit tailings deposition has been completed.
- Likewise, deposition of relatively warm in-pit tailings (+1°C) in WES05 followed by dry cover placement was also predicted to form an open talik after about 62 years (based on a freezing point depression of -3.4°C), however, the talik was predicted to close about 360 years after pit closure.
- Deposition of relatively cold in-pit tailings (-1°C) in WES05 that are water-covered after pit closure was predicted to form an open talik after about 390 years.
- Deposition of relatively cold in-pit tailings (-1°C) in WES05 that are followed by dry cover placement after pit closure was predicted to *not* form an open talik.

The main findings of simulations on WN01, an elongate pit situated in an existing open talik, are summarized as follows:

- Excavation of the WN01 pit over four years was predicted to cause frost penetration in the pit walls and floor of approximately 20 m based on a 0°C freezing temperature or approximately 7 m based on a -3.4°C freezing temperature (the latter freezing temperature corresponding to a TDS concentration of 60,000 mg/L in the bedrock groundwater). These two freezing temperatures correspond to the full spectrum of measured TDS concentrations in the groundwater at the Meliadine Project.
- Deposition of relatively warm tailings (+1°C) in WN01 that are water-covered after pit closure was predicted to re-open the talik within 5 years of tailings deposition based on a -1°C freezing temperature (corresponding to an anticipated tailings porewater TDS concentration of 18,000 mg/L).
- Deposition of cold in-pit tailings (-1°C) in WN01 that are water-covered after pit closure was predicted to re-open the talik within 20 years of tailings deposition based on a -1°C freezing temperature.

Note that a thermal analysis of pit WN01 with dry cover placement was not undertaken because its planned footprint intersects the existing Lake B5, and as such, it was assumed that water cover would be the preferred tailings cover for pit WN01. Furthermore, because the WN01 pit will be located over the existing open talik of Lake B5, use of a dry cover to promote freezing at the top of the tailings is expected to have little utility for containment of dissolved tailings constituents in groundwater.

Overall, when open pits are sited in permafrost (*i.e.*, not within existing taliks), the permafrost can be best preserved when the tailings are deposited in a mostly frozen state, and when a dry tailings cover is used. However, if a dry tailings cover is not an option, then frozen tailings deposition still provides significant benefits for permafrost preservation as it will slow the time for an open talik to develop. In the very long-term however (*i.e.*, nearly 400 years), a talik will form beneath pits having water-covered tailings.

The groundwater analysis was undertaken in two stages to assess groundwater travel times and seepage fluxes from pits considered for tailings backfill under the presumption that the pits are water-covered upon closure and open taliks have formed. In presuming open taliks form, the analysis provides a conservative worst-case scenario for groundwater loadings to receptors. The groundwater analysis does not account for the time it takes groundwater levels to rebound after mining and hydraulic gradients to re-establish towards Meliadine Lake, nor does it consider the time for open taliks to form, post-closure. The first stage of

analysis utilized fundamental analytical solutions while the second stage comprised simplified 2D numerical flow and transport modelling for the pit with the least favorable outcomes to be conservative (WES05; discussed further below).

In the mathematical analysis, seepage fluxes were calculated via the Darcy equation for advective flow through a porous medium. The gradient used to drive seepage fluxes from the backfilled pits was determined using the difference in elevation between the backfilled pit water cover elevation and Meliadine Lake and travel pathway lengths specific to each pit. Pit water cover elevations were based on the spill points of the pits. The hydraulic conductivity of the flowpath was computed using a distance-weighted harmonic mean of units encountered along the flowpath, utilizing calibrated hydraulic conductivity values from the site-wide groundwater model and tailings hydraulic conductivity based on laboratory measurements from slurry tailings produced from the Meadowbank Amaruq mine site.

For pits that are intersected by faults (WES05, WN01, WES01), the fastest groundwater travel time was associated with the fault flowpath, while the slowest travel time is associated with the flowpath which lies fully (or partially) in competent bedrock. For pits not directly intersected by faults (WES04, PUM01, and PUM03), a single travel time was calculated, representing the flowpath that begins in competent bedrock and then follows either a competent or faulted bedrock pathway thereafter.

The main findings from the mathematical analysis are:

- The lowest seepage fluxes were calculated for PUM01 and WES04 pits ( $0.01 \text{ m}^3/\text{d}$ ). Travel times for seepage from PUM01 and WES04 to Meliadine Lake were 18,900 and 7,000 years, respectively.
- WES01 and PUM03 pits also produced a relatively low amount of seepage ( $0.03 \text{ m}^3/\text{d}$ ). Travel time for seepage to Meliadine Lake was 920 years for WES01 and 12,600 years for PUM03. The faster travel time for WES01 is associated with the RM175 fault pathway.
- A slightly higher amount of seepage was predicted for the WN01 pit ( $0.06 \text{ m}^3/\text{d}$ ). The fastest travel time to Meliadine Lake was 590 years along the RM175 flowpath. This pit is situated in an existing open talik underlying Lake B5.
- WES05 was estimated to generate the most ( $1.24 \text{ m}^3/\text{d}$ ) and fastest traveling seepage (14 years) of any facility towards Meliadine Lake. WES05 is transected by highly a permeable fault (WM-D), and has a higher spill point with supports a steeper hydraulic gradient towards Meliadine Lake. This is compounded by a shorter flowpath to Meliadine Lake than the other pits (1 km versus over 2 km).

Two 2D numerical flow and transport models were constructed in FEFLOW to simulate two seepage flowpaths from WES05. The simulation represents the fast flowpath along the WM-D fault, while the second simulation represents the slow flowpath originating in competent ground and then following the WM-B fault to Meliadine Lake. The main findings from the numerical modelling analysis are as follows:

- The flow models essentially confirmed the seepage flux calculated for the WES05 pit determine in the mathematical analysis.
- The first arrival of the plume, as defined by 10% of the source concentration, is 8.5 years, and simulated to report near the shoreline of the lake. Arrival times for the 50 mg/L and 100 mg/L plume are 14.5 and 25 years, respectively. This illustrates the influence of dispersion on the plume, which was not simulated in the mathematical analysis. The simulated transport time for the 50 mg/L plume (*i.e.*, 50% concentration) agrees with the travel time computed in the mathematical analysis.
- The plume traveling along the faster (WM-D) flowpath reaches its maximum (37.5 kg/d) after 100 years. The load following the slower flowpath (WM-B) takes around 3,000 years to materialize in Meliadine Lake. The maximum combined load from both flowpaths (43.3 kg/yr) to Meliadine Lake is predicted occur after 30,000 years.

The tailings pore water source term has been compared to average groundwater quality measured in 2019 to 2021 underground drillhole water intersects to identify potential contaminants of concern (PCOCs) (*i.e.*, parameters that are more concentrated in tailings seepage than background groundwater). Nine parameters have been identified as PCOCs: cyanide, weak acid dissociable (WAD) cyanide, fluoride, ammonia-nitrogen total phosphorous, arsenic, cobalt, copper and selenium. Steady-state loading rates for WES05 tailings seepage for the most elevated PCOCs, scaled from the simulated results for a generic PCOC of 100 mg/L concentration, are: arsenic (1.55 kg/yr), cyanide (0.33 kg/yr), WAD cyanide (0.022 kg/yr) and ammonia-nitrogen (37 kg/yr).

Based on the seepage fluxes and travel times computed for the pits, a simplified scoring scheme was developed to rank the suitability of the pits for tailings disposal. Operational factors have not been considered in the ranking. The pit ranking in order from most suitable to least suitable for tailings storage based on groundwater outcomes is: PUM01, WES04, PUM03, WES01, WN01, and WES05.

The ranking of pit suitability for tailings deposition was predicated on conservative worst-case scenario for groundwater loadings to Meliadine Lake. Depending on how these facilities are operated and closed, open talik formation under the backfilled pits could be limited or avoided altogether, essentially eliminating potential interaction between the pits and the deeper groundwater system.

# ***Table of Contents***

---



**AGNICO EAGLE**



# Table of Contents

EXECUTIVE SUMMARY .....	I
TABLE OF CONTENTS .....	VI
AUTHORSHIP .....	X
<b>1. INTRODUCTION</b>	
1.1 OVERVIEW .....	1-1
1.2 SCOPE OF WORK .....	1-3
1.3 APPROACH .....	1-3
<b>2. DATA SOURCES</b>	
<b>3. THERMAL ANALYSIS OF TALIK DEVELOPMENT</b>	
3.1 BACKGROUND AND OBJECTIVES .....	3-1
3.2 PERMAFROST CONDITIONS AT THE MELIADINE PROJECT SITE .....	3-2
3.3 THERMAL ANALYSIS METHODOLOGY .....	3-5
3.3.1 MATERIAL PROPERTIES .....	3-6
3.3.2 MODEL DOMAIN, BOUNDARY CONDITIONS AND MODEL CALIBRATION .....	3-6
3.3.3 SALINITY AND FREEZING POINT DEPRESSION .....	3-7
3.3.4 TAILINGS DEPOSITIONAL TEMPERATURE .....	3-8
3.4 TALIK DEVELOPMENT BELOW WATERBODIES .....	3-9
3.5 TALIK DEVELOPMENT BELOW WES05 PIT .....	3-13
3.5.1 THERMAL ANALYSIS SETUP .....	3-13
3.5.2 TALIK DEVELOPMENT – UNFROZEN TAILINGS, WET COVER .....	3-16
3.5.3 TALIK DEVELOPMENT – UNFROZEN TAILINGS, DRY COVER .....	3-17
3.5.4 TALIK DEVELOPMENT – FROZEN TAILINGS, WET COVER .....	3-19
3.5.5 TALIK DEVELOPMENT – FROZEN TAILINGS, DRY COVER .....	3-22
3.6 TALIK DEVELOPMENT BELOW WN01 PIT .....	3-23
3.6.1 THERMAL ANALYSIS SETUP .....	3-23
3.6.2 TALIK DEVELOPMENT – UNFROZEN TAILINGS, WET COVER .....	3-24
3.6.3 TALIK DEVELOPMENT – FROZEN TAILINGS, WET COVER .....	3-27
3.7 UNCERTAINTIES AND LIMITATIONS .....	3-31
3.8 SUMMARY .....	3-32
<b>4. GROUNDWATER ANALYSIS</b>	
4.1 OVERVIEW .....	4-1
4.2 CONCEPTUAL MODEL .....	4-1
4.2.1 BASELINE CONDITIONS .....	4-1
4.2.2 POST-CLOSURE CONDITIONS .....	4-4
4.3 MATHEMATICAL MODEL .....	4-6
4.3.1 ANALYTICAL METHODS .....	4-6
4.3.1.1 GOVERNING EQUATIONS .....	4-6
4.3.1.2 PARAMETER VALUES .....	4-7
4.3.2 ANALYTICAL RESULTS .....	4-9
4.3.2.1 TRAVEL TIMES .....	4-9
4.3.2.2 SEEPAGE FLUXES .....	4-10
4.3.3 DISCOVERY PIT WASTE ROCK DISPOSAL .....	4-10
4.4 NUMERICAL FLOW AND TRANSPORT MODEL .....	4-12
4.4.1 MODELLING METHODS .....	4-12
4.4.1.1 MODEL DOMAIN .....	4-13
4.4.1.2 MODEL BOUNDARY CONDITIONS .....	4-13
4.4.1.3 MODEL SETTINGS .....	4-13
4.4.1.4 MODEL PARAMETERIZATION .....	4-16
4.4.2 MODELLING RESULTS .....	4-17

4.4.2.2	VOLUMETRIC FLUXES .....	4-17
4.4.2.3	CONCENTRATIONS .....	4-18
4.4.2.4	LOADING RATES .....	4-22
4.4.3	PARAMETERS OF CONCERN.....	4-24
4.5	CONSERVATISM, UNCERTAINTY, AND LIMITATIONS .....	4-27
4.6	SUMMARY.....	4-28
<b>5. PIT SUITABILITY FOR TAILINGS DEPOSITION</b>		
<b>6. CONCLUSIONS</b>		
6.1	THERMAL MODELLING .....	6-1
6.2	GROUNDWATER SEEPAGE ANALYSIS .....	6-2
<b>REFERENCES.....</b>		<b>R1</b>

## LIST OF FIGURES

FIGURE 1-1	SITE LAYOUT FOR END OF OPERATIONS (2043) .....	1-2
FIGURE 3-1	DEEP TEMPERATURE PROFILE AWAY FROM LAKE TALIKS (GOLDER 2014B, APPENDIX E) .....	3-4
FIGURE 3-2	CALIBRATED THERMAL MODEL .....	3-7
FIGURE 3-3	TOTAL DISSOLVED SOLIDS VERSUS DEPTH (FROM GOLDER 2021C) .....	3-8
FIGURE 3-4	MODEL DOMAIN AND WATERBODY BOUNDARY CONDITIONS .....	3-10
FIGURE 3-5	OPEN TALIK DEVELOPMENT BELOW CIRCULAR WATERBODY WITH RADIUS OF 240 M (FRESH WATER, 0°C FREEZING POINT).....	3-11
FIGURE 3-6	TALIK DEPTH VERSUS CIRCULAR WATERBODY SIZE (FRESH WATER, 0°C FREEZING POINT) .....	3-12
FIGURE 3-7	TALIK DEPTH VERSUS ELONGATED WATERBODY SIZE (FRESH WATER, 0°C FREEZING POINT) .....	3-13
FIGURE 3-8	THERMAL ANALYSIS SECTION THROUGH WES05 AND WN01 PITS .....	3-15
FIGURE 3-9	WES05 PIT AXISYMMETRIC THERMAL MODEL DOMAIN.....	3-16
FIGURE 3-10	WES05 PIT, +1°C INITIAL TAILINGS TEMPERATURE, WET COVER, 62 YEARS AFTER PIT CLOSURE.....	3-17
FIGURE 3-11	WES05 PIT, +1°C INITIAL TAILINGS TEMPERATURE, DRY COVER, 62 YEARS AFTER PIT CLOSURE .....	3-18
FIGURE 3-12	WES05 PIT, +1°C INITIAL TAILINGS TEMPERATURE, DRY COVER, 200 YEARS AFTER PIT CLOSURE.....	3-18
FIGURE 3-13	WES05 PIT, +1°C INITIAL TAILINGS TEMPERATURE, DRY COVER, 360 YEARS AFTER PIT CLOSURE .....	3-19
FIGURE 3-14	WES05 PIT, -1°C INITIAL TAILINGS TEMPERATURE, WET COVER, 62 YEARS AFTER PIT CLOSURE .....	3-20
FIGURE 3-15	WES05 PIT, -1°C INITIAL TAILINGS TEMPERATURE, WET COVER, 62 YEARS AFTER PIT CLOSURE, CLOSE-UP VIEW OF TEMPERATURES IN TAILINGS .....	3-21
FIGURE 3-16	WES05 PIT, -1°C INITIAL TAILINGS TEMPERATURE, WET COVER, 390 YEARS AFTER PIT CLOSURE.....	3-21
FIGURE 3-17:	WES05 PIT, -1°C INITIAL TAILINGS TEMPERATURE, WET COVER, 1000 YEARS AFTER PIT CLOSURE .....	3-22
FIGURE 3-18:	WES05 PIT, -1°C INITIAL TAILINGS TEMPERATURE, DRY COVER, 62 YEARS AFTER PIT CLOSURE .....	3-23
FIGURE 3-19:	WN01 PIT CROSS-SECTION THERMAL MODEL DOMAIN AND INITIAL TEMPERATURE CONDITIONS (OPEN TALIK BELOW LAKE B5).....	3-24
FIGURE 3-20	WN01 PIT, END OF 4 <sup>TH</sup> YEAR OF PIT EXCAVATION .....	3-26
FIGURE 3-21	WN01 PIT, +1°C INITIAL TAILINGS TEMPERATURE, END OF 1 <sup>ST</sup> YEAR OF PIT FILLING (ELAPSED YEAR 5) .....	3-26
FIGURE 3-22	WN01 PIT, +1°C INITIAL TAILINGS TEMPERATURE, WET COVER, 20 YEARS AFTER PIT CLOSURE .....	3-27
FIGURE 3-23:	WN01 PIT, -1°C INITIAL TAILINGS TEMPERATURE, AT PIT CLOSURE .....	3-29
FIGURE 3-24	WN01 PIT, -1°C INITIAL TAILINGS TEMPERATURE, WET COVER, 20 YEARS AFTER PIT CLOSURE .....	3-29

FIGURE 3-25	WN01 PIT, -1°C INITIAL TAILINGS TEMPERATURE, WET COVER, 100 YEARS AFTER PIT CLOSURE .....	3-30
FIGURE 3-26	WN01 PIT, -1°C INITIAL TAILINGS TEMPERATURE, WET COVER, 1000 YEARS AFTER PIT CLOSURE .....	3-30
FIGURE 4-1	CONCEPTUAL MODEL OF GROUNDWATER FLOW (BASELINE CONDITIONS) .....	4-3
FIGURE 4-2	CONCEPTUAL MODEL OF GROUNDWATER FLOW (POST-CLOSURE CONDITIONS) .....	4-5
FIGURE 4-3	CROSS-SECTION OF WES05 FLOWPATH ALONG WM-D (TOP PANE) AND WM-B (BOTTOM PANE) FAULT PATHS USED TO PARAMETERIZE THE 2D NUMERICAL FLOW AND TRANSPORT MODELS. ....	4-14
FIGURE 4-4	WES05 FLOW AND TRANSPORT MODEL SETUP FOR WM-D (TOP PANE) AND WM-B (BOTTOM PANE) FAULT FLOW PATHS. DOTS REPRESENT CONCENTRATION PREDICTION POINTS A, B1, B2, B3, C, D AND E. ....	4-15
FIGURE 4-5	CONCENTRATION VERSUS TIME FOR WES05 WM-D (TOP PANE) AND WM-B (BOTTOM PANE) FAULT FLOW PATHS. LOCATION OF PREDICTION POINTS SHOWN ON RIGHT HAND SIDE. SOURCE CONCENTRATION IS 100 MG/L. ....	4-19
FIGURE 4-6	SIMULATED CONCENTRATIONS FOR WES05 WM-D FLOWPATH AFTER 5, 10 AND 25 YEARS. SOURCE CONCENTRATION IS 100 MG/L.....	4-20
FIGURE 4-7	SIMULATED CONCENTRATIONS FOR WES05 WM-B FLOWPATH AFTER 1,000, 3,000 AND 4,500 YEARS. SOURCE CONCENTRATION IS 100 MG/L.....	4-21
FIGURE 4-8	SIMULATED LOADING RATES FOR WM-D FLOWPATH ASSUMING A CONSTANT SOURCE CONCENTRATION OF 100 MG/L. ....	4-23
FIGURE 4-9	SIMULATED LOADING RATES FOR WM-B FLOWPATH ASSUMING A CONSTANT SOURCE CONCENTRATION OF 100 MG/L. ....	4-23
FIGURE 4-10	SIMULATED COMBINED LOADING RATES AND CUMULATIVE LOADS TO MELIADINE LAKE FROM THE WM-D AND WM-B FLOWPATHS ASSUMING A CONSTANT SOURCE CONCENTRATION OF 100 MG/L. ....	4-24

## LIST OF TABLES

TABLE 1-1	OPEN PIT AREAS IDENTIFIED FOR POTENTIAL IN-PIT TAILINGS STORAGE.....	1-1
TABLE 3-1	BEDROCK AND TAILINGS THERMAL PROPERTIES .....	3-6
TABLE 4-1	CALIBRATED HYDRAULIC CONDUCTIVITY FOR COMPETENT BEDROCK AND SELECTED FAULTS AFTER GOLDR (2021B).....	4-2
TABLE 4-2	TAILINGS SEEPAGE ANALYSIS PARAMETERS AND RESULTS.....	4-8
TABLE 4-3	DISCOVERY IN-PIT WASTE ROCK SEEPAGE ANALYSIS PARAMETERS AND RESULTS .....	4-11
TABLE 4-4	SIMULATED FLOW AND TRANSPORT MODEL RESULTS FOR WES05 PIT .....	4-17
TABLE 4-5	POTENTIAL CONTAMINANTS OF CONCERN IN TAILINGS SEEPAGE .....	4-25
TABLE 4-6	STEADY-STATE PCOC GROUNDWATER LOADS TO MELIADINE LAKE FROM WES05.....	4-26
TABLE 5-1	RANKING OF PIT SUITABILITY FOR TAILINGS DEPOSITION BASED ON GROUNDWATER OUTCOMES. ....	5-1

## ***Authorship***

---



**AGNICO EAGLE**

## Authorship

This report was prepared by Ardent Innovation Inc. (Ardent) and Lorax Environmental Services Ltd. (Lorax) for Agnico Eagle Mines Ltd. (Agnico Eagle). This report was written by Ron Coutts, M.Sc., P.Eng., of Ardent and Laura-Lee Findlater, B.Sc., P.Geo., of Lorax, and reviewed by Justin Bourne, M.Eng., P.Eng., of Lorax. Lorax and Ardent have relied on information available in scientific literature and information supplied by Agnico Eagle in preparing this report.

per:



*Dec. 16, 2022*  
(for thermal aspects only)


**Ron Coutts, M.Sc., P.Eng.**  
Senior Geological Engineer  
Ardent Innovation Inc.



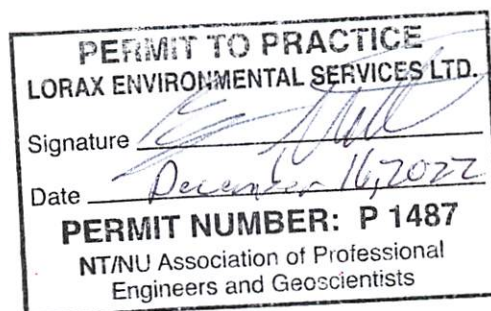
*Dec. 16, 2022*  
(for hydrogeology aspects only)

**Laura-Lee Findlater, B.Sc., P.Geo.**  
Senior Hydrogeologist  
Lorax Environmental Services, Ltd.

Reviewed by:



**Justin Bourne, M.Eng., P.Eng.**  
Senior Hydrogeological Engineer  
Lorax Environmental Services, Ltd.



# ***1. Introduction***

---



**AGNICO EAGLE**

# 1. Introduction

## 1.1 Overview

Agnico Eagle Mines Limited (Agnico Eagle) operates the Meliadine Project (the Project) 25 km north of Rankin Inlet in the Kivalliq region of Nunavut. The Project is composed of seven known gold deposits (Tiriganiaq, Wesmeg, Wesmeg North, Pump, F Zone, Discovery, Wolf) which are being developed in a phased approach. The initial phase of development (Phase 1) is currently in operations and is focused on development of the Tiriganiaq gold deposit (both open pit and underground). The Meliadine Extension comprises an extension of mine life to 2043 with new underground mining activity planned for previously approved open pit areas and one new deposit area.

Agnico Eagle is evaluating in-pit deposition of slurry tailings in six different open pits in support of a pre-feasibility study and permitting of the Meliadine Extension. Currently, tailings are either backfilled into the underground mine as cemented paste backfill or stored in an above ground dry-stack tailings facility comprised of two cells. The candidate pits identified by Agnico Eagle are listed in Table 1-1 and shown in Figure 1-1.

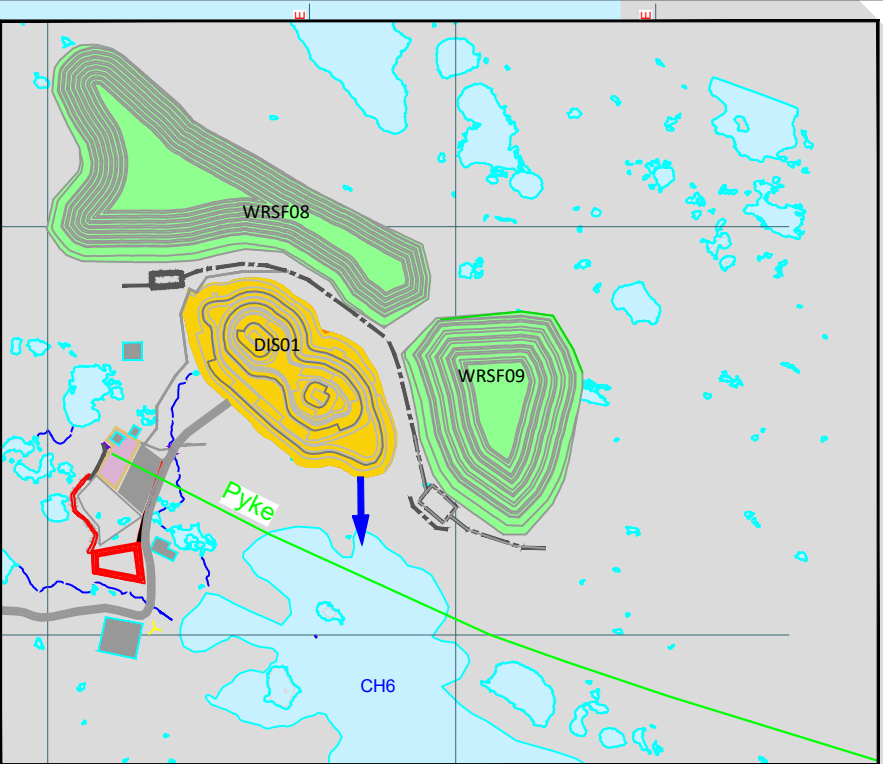
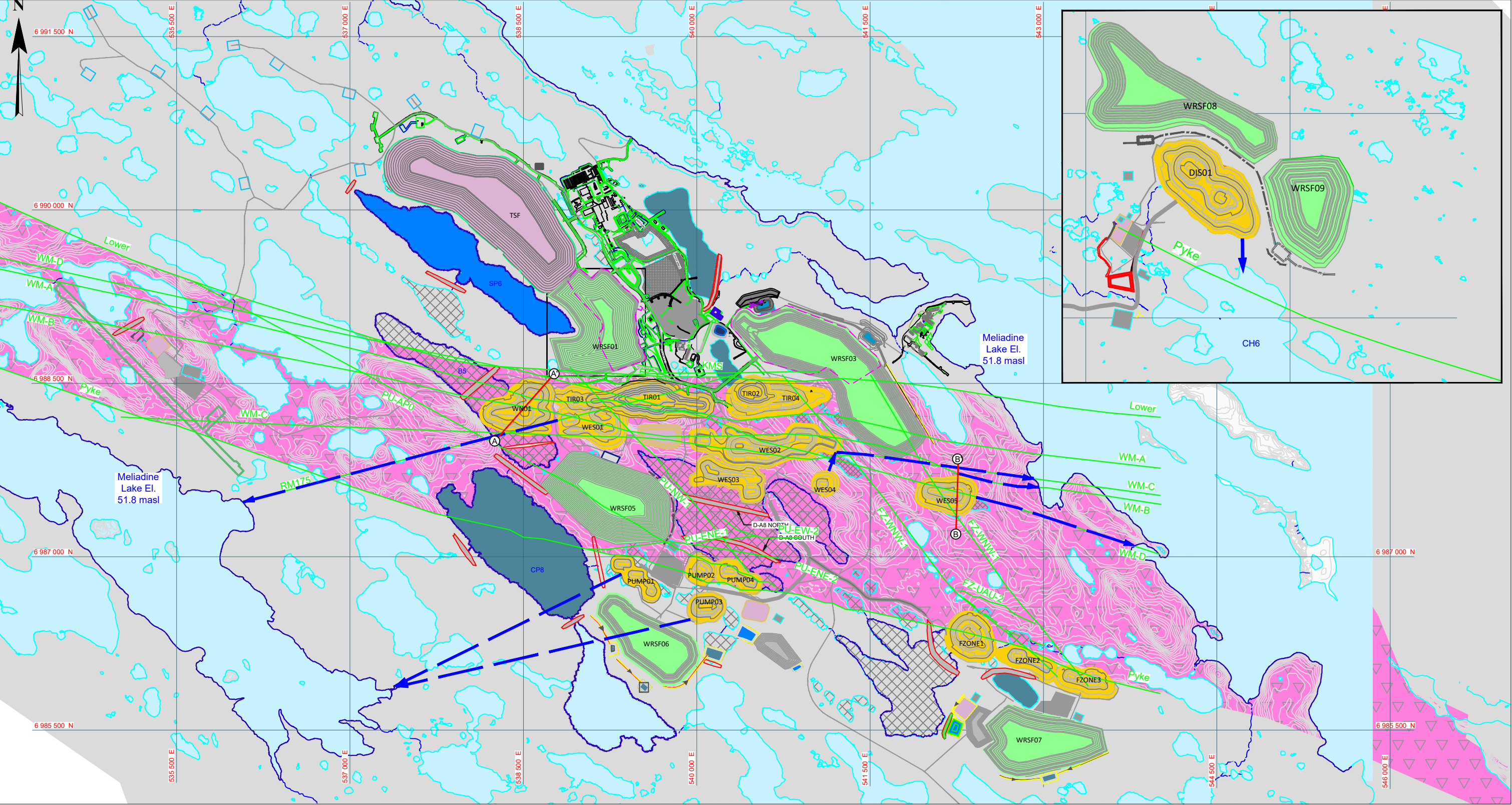
**Table 1-1:  
Open pit areas identified for potential in-pit tailings storage**

Pit	Ore First Extracted <sup>1</sup>	Year pit available <sup>1</sup>	Pit Volume below Overburden (m <sup>3</sup> ) <sup>1</sup>	Connection with Underground <sup>1</sup>
Wesmeg 01 (WES01)	2026	2029	2,340,568	Pit bottom connects to stopes
Wesmeg 04 (WES04)	2024	2025	126,226	No
Wesmeg 05 (WES05)	2040	2043	2,936,368	No
Wesmeg North 01 (WN01)	2027	2031	7,162,482	Stopes located 10-20 m below pit bottom
Pump 01 (PUM01)	2030	2032	375,218	Stopes located at least 35 m below pit bottom
Pump 03 (PUM03)	2028	2031	1,027,283	Stopes located along bottom for one level only

**Notes:**

1. Agnico Eagle (2021a).





**LEGEND**

MAJOR AND MINOR CONTOURS FOR PITS

EXISTING GROUND

ROAD

CROSS-SECTION POST-CLOSURE

SEEPAGE FLOW PATH LAKE WITH OPEN TALUK (SIMULATED)

FAULT

DIVERSION CHANNEL

CONTACT WATER POND

SALINE POND

WATER

DEWATERED

OPEN PITS COMPLETED

TAILINGS STORAGE FACILITY COMPLETED

WASTE ROCK STORAGE FACILITY COMPLETED

MAFIC VOLCANIC BEDROCK

SEDIMENTARY BEDROCK

DATE SAVED:

Dec 14, 2022

DRAWN BY:

GM

REVIEWED:

LF

VERSION:

3

Source data: Bedrock lithology according to Golder (2021b) groundwater model.

CLIENT:

AGNICO EAGLE

LORAX ENVIRONMENTAL

PROJECT:

Meliadine Phase 2 Extension In-Pit Tailings Study

TITLE:

Site Layout for End of Operations (2043)

PROJECT #:

A574-6

FIGURE:

1-1

P:\@Drafting\Meliadine\Drafting Figures\Autocad\Cross Sections\In-pit Tailings Study\Site Layout for EOP -2043\_20221214.dwg

## **1.2 Scope of Work**

Agnico Eagle has contracted Lorax Environmental Services Ltd. (Lorax) to undertake this in-pit tailings disposal study, which is comprised of both thermal and groundwater analysis components. Lorax has subcontracted Ardent Innovation Inc. (Ardent) to undertake the thermal analysis supporting this study. The objectives of this study are to:

- Evaluate the timing and extent of permafrost degradation below pits proposed for potential tailings storage;
- Estimate the quantity of seepage emanating from the backfilled pits and associated travel times to receiving waterbodies;
- Conduct transport modeling for the pit with the least favorable outcomes; and,
- Provide a ranking of the suitability of the candidate pits for tailings disposal based on thermal and groundwater outcomes.

## **1.3 Approach**

This report comprises a combined thermal and hydrogeological pre-feasibility level assessment of in-pit tailings disposal which will ultimately inform an alternatives assessment for an application of a Final Environmental Impact Statement (FEIS) Addendum to the Nunavut Impact Review Board (NIRB).

The thermal analysis was conducted in two phases. The first phase of thermal modelling explored the relationship of hypothetical waterbodies of different size, morphology, and temperature on open talik formation in ground experiencing thermal conditions consistent with the Project. The second phase of modelling simulated tailings deposition in two pit end-members where key operational and closure strategies were examined for their expected impact on permafrost conditions.

The groundwater analysis was also conducted in two phases. The first phase involved a mathematical analysis using fundamental analytical solutions to estimate travel times and seepage fluxes from all pits considered for tailings backfill under the presumption that open taliks form. In presuming the formation of open taliks, the analysis provides a conservative worst-case scenario for groundwater loadings to receptors. The second phase of analysis comprised 2D numerical flow and transport modelling of the pit with the least favorable outcomes (WES05) to determine first arrival times and loading rates to Meliadine Lake for potential contaminants of concern (PCOCs). Ultimately, the pits were ranked according to groundwater outcomes which were then qualified by findings from the thermal modelling.

## ***2. Data Sources***

---



**AGNICO EAGLE**

## **2. Data Sources**

---

The data sources listed herein directly informed the thermal and groundwater analysis presented in this report. The data sources include the following reports:

- Golder, 2021a. Meliadine Extension – 2020 Thermal Assessment. Document No. 20136436-815-R-Rev2. Report Dated December 2021.
- Golder, 2021b. Meliadine Extension – Hydrogeology Modelling Report. Document No. 20136436-857-R-Rev3-2300. Report dated December 2021.
- Agnico Eagle, 2019. Meadowbank Gold Project 2018 Annual Report. Report dated April 8, 2019.
- Golder, 2017. Whale Tail Project, Laboratory Testing on Process Plant Tailings. Document No. 001-1775467-MTA-Rev 0. Technical Memorandum dated December 14, 2017.
- Golder, 2014b. SD 6-1 Permafrost Thermal Regime Baseline Studies – Meliadine Gold Project, Nunavut. Document No. 225-1314280007. Ver. 0. Report dated April 2014.

Data contained in the following unpublished datafiles and email transmissions were also incorporated into the thermal and groundwater analyses:

- Pit tailings storage volumes computed from Version 8 Mine Layout (Agnico Eagle, 2021a)
- Spatial extents of pits per CAD file (2043 Year Over Site Layout.dwg) generated by Golder (April 29, 2021) (Golder, 2021d)
- Meliadine Lake Elevation per “PLOM2021\_MEL\_ENG\_edits\_V1-Base.dwg” generated by Agnico Eagle (Agnico Eagle, 2021d)
- Spatial extents of underground per Leapfrog File (Geochem\_Samples\_New.lfview) generated by Agnico Eagle (June 20, 2020) and based on the Version 8 Mine Layout
- Water analyses of detoxified tailings (TR291\_WATER QUALITY MONITORING\_August4and8th.xlsx) provided by H. Murphy (August 13, 2021) (Agnico Eagle, 2021c)

### ***3. Thermal Analysis of Talik Development***

---



**AGNICO EAGLE**

### **3. Thermal Analysis of Talik Development**

---

This section presents the background, objectives, methodology and results from thermal finite element analyses (FEAs) to assess the development of taliks beneath pits where in-pit tailings deposition may occur within the Meliadine Project area.

Key terms used herein are defined as follows:

- *Permafrost*, or *perennially frozen ground*, is defined as soil or rock having temperatures below 0°C during at least two consecutive winters and the intervening summer (Andersland and Ladanyi 2004).
- *Talik* is a layer or body of unfrozen ground within permafrost, “closed” when entirely surrounded by permafrost, and “open” when only partially surrounded by permafrost (Andersland and Ladanyi 2004).
- *Active layer* is the top layer of ground in which temperature fluctuates above and below 0°C during the year (Andersland and Ladanyi 2004).

#### **3.1 Background and Objectives**

The main objective of the work reported herein was a pre-feasibility evaluation of in-pit tailings deposition in support of permitting for the Meliadine Extension. As part of that evaluation, the following information was reviewed as it related to thermal analysis of talik development:

- Previous thermal analysis reports (Golder 2021a, Golder 2014b)
- Available ground temperature data (Agnico Eagle 2021b, Golder 2014b)
- Sections of other relevant reports (Agnico Eagle 2021a, Golder 2014b)

The pre-feasibility evaluation included thermal analyses of the long-term development of taliks below the pits where in-pit tailings deposition may occur. The objectives of the thermal analyses were to:

- Quantitatively show the thermal steady-state relationship between waterbody (*i.e.*, in-pit water-covered tailings) areal footprint size and the long-term underlying talik depth.
  - The objective of these thermal analyses was to improve the understanding of the conditions under which open taliks could develop beneath water-covered in-pit tailings.



- Determine the timeframes for talik development beneath prototypical open pits at the Meliadine Project where in-pit tailings disposal may occur.
  - For this, the Wesmeg05 (WES05) pit and the Wesmeg North Pit (WN01) were chosen as they were considered representative of the range of pits at the Meliadine Project which have generally circular or elongated areal footprints, respectively.
- Assess the sensitivity to physical parameters to which talik development (or talik depletion) below pits with in-pit tailings deposition are particularly sensitive. The long-term thermal response below pits with in-pit tailings deposition is sensitive to:
  - mean annual tailings deposition temperature (*i.e.*, initial tailings temperature); and,
  - long-term tailings cover type (*i.e.*, water-covered [wet cover] or soil/rock covered [dry cover]).

Thermal sensitivity analyses to tailings deposition temperature (unfrozen or frozen) was completed for both the WES05 and WN01 pits. In the long-term, a wet cover imparts significantly more heat to the subsurface than a dry cover. Thermal sensitivity analyses to tailings cover type (wet or dry) was completed for the WES05 pit, but was not undertaken for the WN01 pit because the latter pit footprint intersects the existing Lake B5, and as such, it was assumed that water cover would be the preferred option for pit WN01. Furthermore, because the WN01 pit will be located over the existing open talik of Lake B5, use of a dry cover to promote freezing at the top of the tailings is expected to have little utility for containment of dissolved tailings constituents in groundwater.

Potential climate warming effects in the decades following mine closure would also cause warming of the upper permafrost and other associated effects such as increased active layer depth. However, thermal analyses of climate warming effects were outside of the scope for this pre-feasibility thermal assessment.

### **3.2 Permafrost Conditions at the Meliadine Project Site**

The Meliadine Project is located approximately 25 km north of Rankin Inlet, Nunavut, in the continuous permafrost zone (NRCan 1995). At Rankin Inlet, the mean annual air temperature from 30-year climate normals data is -10.5°C (Environment Canada 2021). Consequently, the permafrost at the Meliadine Project area is characterized as cold and deep. This characterization is also evidenced by deep borehole temperature measurements. Figure 3-1 shows temperature measurements made from a borehole installed by EBA

Engineering Consultants in October 1998 (borehole ID M98-195) and monitored over a subsequent two-year period (Golder 2014b). It is evident from Figure 3-1 that:

- The depth of zero annual amplitude (*i.e.*, the depth at which annual temperature variations do not occur) is about 20 m. Based on professional experience, this is a relatively deep depth for zero annual amplitude and is hence indicative of generally low moisture content as would be expected in bedrock.
- The mean annual ground temperature (MAGT) at the ground surface is between about -7.5°C and -8.0°C, based on extrapolation of the ground temperature profile from below 25 m depth to the ground surface. This MAGT is congruent with the observed mean annual air temperature (MAAT) of -10.5°C as the MAGT is often about 3°C to 4°C warmer than the MAAT in permafrost environments, depending on the thickness and moisture content of organics at the ground surface, if any.
- The base of the permafrost (based on the 0°C isotherm) is at a depth of approximately 460 m, based on extrapolation of the almost linear temperature profile along the lower portion of the borehole. Note that elevated porewater salinity at the base of the permafrost will depress the freezing point of water. For a total dissolved solids (TDS) concentration of 60,000 mg/L, the freezing point is about -3.6°C.

The measured ground temperature profile in Figure 3-1 is especially important because the M98-195 borehole is located well away from the many lakes in the Meliadine project area and as such, the ground temperature at the borehole location is not influenced by the ground warming effects of lakes as is evident in many of the other ground temperature profile data sets in the area. Hence, the data in Figure 3-1 serves as an excellent baseline of ground temperature conditions for thermal FEA model calibration.

It is also noteworthy that the almost linear ground temperature profile shown in Figure 3-1 combined with a reasonable value of the bulk bedrock thermal conductivity over the depth interval (*i.e.*, to a depth of about 460 m) can then be used to back-calculate the geothermal energy flux from Earth's interior. Accordingly, using the MAGT at the ground surface (-7.0°C), the thermal FEA model can be calibrated to reproduce the observed depth to the base of the permafrost by adjusting the geothermal energy flux in the thermal model until the observed 460 m depth to the base of the permafrost is matched by that in the thermal model.



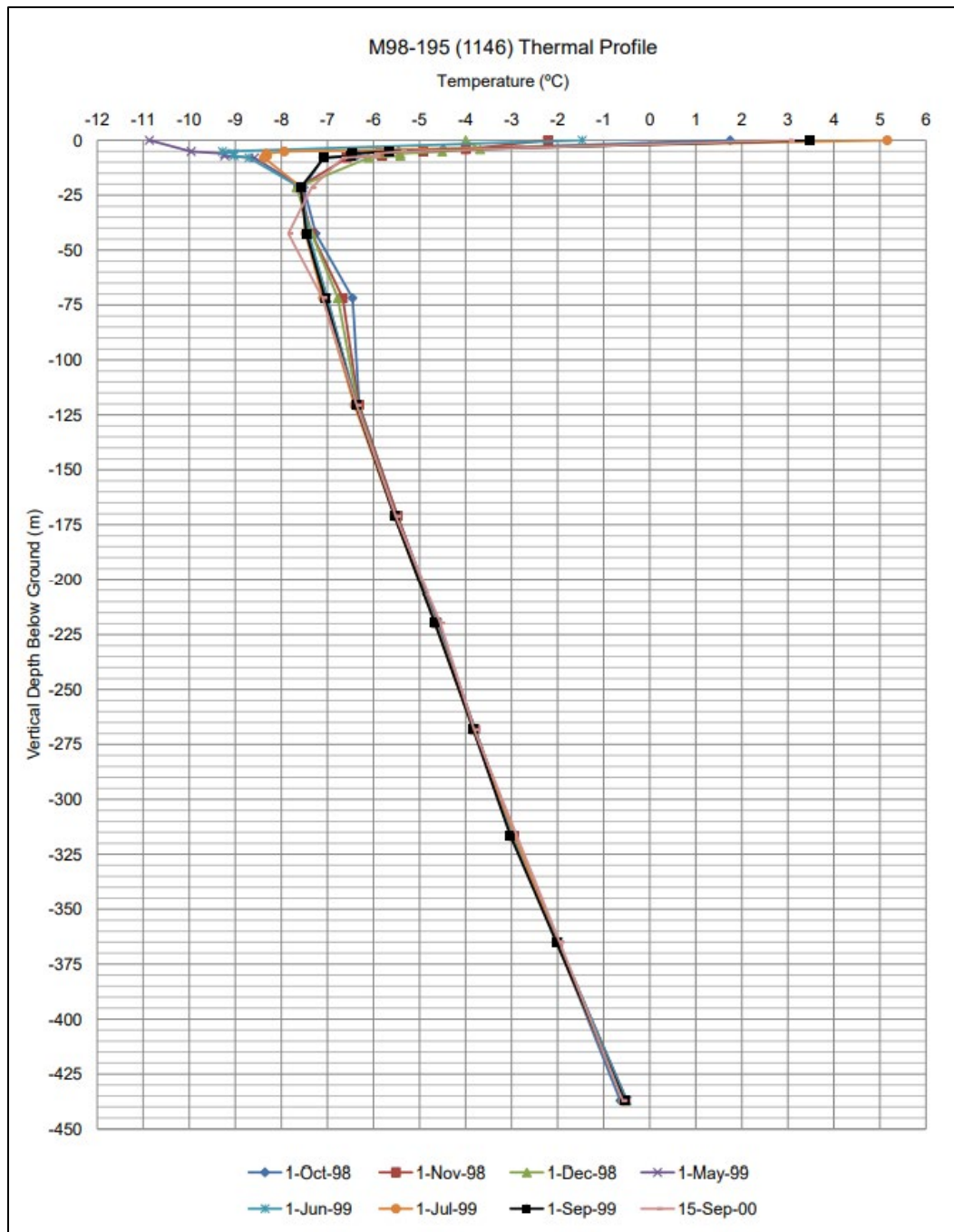


**Figure 3-1: Deep temperature profile away from lake taliks (Golder 2014b, Appendix E)**

### 3.3 Thermal Analysis Methodology

The thermal analysis approach proceeded as follows:

- A 2D thermal finite element analysis (FEA) model was setup using the observed ground surface MAGT and was then calibrated by adjustment of the geothermal energy flux until the depth to the base of the permafrost in the model matched that observed in the borehole (Figure 3-1).
  - The bedrock thermal conductivity values used were those from previous modelling work for the Meliadine Project (Golder 2021a) and are considered reasonable based on published sources (*e.g.*, Andersland and Ladanyi 2004).
  - Overburden was not included in the thermal FEA model because of the very small scale of the overburden depths (2 m to 18 m as reported in Golder 2021a) relative to scale of the bedrock depth (700 m) in the model domain. Furthermore, the exclusion of the overburden from the thermal model was consistent with previous thermal modelling (Golder 2021a).
- A series of 2D steady-state thermal FEAs were completed to assess the effect of waterbody areal footprint size on the long-term talik depth beneath the waterbody.
  - Both 2D axisymmetric and 2D cross-section planar model domain geometries were assessed to consider circular- and elongated-shaped waterbodies, respectively.
  - The differences between these two geometries will be discussed further when thermal analysis results are presented later in this document.
- Transient 2D thermal FEAs were completed to assess temporal changes to the ground temperatures near and beneath open pits during excavation, filling with in-pit tailings, and for the longer-term following pit closure.
  - These analyses were performed for a prototypical circular-shape pit (WES05) and for a prototypical elongated-shape pit (WN01).
  - The thermal analyses also included sensitivity analyses to initial pit tailings temperatures (WES05 and WN01 pits), and to wet (water covered) versus dry (soil/rock) tailings covers (WES05 pit only).

All thermal FEA modelling was performed using GeoStudio TEMP/W 2021.3 (Seequent 2021). It is important to note that the methodology used for the thermal analysis reported herein was specific to the objectives related to in-pit talik development, and that the methodologies employed by other previous (or future) thermal analyses may differ to meet the specific objectives of those analyses. Consequently, any differences in overall thermal

analysis methodology between different thermal analysis efforts are often a result of the necessity to use different approaches address different technical issues and objectives.

### 3.3.1 Material Properties

Bedrock material thermal properties reported in Golder (2021a) were reviewed and confirmed to be consistent with those for bedrock reported in Andersland and Ladanyi (2004) and were subsequently used for the thermal modelling reported herein.

Soil index properties for slurry tailings were based on communications with Agnico Eagle and tailings slurry properties reported for Meadowbank (Agnico Eagle 2019). Thermal properties for the tailings were subsequently estimated based on relationships between soil index properties (gravimetric moisture content, dry density, and assumed 100% water saturation) and thermal properties (Andersland and Ladanyi 2004).

The thermal properties for the bedrock and tailings used in the thermal modelling are shown in Table 3-1.

**Table 3-1:**  
**Bedrock and Tailings Thermal Properties**

Property	Bedrock	Tailings Slurry
Volumetric Water Content (%)	1.0	72
Frozen Thermal Conductivity (W/m-°C)	3.0	2.1
Unfrozen Thermal Conductivity (W/m-°C)	3.0	0.70
Frozen Heat Capacity (kJ/m <sup>3</sup> -°C)	2000	2100
Unfrozen Heat Capacity (kJ/m <sup>3</sup> -°C)	2000	3600

### 3.3.2 Model Domain, Boundary Conditions and Model Calibration

Based on the objective of determining the long-term development of open talik beneath pits with in-pit tailings deposition, and because of the deep depth to the base of the permafrost (nominally 460 m depth, away from the warming influence of lakes), the thermal model domain covered a depth interval from ground surface to 700 m for all thermal analyses. The horizontal extent of the model domain varied from 1000 m to 3200 m depending on the requirements of the thermal analysis.

Figure 3-2 shows the calibrated steady-state thermal model. In this case the thermal model domain is a symmetric half-space where the left boundary is an axis of symmetry. The WES05 open pit mine profile (idealized using straight lines) is shown in the top left corner of the model domain for reference, but the pit was not included in the model calibration. Because of the large spatial scale and long temporal scale considered in this modelling work, it was appropriate to perform the model calibration using a steady-state thermal

analysis. Accordingly, the ground surface boundary condition was set to the representative MAGT of the ground surface ( $-7^{\circ}\text{C}$ ) and the geothermal energy flux at the lower boundary was adjusted until the depth of base of the permafrost as calculated by the model matched that observed at the Meliadine Project area (460 m, as shown in Figure 3-1). The calibrated geothermal energy flux boundary condition at the base of the model was  $4.0 \text{ kJ/d-m}^2$  ( $0.046 \text{ W/m}^2$ ).

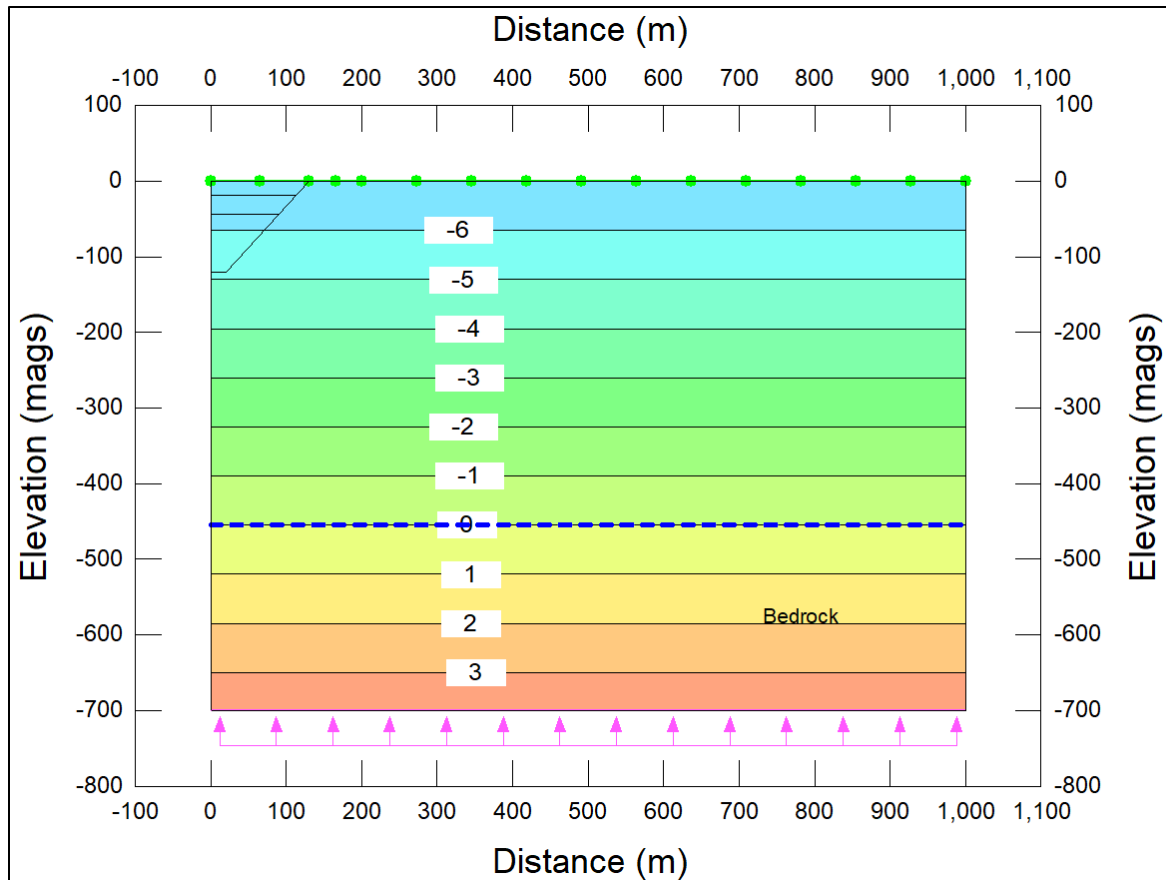


**Figure 3-2: Calibrated thermal model**

### 3.3.3 Salinity and Freezing Point Depression

Porewater salinity causes a depression of the freezing point of water. As a point of reference, seawater with a typical salinity of 35,000 mg/L (35 ppt) has a freezing point of about  $-2.0^{\circ}\text{C}$ . Figure 3-3 (reproduced from Golder 2021c) shows that in the Meliadine Project area, TDS reaches 60,000 mg/L (60 ppt) with a corresponding freezing point of about  $-3.4^{\circ}\text{C}$ . Consequently, the delineation of frozen and unfrozen zones (*i.e.*, taliks) depends both on the distribution of both temperature and salinity within the bedrock. Furthermore, porewater salinity and the associated freezing point depression significantly complicates prediction of talik delineation in the bedrock at the Meliadine Project area using thermal modelling analysis. Despite this complicating factor, thermal analysis results

are still useful to predict the temperature distribution within the bedrock, and from there, talik delineation can be based on a specific temperature isotherm, such as  $-3.4^{\circ}\text{C}$  if a 60,000 mg/L salinity is assumed throughout the bedrock mass.

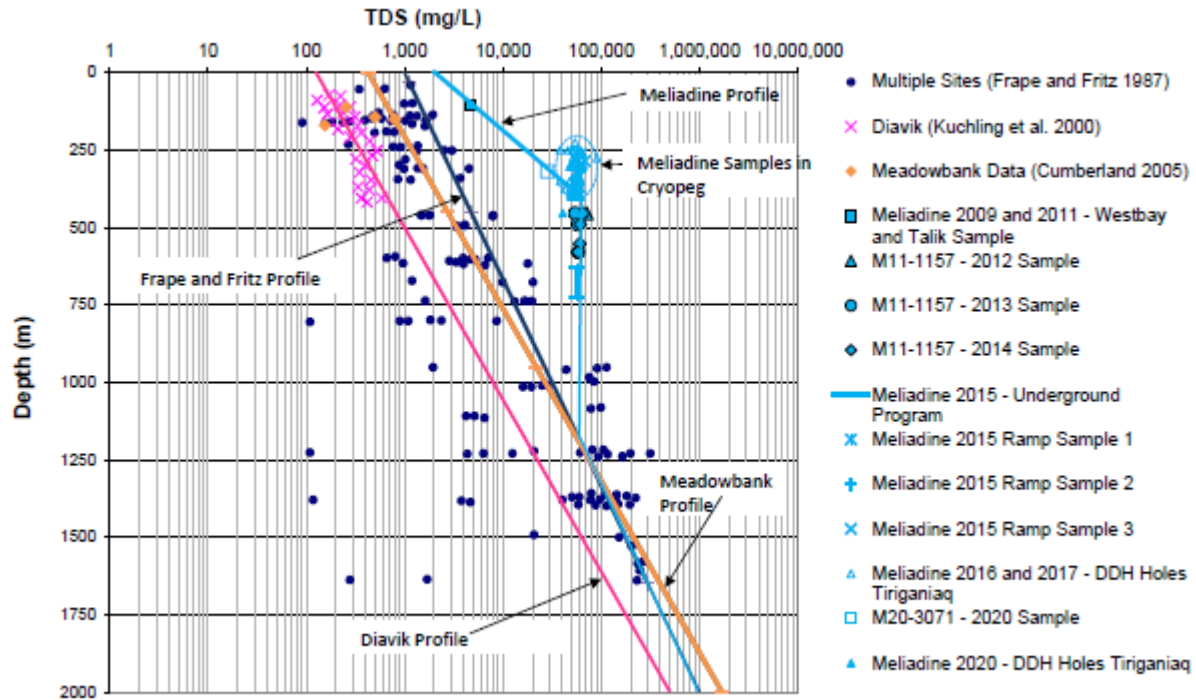


**Figure 3-3: Total dissolved solids versus depth (from Golder 2021c)**

It is important to note that in the tailings, freezing can occur over a range of temperatures because of the small pore spaces in the fine-grained tailings. Accordingly, discussion of a particular freezing temperature of the tailings later in this report is meant as a shorthand to simply indicate the freezing point depression, and hence, the temperature at which ice initiation occurs in the tailings pore spaces.

### 3.3.4 Tailings Depositional Temperature

Talik development beneath pits filled with tailings will be sensitive to the average initial tailings temperature when in-pit tailings deposition is completed; specifically, whether the bulk mass of the tailings is generally unfrozen, or frozen, and hence the degree to which the latent heat of fusion remains in the tailings or has been liberated, respectively. When tailings are frozen, their latent heat of fusion has already been liberated, and as such, they have relatively little heat content to dissipate relative to unfrozen tailings. Depending on tailings deposition operating conditions, tailings may become frozen during deposition because of the extremely cold climate at the Meliadine Project area.

It is noteworthy that the exact initial tailings subfreezing temperature is not of key importance in these thermal analyses with frozen tailings, but instead, of key importance is that the latent heat of fusion is not present in the tailings after pit closure. Accordingly, the term “frozen tailings” used later in this report refers to tailings where most or all of their latent heat has been liberated during tailings deposition, whereas the term “unfrozen tailings” applies to tailings where most of the latent heat has been retained at the time of pit closure.

### **3.4 Talik Development below Waterbodies**

An open pit excavation subsequently filled with in-pit tailings and capped with water is, from a thermal perspective, like other waterbodies such as lakes, where the maximum winter ice thickness does not freeze to bottom of the water column. At the Meliadine Project area, it is expected that the maximum winter ice thickness will be around 1.5 m and the water cover depths above the tailings will exceed this depth. Taliks exist below waterbodies in permafrost environments because the water attenuates the extremely cold winter temperature conditions experienced at the bottom of the waterbody. When the water depth is greater than the maximum ice cover depth, liquid water (at 0°C or warmer) persists at the bottom of the waterbody throughout the winter. Hence, the depth of the talik below the waterbody depends on whether the water depth exceeds the maximum winter ice depth, and on the mean annual water temperature. Furthermore, talik depth also depends on the areal size of the waterbody itself (talik depth increases with waterbody size because the water cover acts like insulation that prevents subsurface freezing below the waterbody).

The overall shape of a waterbody will also affect the depth of its underlying talik. All else being equal, the talik depth below a circular waterbody having a 300 m diameter for example, will be less than that of an elongated waterbody of 300 m width. This is because when considered in plan view, a circular waterbody has an aspect (length to width ratio of 1.0, whereas an elongated waterbody will have an aspect ratio well above 1.0.

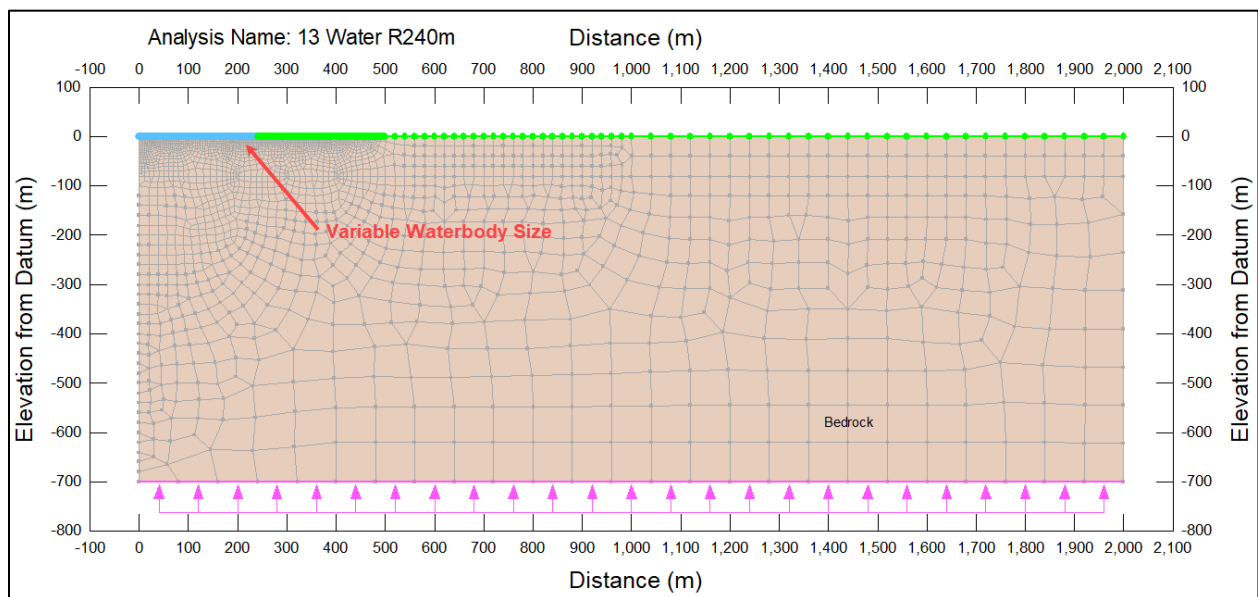
To quantify the relationship between waterbody parameters (waterbody size, shape, and temperature) and the long-term talik depth, a series of 2D steady-state thermal FEAs were completed over a range of waterbody sizes and water temperatures for both circular and elongated waterbodies in the Meliadine Project area. Figure 3-4 shows a 2D model domain where the ground surface boundary condition for dry land (shown by green symbols) was set to -7°C (consistent with the calibrated thermal FEA for the Meliadine Project area shown earlier) and where the waterbody temperature (blue symbols) was set to either +1°C or +4°C. A temperature of +1°C was selected to represent a reasonable estimate of mean annual water temperature, and +4°C was selected because the maximum density of water occurs at +4°C, and because shallow waterbodies experience very little seasonal lake turnover, it was reasonable to use this temperature as an upper bound for the sensitivity

analysis. For each of the two waterbody temperatures, the waterbody size was varied to determine the long-term talik depth.

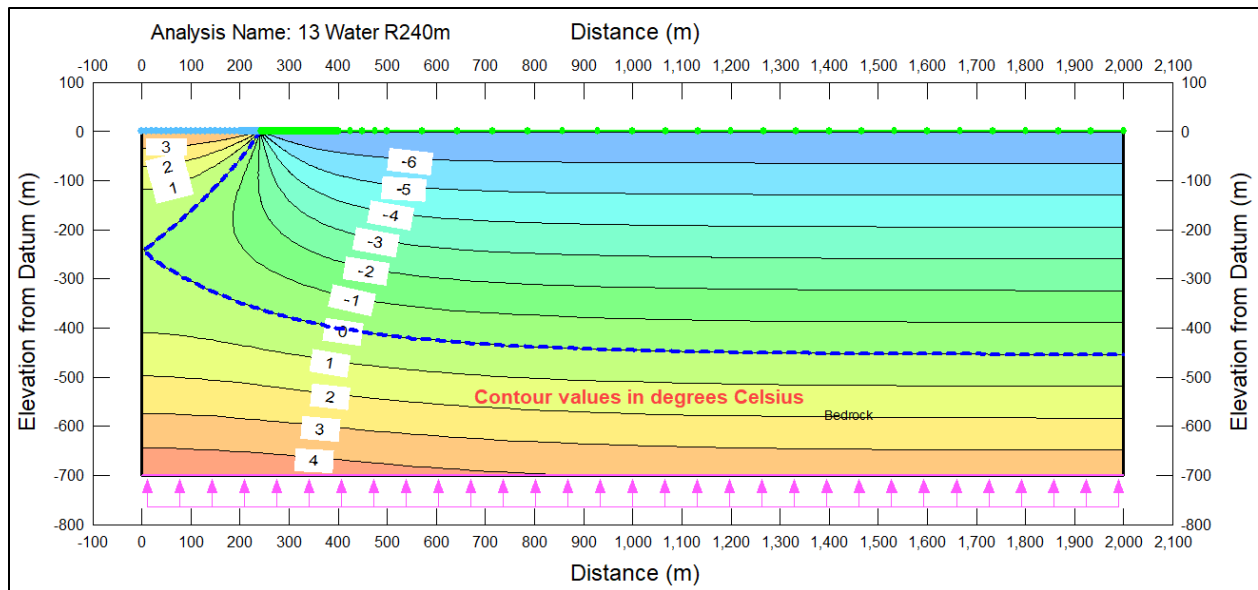
For circular waterbodies, a 2D axisymmetric model domain was used where the 2D model domain represents a cylindrical domain which is symmetric around the left-hand side of the model domain. For elongated waterbodies, a 2D planar cross-section model domain was used where the 2D model domain represents a cross-section that extends infinitely in the third dimension (*i.e.*, “into the page”).

Figure 3-5 shows the temperature distribution for a circular waterbody with a radius of 240 m with a mean annual water temperature of +4°C. From this figure it is noted that:

- The talik depth below the waterbody reaches a depth of about 230 m below the centre of the waterbody.
- The warming effect of the waterbody causes a decreased depth to the base of the permafrost (*i.e.*, the base of the permafrost rises in elevation beneath waterbodies). As shown in the figure, the base of the permafrost is elevated to the same depth of the talik below the waterbody.
- In this case the 240 m waterbody radius represents the critical size below which an open-talik would not develop in the long-term, and above which an open talik would develop.
- Away from the waterbody, on the right side of the model domain, the depth to the base of the permafrost (*i.e.*, the depth to the 0°C isotherm) is about 460 m, which is consistent with the calibrated thermal model.



**Figure 3-4: Model domain and waterbody boundary conditions**



**Figure 3-5: Open Talik Development Below Circular Waterbody with Radius of 240 m (fresh water, 0°C freezing point)**

Figure 3-6 summarizes the results from 29 steady-state thermal FEA runs and shows how talik depth and base of permafrost depth varies in relation to the circular waterbody size and temperature in the Meliadine Project area. This figure also shows the waterbody radius necessary to develop an open talik under non-saline groundwater conditions. As shown in the figure, for mean annual waterbody temperatures of +4°C and +1°C, an open talik will develop if the waterbody radius exceeds 240 m and about 325 m, respectively. Note that under saline groundwater conditions, these radii will be less than those for non-saline groundwater given the effect of freezing point depression.

For elongated waterbodies, another series of 15 2D thermal FEAs was completed with the results summarized in Figure 3-7. For elongated waterbodies with water temperatures of +4°C and +1°C, an open talik develops when the waterbody half-width across the short axis is about 120 m and 185 m, respectively.



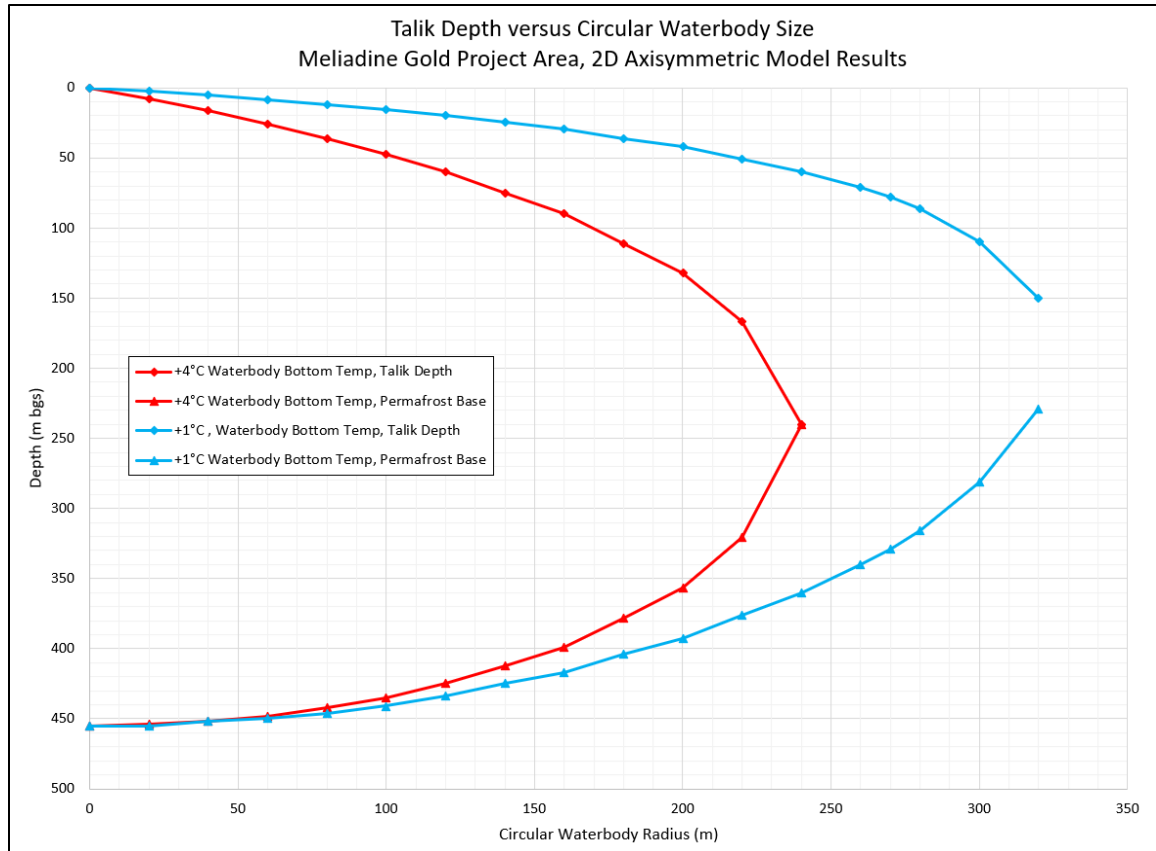


**Figure 3-6: Talik Depth versus Circular Waterbody Size (fresh water, 0°C freezing point)**

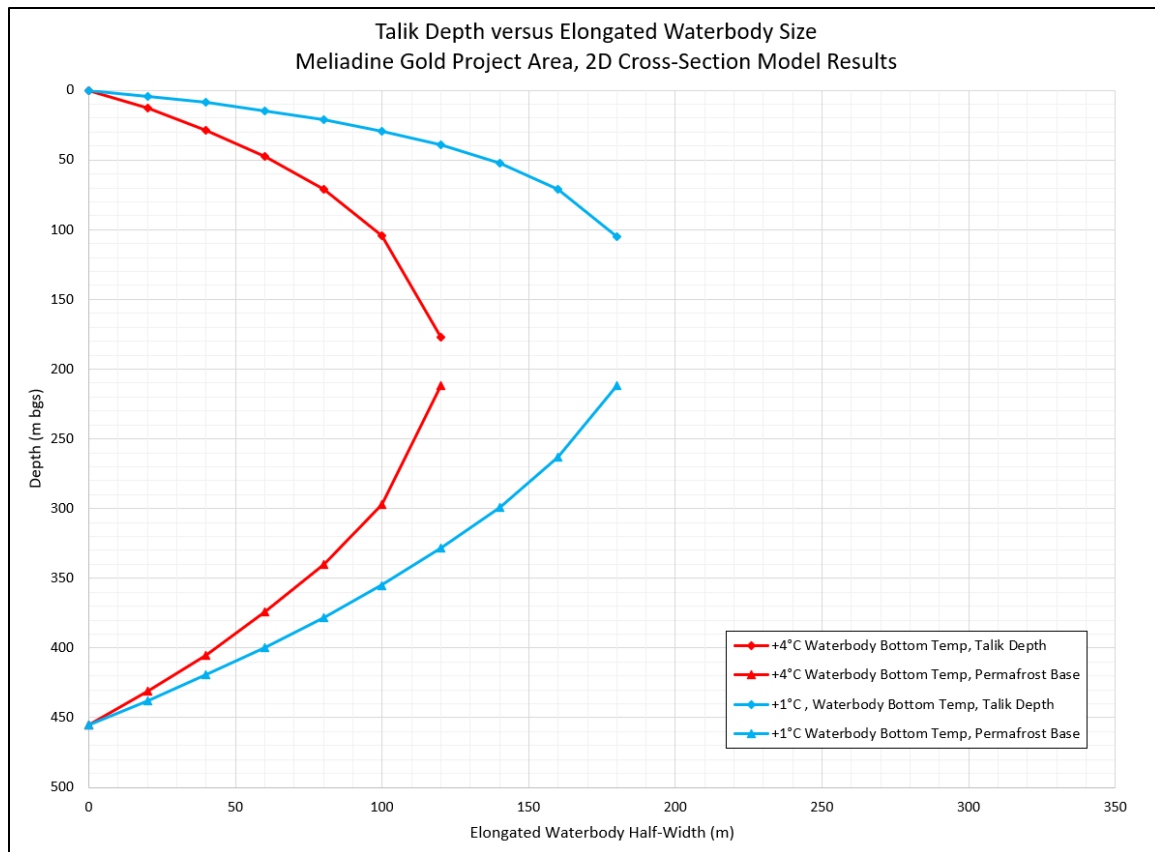


**Figure 3-7: Talik Depth versus Elongated Waterbody Size (fresh water, 0°C freezing point)**

### 3.5 Talik Development below WES05 Pit

#### 3.5.1 Thermal Analysis Setup

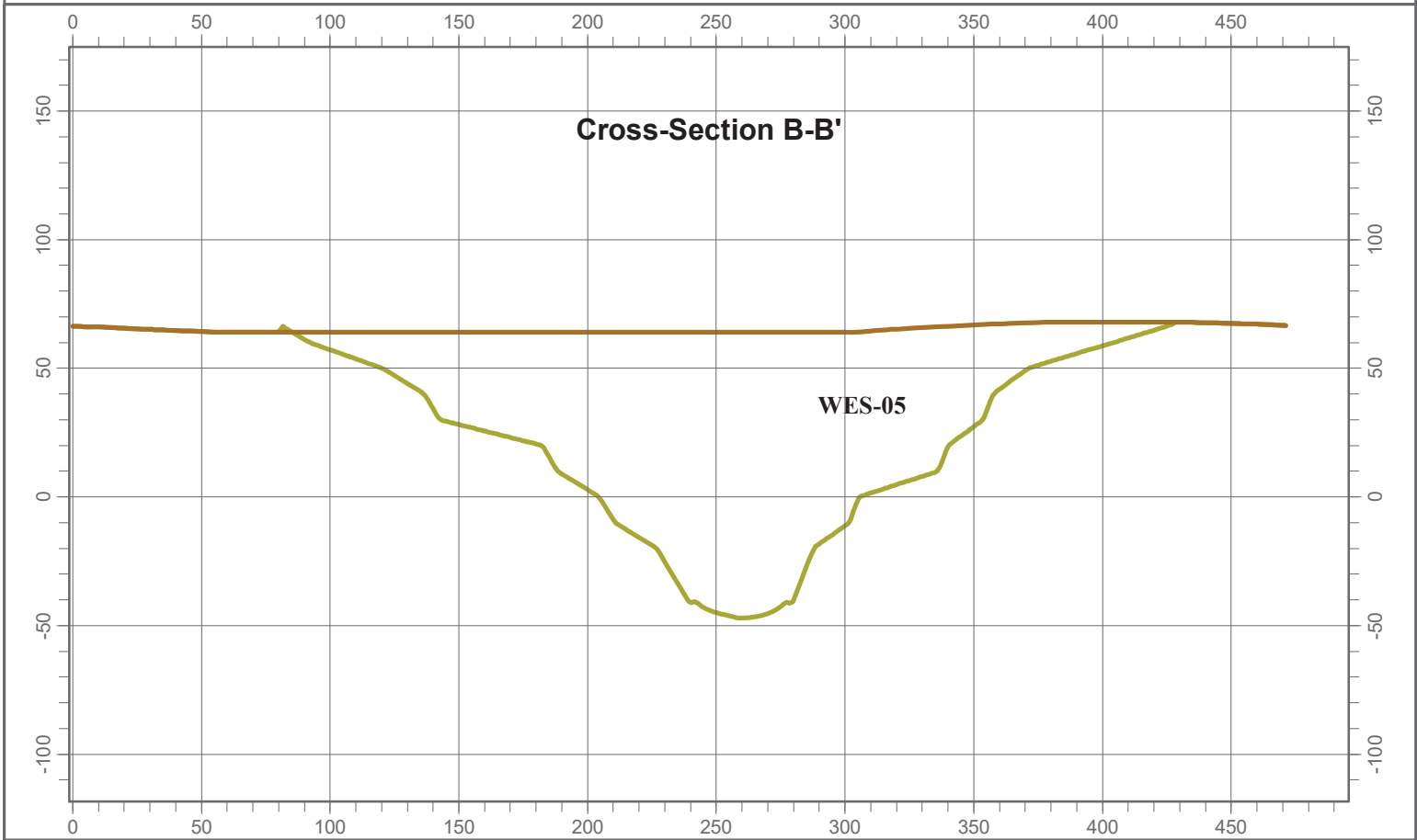
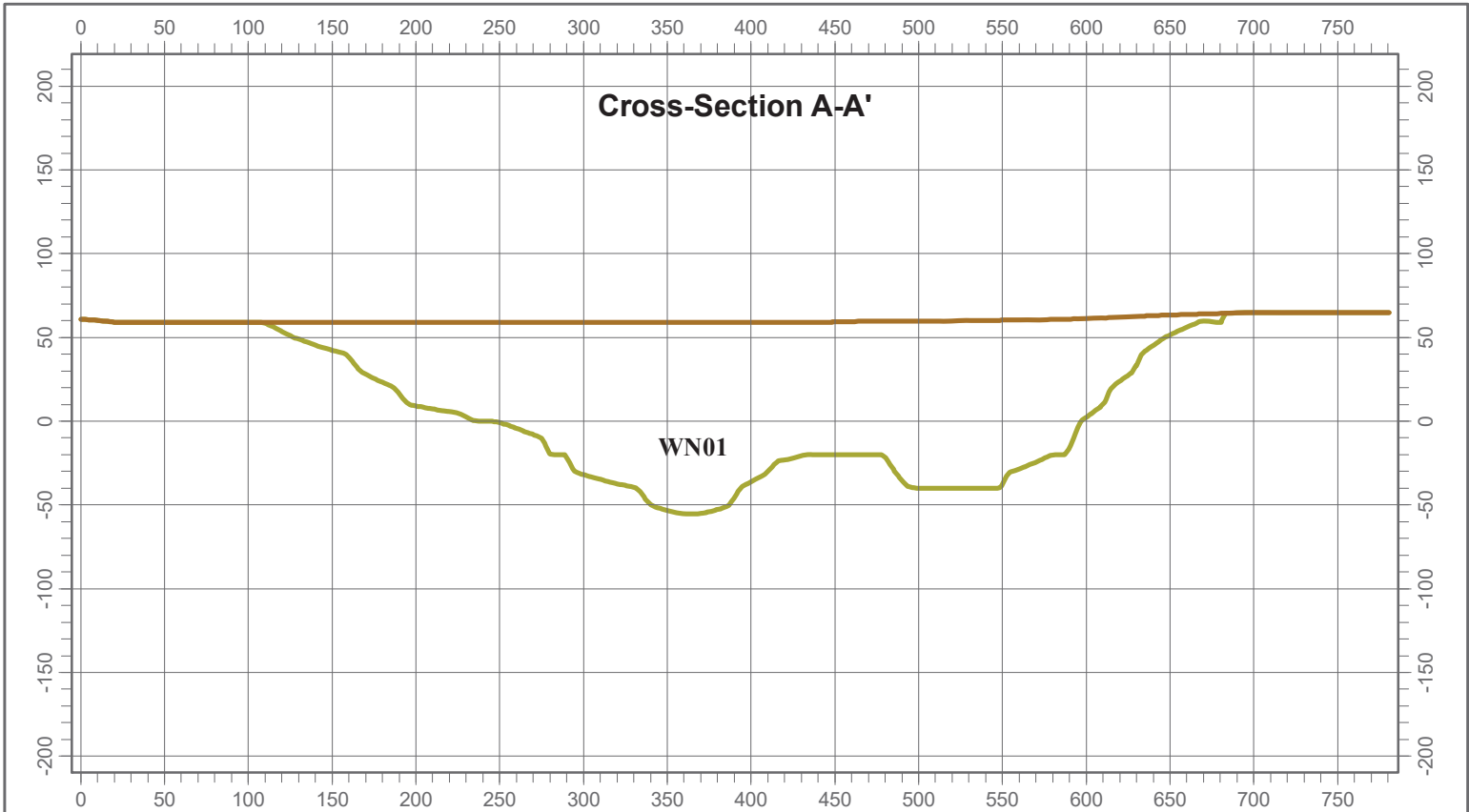
A transient 2D thermal analysis was performed to assess the timeframe for talik development beneath the WES05 pit with in-pit tailings and water cover. As discussed earlier in this report, water cover on the in-pit tailings will cause a talik to develop or enlarge in the long-term because of the insulative and consequently warming influence of the water cover. Consequently, an additional thermal analysis was performed to assess the thermal response to in-pit tailings at WES05 using a dry cover for the in-pit tailings.

While setting up these thermal analyses, it was evident that the long-term thermal response to in-pit tailings deposition would be sensitive to the average tailings deposition temperature and in particular, the amount of latent heat of fusion that could remain in the tailings after they have been deposited. Given the very cold climate at the Meliadine Project area and depending on the tailings slurry temperature and currently unknown operational details regarding tailings deposition, the deposited tailings could have an average temperature that is either below or above freezing. If the average tailings temperature after

deposition is above freezing, a significant amount of heat energy will be imparted over the long-term to the bedrock surrounding a pit as the tailings freeze. To assess the uncertainty of the average initial temperature of the pit tailings, additional transient thermal analyses were completed using initial tailings temperatures of +1°C and -1°C (referred to herein as “unfrozen tailings” and “frozen tailings”, respectively).

The WES05 pit was selected for thermal analysis as a prototypical pit with a somewhat circular areal footprint, and as such, WES05 was intended to serve as a proxy for any circular shaped pit in the Meliadine Project area located away from existing taliks near lakes. The location of the WES05 cross-section in plan-view is shown on Figure 1-1, and the corresponding WES05 cross-section elevation profile used in the thermal analysis is shown in Figure 3-8. The axisymmetric model domain used for the WES05 thermal analyses is shown in Figure 3-9. The axis of symmetry is the left side boundary of the model domain.

Agnico Eagle (2021a) indicates that the WES05 pit would be completely excavated in three years, and based on projected mill throughput, the pit would then be filled with in-pit tailings over the subsequent three years. Accordingly, to simulate excavation and filling with tailings in the thermal FEA, two intermediate pit bottom levels were established such that their elevations delineate three elevation zones within the pit wherein each pit zone has equal volume. These three pit bottom levels are shown in the top left corner of the model domain within the pit boundary (Figure 3-9). The boundary condition at the pit bottom was set to the MAGT of -7°C during the three stages of excavation (over the first three years) and during the subsequent three stages of in-pit tailings deposition (over the next three years). After pit closure, the boundary condition at the top of the tailings was set to +2°C for wet (water) cover tailings, and to the MAGT of -7°C for dry cover tailings. The simulations were run to 1000 years.



**LEGEND**

- Natural Ground
- EOM

DATE SAVED: Jan 07, 2022  
 DRAWN BY: GM  
 REVIEWED: LF  
 VERSION: 1

CLIENT:



**AGNICO EAGLE**



**LORAX**  
ENVIRONMENTAL

PROJECT:

**Meliadine Extension  
In-Pit Tailings Study**

TITLE:

Thermal Analysis Section  
through WES05 and WN01 Pits

PROJECT #:

A574-6

FIGURE:

3-8

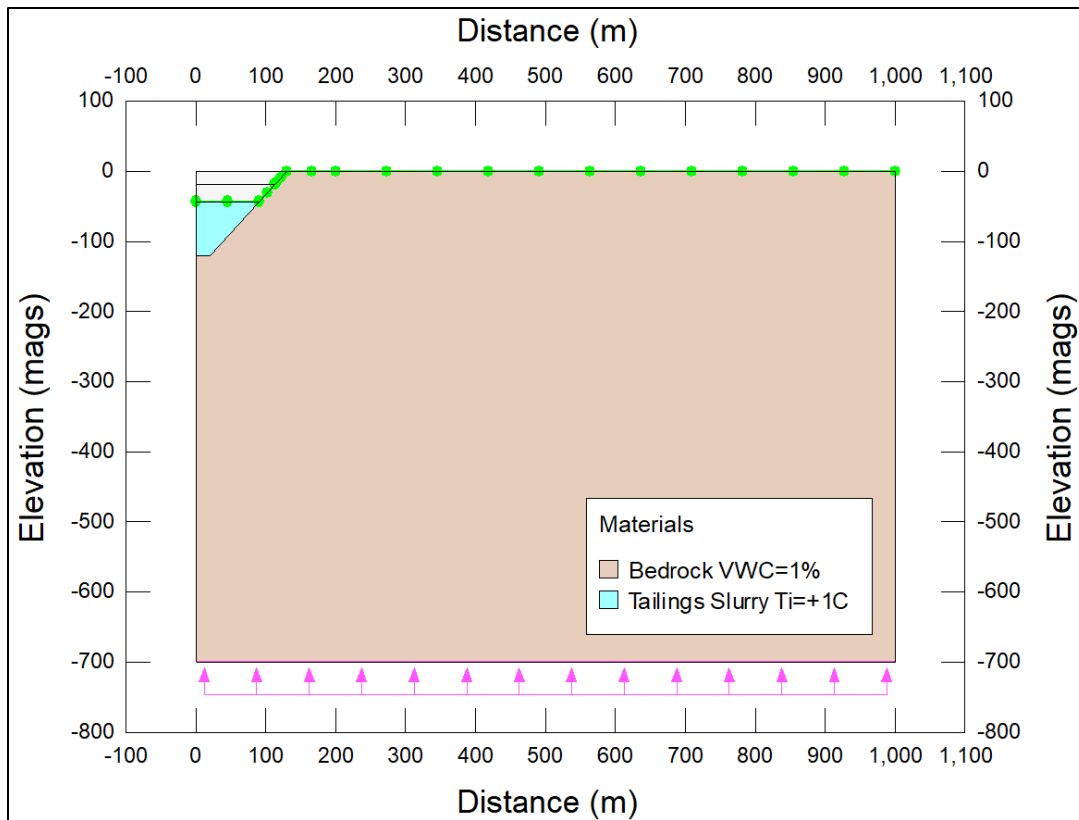


**Figure 3-9: WES05 Pit Axisymmetric Thermal Model Domain**

### 3.5.2 Talik Development – Unfrozen Tailings, Wet Cover

Figure 3-10 shows the thermal FEA results for the case with an average initial tailings temperature of +1°C (*i.e.*, unfrozen tailings) and with wet cover (+2°C mean annual water cover temperature). The figure shows the temperature distribution 62 years after pit closure (68 years from beginning of pit excavation), just at the point of time when the talik below the pit opens to the sub-permafrost talik at a depth of about 200 m.

Note that the talik delineated in Figure 3-10 is based on the -3.4°C isotherm, which corresponds to a groundwater TDS concentration of 60,000 mg/L. Delineating the talik based on the -3.4°C isotherm is conservative because lower groundwater TDS concentration would result in a warmer freezing temperature and would significantly increase the timeframe before the talik would open to the sub-permafrost talik. For example, as shown by the isotherms in Figure 3-10, if the freezing point depression was -3.0°C, then 62 years after pit closure, there would remain about 100 m of frozen bedrock below the bottom of the talik delineated by the -3.0°C isotherm. Similarly, for a -2.0°C freezing point, about 200 m of frozen bedrock would remain below the pit talik 62 years after pit closure.

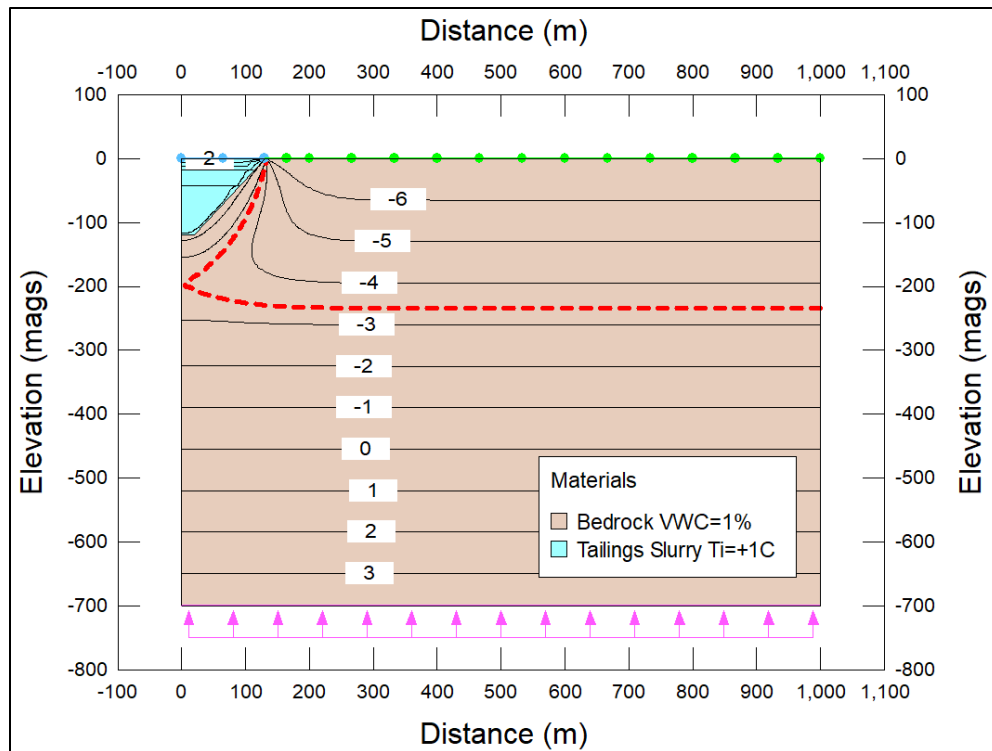


**Figure 3-10: WES05 Pit, +1°C Initial Tailings Temperature, Wet Cover, 62 Years after Pit Closure**

### 3.5.3 Talik Development – Unfrozen Tailings, Dry Cover

An identical thermal FEA was performed using unfrozen tailings except with a dry tailings cover. As shown by comparison of Figure 3-11 with Figure 3-10, the temperature distribution below the pit 62 years after pit closure is not affected by the use of a dry tailings cover versus a wet tailings cover; this is because the ground temperatures below about 50 m depth after 62 years are not affected by the temperature conditions at the tailings surface, but are instead governed by the initial tailings temperature. Consequently, if the average tailings are generally unfrozen when they are deposited (*i.e.*, retain most of their latent heat of fusion), then even with a dry tailings cover, an open-talik will develop about 62 years after pit closure and will continue to enlarge thereafter as shown in Figure 3-12 which shows the talik development 200 years after pit closure with dry tailings cover.

It is worth noting that in the very long term (more than 300 years), heat loss through the dry cover will cause the open talik to shrink and become a closed talik contained within and just below the pit. Figure 3-13 shows the point in time when the open talik becomes closed about 360 years after pit closure. In the very long-term (about 800 years after pit closure), the subsurface temperature distribution fully reinstates itself to pre-mining conditions when a dry tailings cover is present, whereas a permanent open talik remains below the pit when wet tailings cover is used.

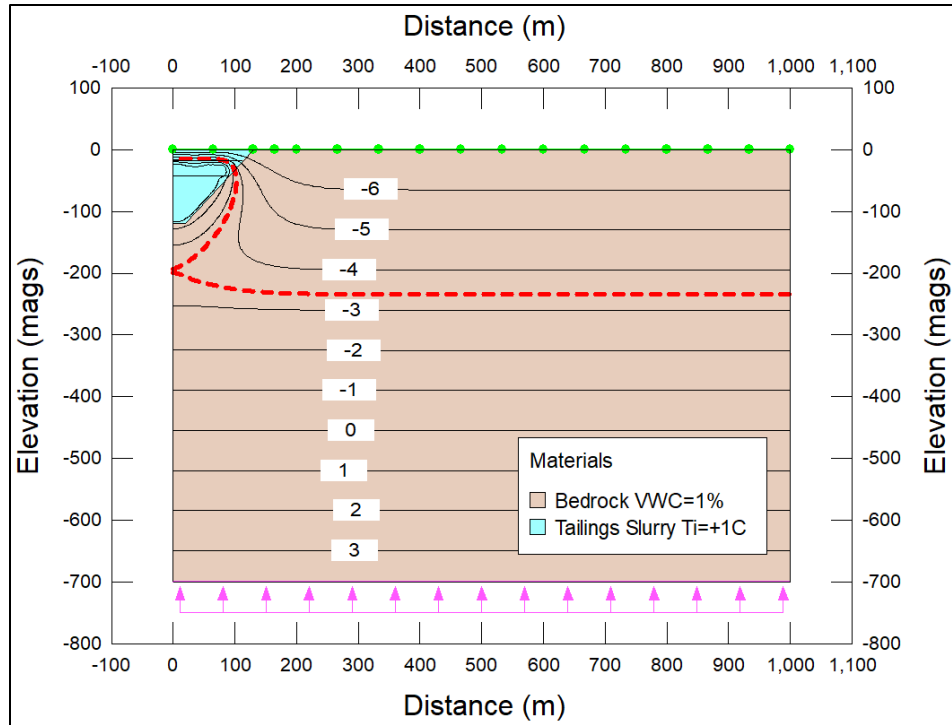


**Figure 3-11: WES05 Pit, +1°C Initial Tailings Temperature, Dry Cover, 62 Years after Pit Closure**

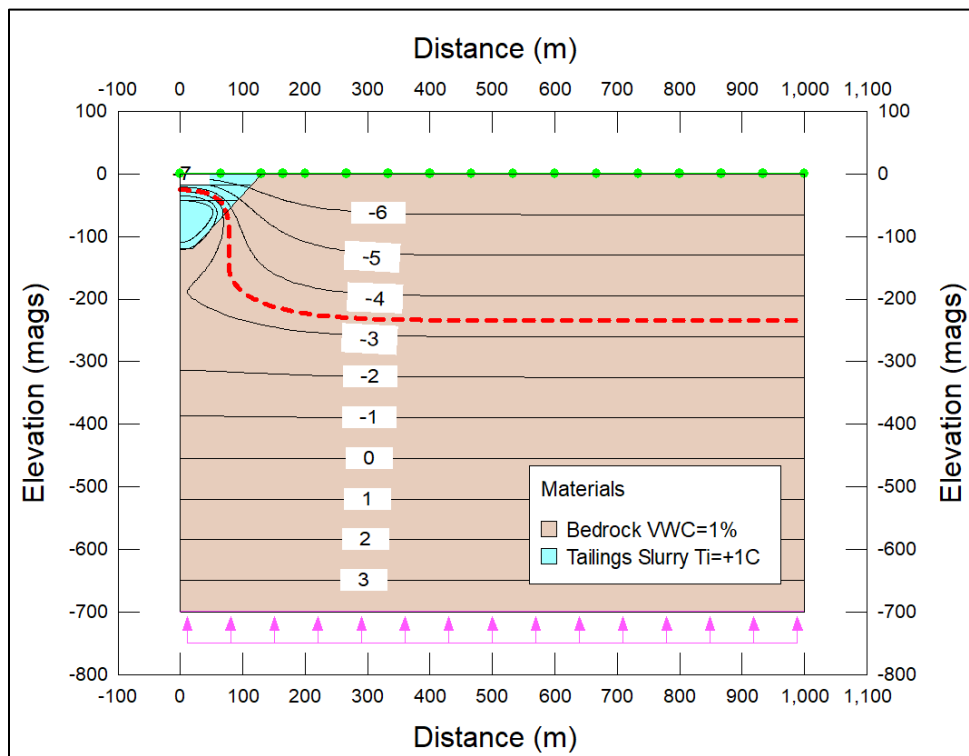


**Figure 3-12: WES05 Pit, +1°C Initial Tailings Temperature, Dry Cover, 200 Years after Pit Closure**

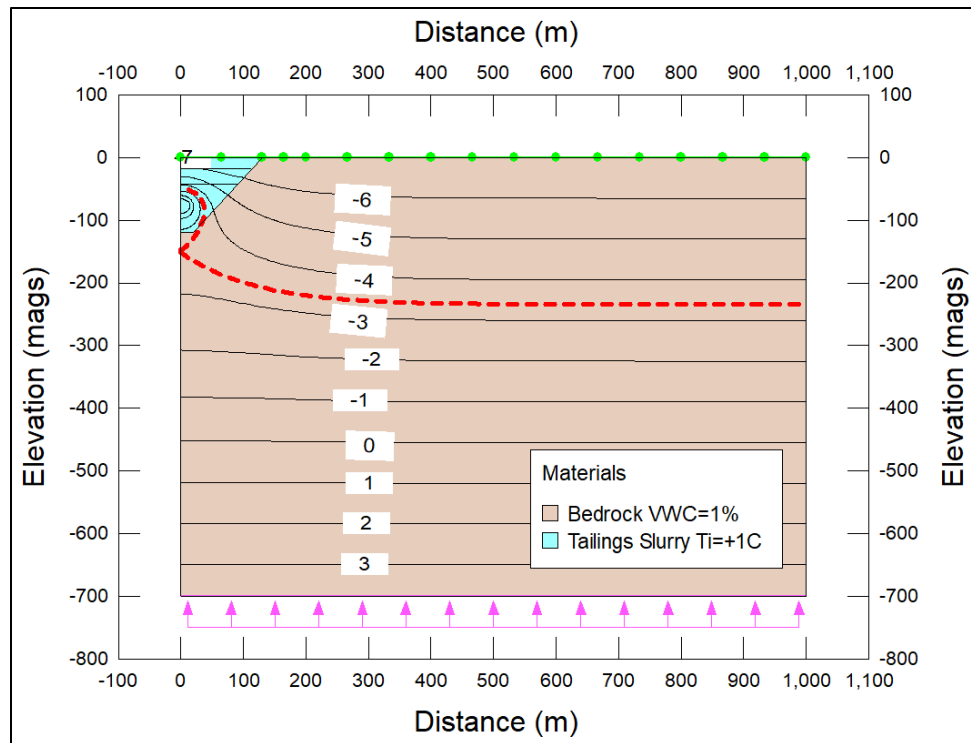


**Figure 3-13: WES05 Pit, +1°C Initial Tailings Temperature, Dry Cover, 360 Years after Pit Closure**

### 3.5.4 Talik Development – Frozen Tailings, Wet Cover

Based on the thermal FEA results in the previous section, it is evident that talik development beneath pits filled with tailings will be sensitive to the average initial tailings temperature when in-pit tailings deposition is completed.

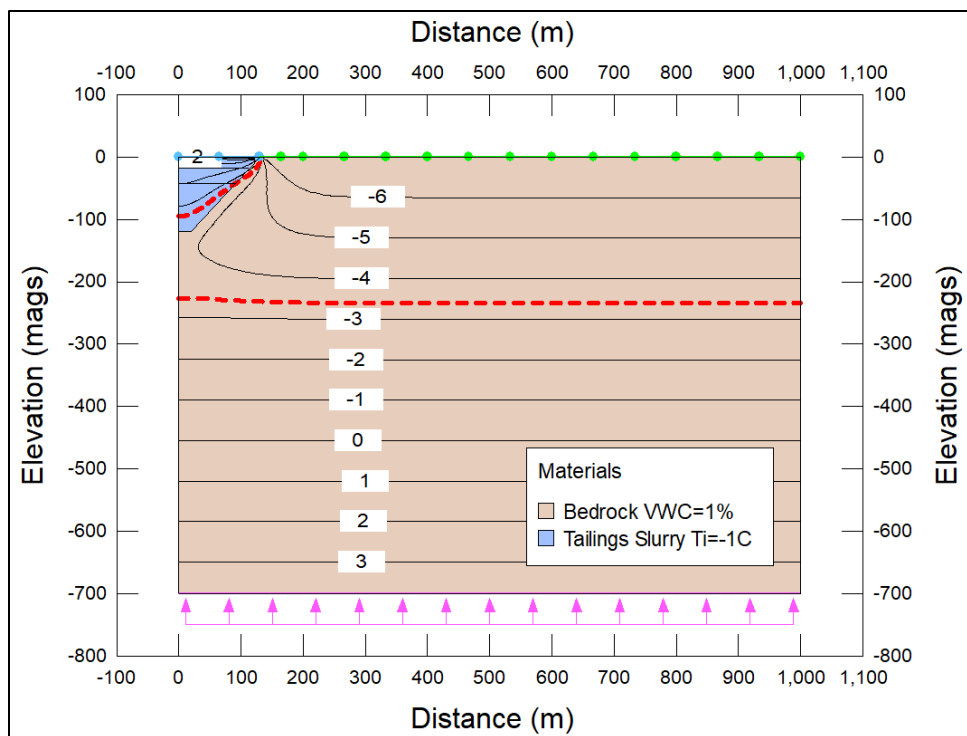
Figure 3-14 shows the temperature distribution in the subsurface 62 years after pit closure for the case with frozen tailings having an initial temperature of -1°C and with a wet tailings cover (+2°C water temperature). At this point in time most of the tailings remain below 0°C as shown in the close-up view of the tailings' temperatures shown in Figure 3-15. Note that the -3.4°C isotherm shown within the in-pit tailings in Figure 3-15 (red dashed line) represents a freezing point depression corresponding to a TDS concentration of 60,000 mg/L, however, according to water quality analysis of current detoxified tailings water (Agnico Eagle, 2021c), TDS concentrations in slurry water are anticipated to be 18,000 mg/L or less, in which case the freezing point of the tailings would be about -1.0°C. Consequently, 62 years after pit closure, much the tailings volume may remain frozen, depending on the TDS concentration and the corresponding freezing point depression.

Figure 3-15 also shows that the water cover causes long-term thawing of the initially frozen tailings. By 62 years after pit closure, the 0°C isotherm reaches a depth of about 5 m below



the top of the tailings surface whereas the  $-3.4^{\circ}\text{C}$  isotherm reaches a depth of about 95 m at this same time. Accordingly, the talik depth below the tailings surface will be highly dependent on the freezing point depression of the tailings porewater, which in turn depends on the overall TDS concentration within the tailings porewater.

The thawing caused by the water cover will continue over the long-term. Figure 3-16 shows that after about 390 years, an open talik develops (based on the  $-3.4^{\circ}\text{C}$  isotherm). The open talik enlarges slowly over the long-term; Figure 3-17 shows the subsurface temperature distribution after 1000 years and the enlargement of the talik that occurs since the talik first opened about 600 years earlier.



**Figure 3-14: WES05 Pit,  $-1^{\circ}\text{C}$  Initial Tailings Temperature, Wet Cover, 62 Years after Pit Closure**

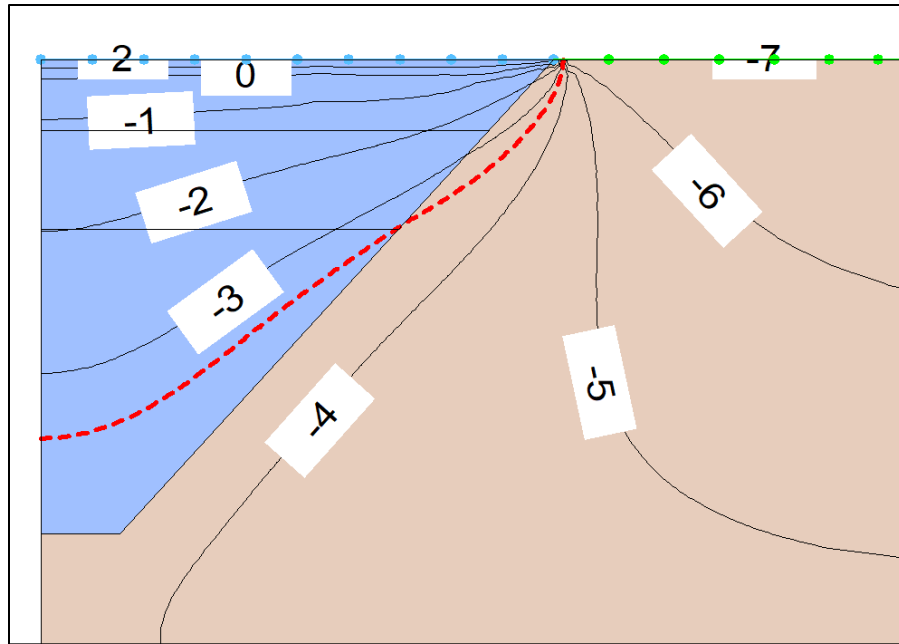


**Figure 3-15: WES05 Pit, -1°C Initial Tailings Temperature, Wet Cover, 62 Years after Pit Closure, Close-up View of Temperatures in Tailings**

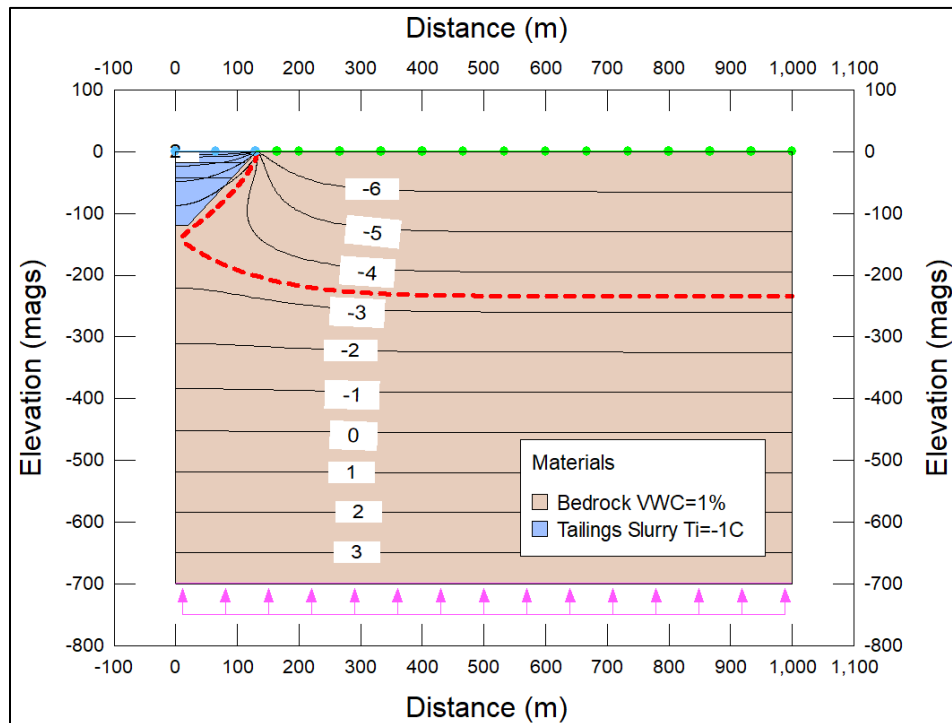


**Figure 3-16: WES05 Pit, -1°C Initial Tailings Temperature, Wet Cover, 390 Years after Pit Closure**

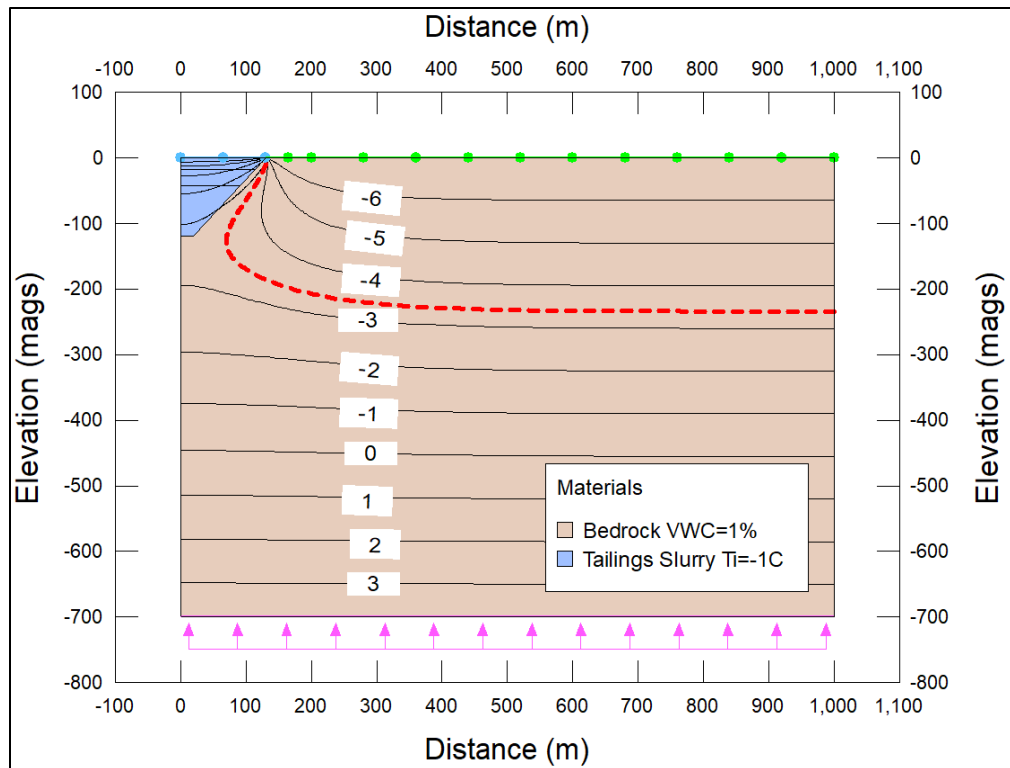


**Figure 3-17: WES05 Pit, -1°C Initial Tailings Temperature, Wet Cover, 1000 Years after Pit Closure**

### 3.5.5 Talik Development – Frozen Tailings, Dry Cover

For the case with initially frozen tailings with dry cover, the subsurface temperature distribution 62 years after pit closure is shown in Figure 3-18. In this case, the dry tailings cover increases the overall heat extraction from the in-pit tailings causing the tailings temperatures to cool over time. With this combination of frozen tailings and dry tailings cover, a talik never develops within or below the pit and the subsurface temperature conditions return to their pre-development state most rapidly of all the cases considered for the WES05 pit. The re-establishment of the subsurface temperatures to pre-development conditions is mostly complete within about 120 years after pit closure when the ground temperatures are nominally 0.5°C warmer than the pre-development temperatures. Thereafter, the ground temperatures continue to cool very slowly.

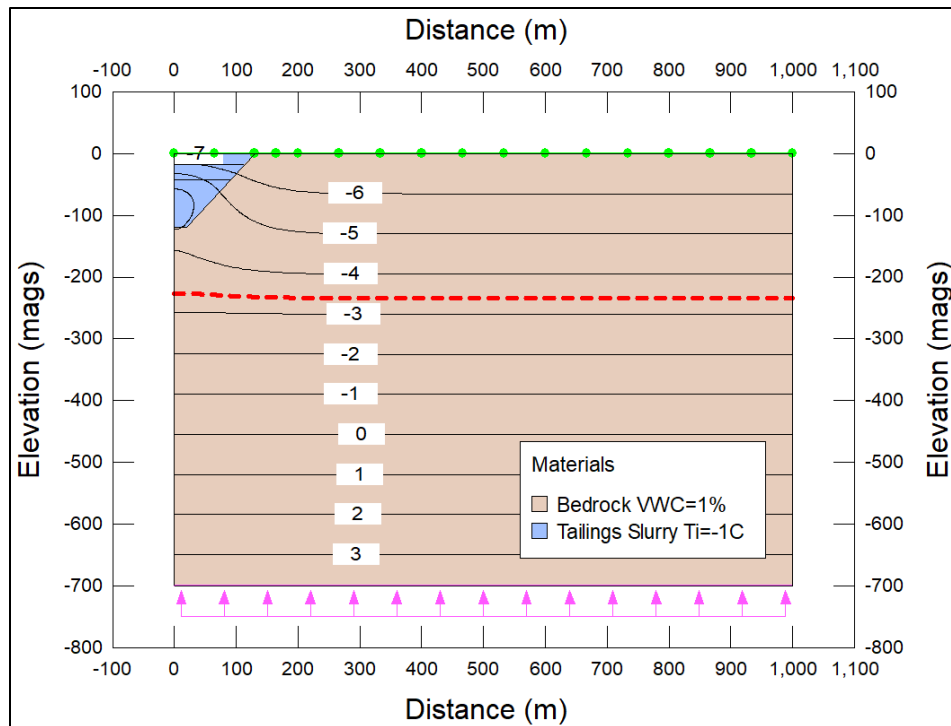


**Figure 3-18: WES05 Pit, -1°C Initial Tailings Temperature, Dry Cover, 62 Years after Pit Closure**

### 3.6 Talik Development below WN01 Pit

#### 3.6.1 Thermal Analysis Setup

A transient 2D thermal analysis was performed to assess the subsurface thermal response to in-pit tailings deposition in the WN01 pit. The WN01 pit footprint intersects Lake B5 (Figure 1-1) and as such represents a prototypical pit excavated into an existing open talik. The cross-section through the WN01 pit and its corresponding elevation profile are also shown in Figure 3-8.

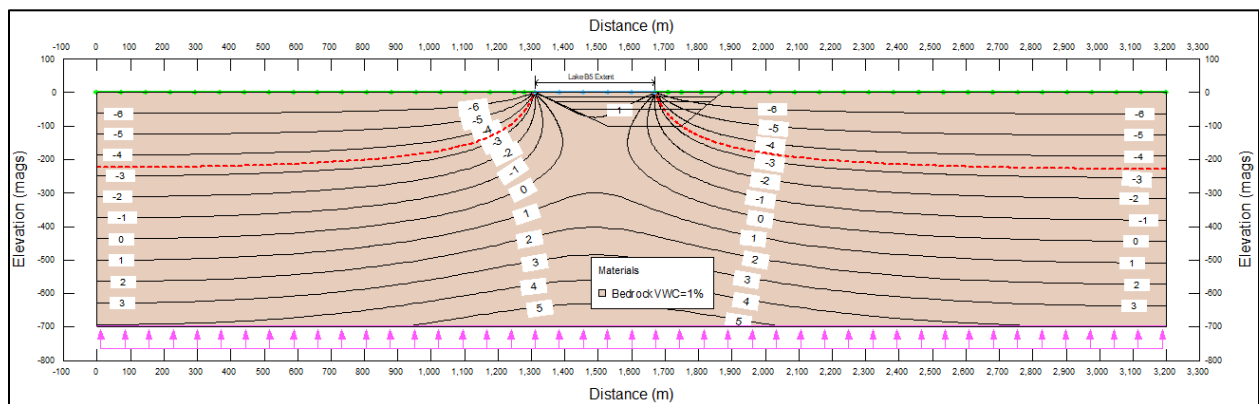
The 2D planar vertical cross-section thermal model domain is shown in Figure 3-19 where the idealized pit excavation profile using straight line segments is shown for reference. The model domain extends 3200 m horizontally and 700 m vertically. There is no axis of symmetry in this model because of the unsymmetric cross-sectional geometry of the pit excavation and its unsymmetric relation to the area of Lake B5.

Figure 3-19 also shows the initial temperature conditions before excavation as calculated using steady-state thermal FEA consistent with the thermal model calibration described earlier in this report. The extent of Lake B5 along the top boundary of the model domain is shown in Figure 3-19 for reference. The open talik below the lake is delineated in this case using the -3.4°C isotherm (corresponding to TDS concentration of 60,000 mg/L). At

the sides of the model domain, the 0°C isotherm is at a depth of about 460 m, consistent with the observed base of permafrost as shown in Figure 3-1.

According to Agnico Eagle (2021a), the WN01 pit is expected to be excavated over an approximately four-year period. It is estimated from the projected mill throughput that filling of the pit with slurry tailings would occur over the following four years. Like the WES05 thermal analysis, staged simulations were undertaken representing three intermediate pit bottom levels corresponding to four elevation zones of equal volume. These four pit bottom levels are illustrated in the model domain shown in Figure 3-19. The boundary condition at the pit bottom was set to the MAGT of -7°C during the excavation stages (over the first four years), and during the in-pit tailings deposition stages (over the next four years). After pit closure, the boundary condition at the top of the tailings was set to +2°C for wet (water) cover tailings. The simulations were run up to 1000 years.

For the thermal analysis of the WN01 pit, the dry cover scenario was not considered as it is expected that post-closure, a water cover would be inevitable because of the presence of Lake B5. In any event, because the WN01 pit will be located over an existing open talik, use of a dry cover to promote freezing at the top of the tailings is expected to have little utility for containment of dissolved tailings constituents in groundwater.



**Figure 3-19: WN01 Pit Cross-Section Thermal Model Domain and Initial Temperature Conditions (Open Talik below Lake B5)**

### 3.6.2 Talik Development – Unfrozen Tailings, Wet Cover

The WN01 planned pit footprint intersects a portion of Lake B5 (Figure 1-1). After a portion of Lake B5 over the WN01 pit area is hydraulically isolated from the remainder of the lake using berms and subsequently drained (Figure 1-1), excavation of the WN01 pit will expose the unfrozen bedrock within the open talik below the lake to cold arctic

environment temperatures. During excavation of WN01, the pit excavation ground surface is reasonably expected to have a MAGT of around  $-7^{\circ}\text{C}$ . Consequently, during the years of excavation, heat loss from the bedrock surrounding the pit will cause frost penetration into the pit walls and floor. Figure 3-20 shows the subsurface temperature distribution after 4 years of WN01 pit excavation from the thermal FEA. At this point in time, the  $0^{\circ}\text{C}$  isotherm will penetrate about 20 m into the pit walls and floor in those areas of the pit excavated into the pre-existing open talik. Similarly at this time, the  $-3.4^{\circ}\text{C}$  isotherm will penetrate about 7 m.

Figure 3-21 shows the subsurface temperature distribution for the WN01 pit after the first year of tailings infilling (end of year 5 in the simulation). At this point in time, the  $0^{\circ}\text{C}$  isotherm along the pit walls and floor has penetrated about 5 m deeper than the previous year. Deposition of unfrozen tailings causes warming of the pit wall bedrock where it is contacted by the tailings and ceases further penetration of the  $-3.4^{\circ}\text{C}$  isotherm relative to the previous year.

Figure 3-22 shows the WN01 pit with unfrozen tailings deposition with water cover 20 years after pit closure. As shown in the figure, there is a layered temperature distribution within the tailings with a temperature range between  $+0.5^{\circ}\text{C}$  and  $-1.4^{\circ}\text{C}$  because of the cooling of each of the four in-pit layers as they were placed one per year in the thermal model. In the actual pit, the tailings layers will have much finer spacing, but a layered thermal distribution within the tailings will still occur because of temperature variations during winter and summer tailings deposition.

Based on the  $-3.4^{\circ}\text{C}$  isotherm (corresponding to TDS concentration of 60,000 mg/L) in Figure 3-22, an open talik would exist across the entire pit footprint. However, TDS concentrations in slurry water are anticipated to be 18,000 mg/L or less (Agnico Eagle, 2021c), in which case the freezing point of the tailings would be about  $-1.0^{\circ}\text{C}$ . As evident in Figure 3-22, the  $-1.0^{\circ}\text{C}$  isotherm also delineates an open talik beneath the pit 20 years after pit closure.

In summary, for pits intersecting existing taliks below and near lakes, and when tailings are deposited as unfrozen (*i.e.*, their latent heat of fusion has not been liberated during deposition), the talik will be temporarily closed during pit excavation because of frost penetration into the pit walls and floor, but the talik will be reopened within about 5 years after in-pit tailings deposition is initiated.

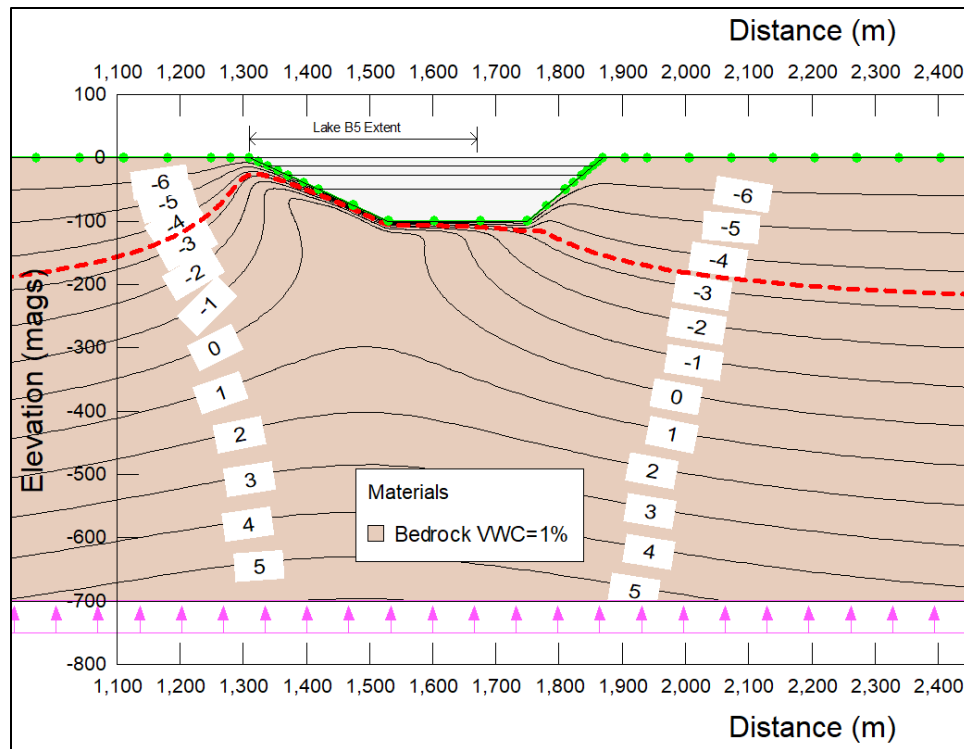


Figure 3-20: WN01 Pit, End of 4<sup>th</sup> Year of Pit Excavation

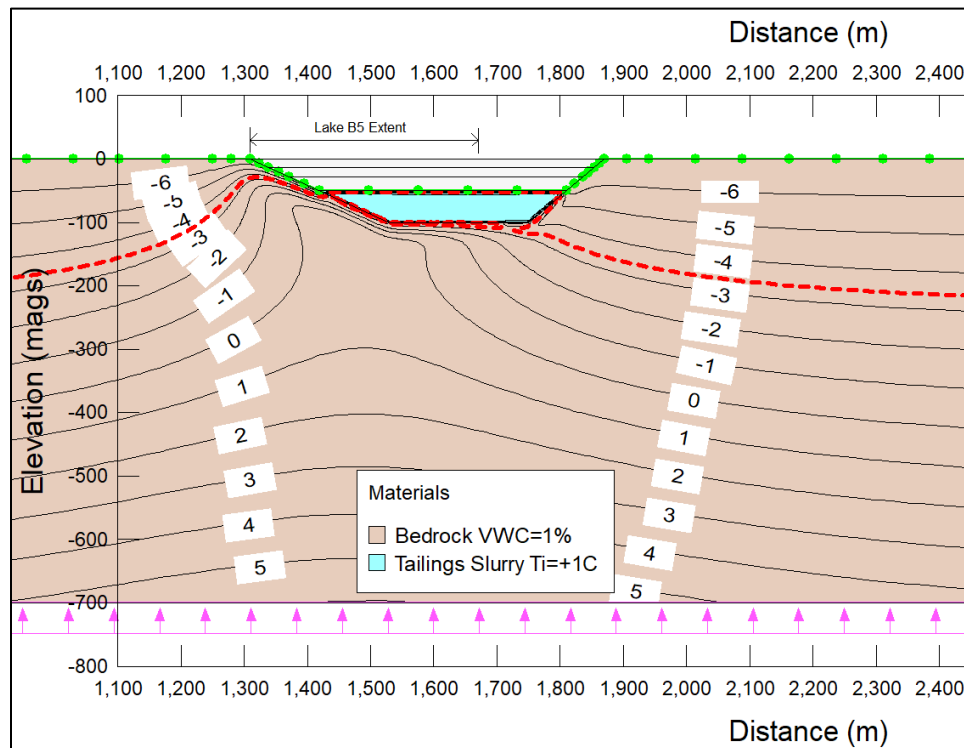
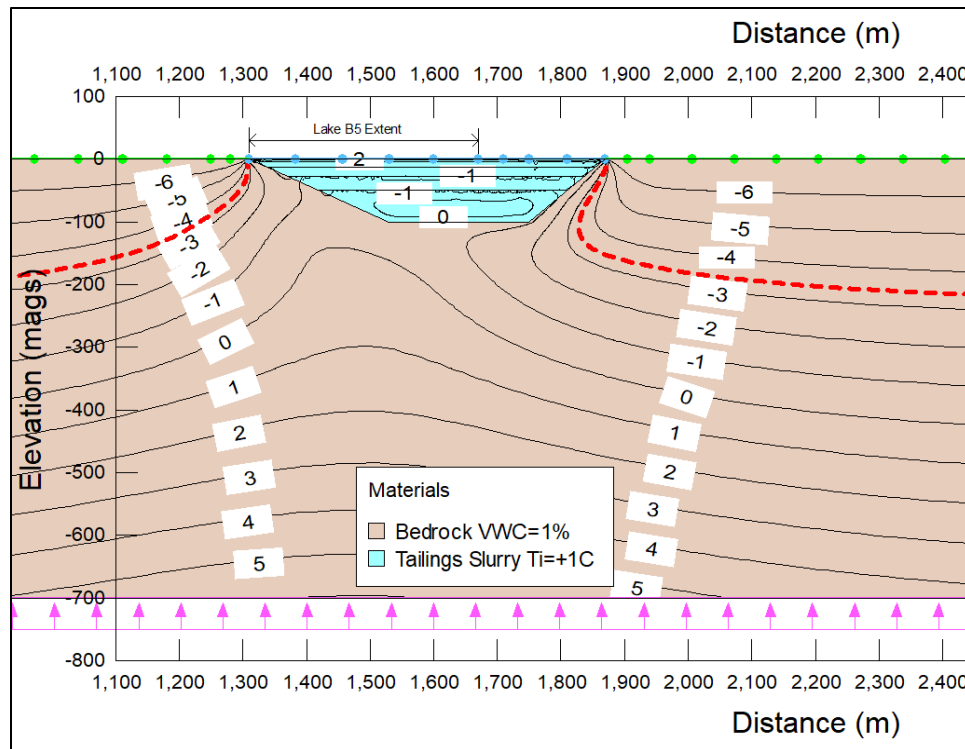


Figure 3-21: WN01 Pit, +1°C Initial Tailings Temperature, End of 1<sup>st</sup> Year of Pit Filling (Elapsed Year 5)



**Figure 3-22: WN01 Pit, +1°C Initial Tailings Temperature, Wet Cover, 20 Years after Pit Closure**

### 3.6.3 Talik Development – Frozen Tailings, Wet Cover

To assess the effect of frozen tailings deposition on talik development for the WN01 pit, and where wet tailings cover is used, a 2D transient thermal analysis was performed where the initial tailings temperature was -1°C. This is identical to the analysis reported in the previous section, except for the colder initial tailings temperature used in the analysis.

Despite specifying an initial tailings temperature of -1°C for each annual lift of tailings deposited in the pit, the average pit tailings temperature distribution will be layered, with a variable temperature within each layer, and an overall average temperature at the end of pit infilling that is colder than -1°C. Tailings temperatures below -1°C result from the exposure to the cold MAGT of -7°C.

Figure 3-23 shows the subsurface temperature distribution at pit closure (*i.e.*, upon conclusion of the fourth year of in-pit tailings deposition). Although the -3.4°C isotherm (red dashed line) intersects the in-pit tailings, it is important to note that the freezing point within the tailings is expected to be -1.0°C or warmer if the tailings porewater TDS concentration is 18,000 mg/L or less. Accordingly, for the case shown in Figure 3-23, the tailings porewater will be, for the most part, frozen and immobilized at the time of pit closure.



As shown in Figure 3-24, the relatively cold initial temperatures within the tailings during deposition keeps the tailings frozen over the first 20 years following pit closure, except at the top of the tailings where the water cover causes tailings thaw to a depth of about 4 m, and at the bottom of the tailings, where slow warming causes the bottom of the tailings to warm to  $-1^{\circ}\text{C}$  on the side of the pit that intersected the pre-existing open talik beneath Lake B5. Hence, after about 20 years, the talik opens at the bottom of the tailings if the freezing point within the bedrock is colder than about  $-1^{\circ}\text{C}$ .

The subsurface temperature distribution 100 years after pit closure is shown in Figure 3-25. The tailings have warmed somewhat over the previous 80 years (by comparison with Figure 3-24) because of the warming effect of the water cover on the tailings. The warming effect causes the tailings to be above  $-1^{\circ}\text{C}$  (thawed) to a depth of about 20 m. Below 20 m depth, the tailings remain at a temperature just below  $-1^{\circ}\text{C}$  (frozen) except near the bottom of the tailings on the side of the pit excavated into the pre-existing talik, where the tailings temperature rises slightly above  $-1^{\circ}\text{C}$ . At this location, the open talik that had developed there 80 years earlier still exists (as one might expect), but the talik has not expanded significantly over the intervening 80 years.

Finally, for completeness, Figure 3-26 shows the subsurface temperature distribution after 1000 years. At this point in time, the warming effect of the wet cover over the tailings has completely thawed the in-pit tailings and the open talik (delineated by the  $-1^{\circ}\text{C}$  isotherm at the base of the pit) has opened completely.

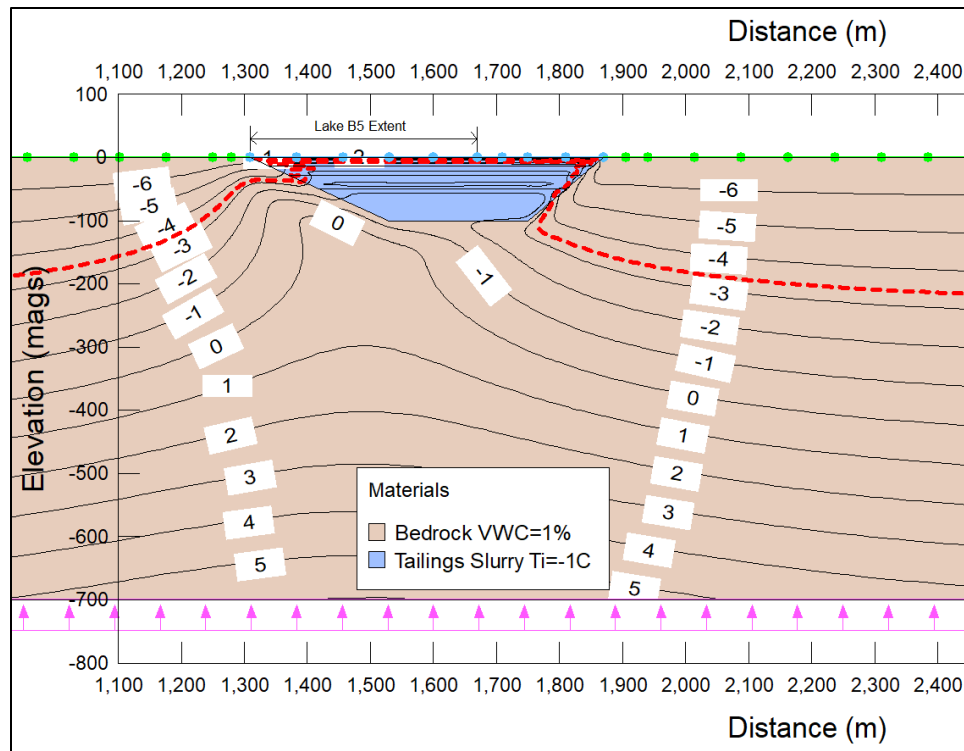


Figure 3-23: WN01 Pit, -1°C Initial Tailings Temperature, at Pit Closure

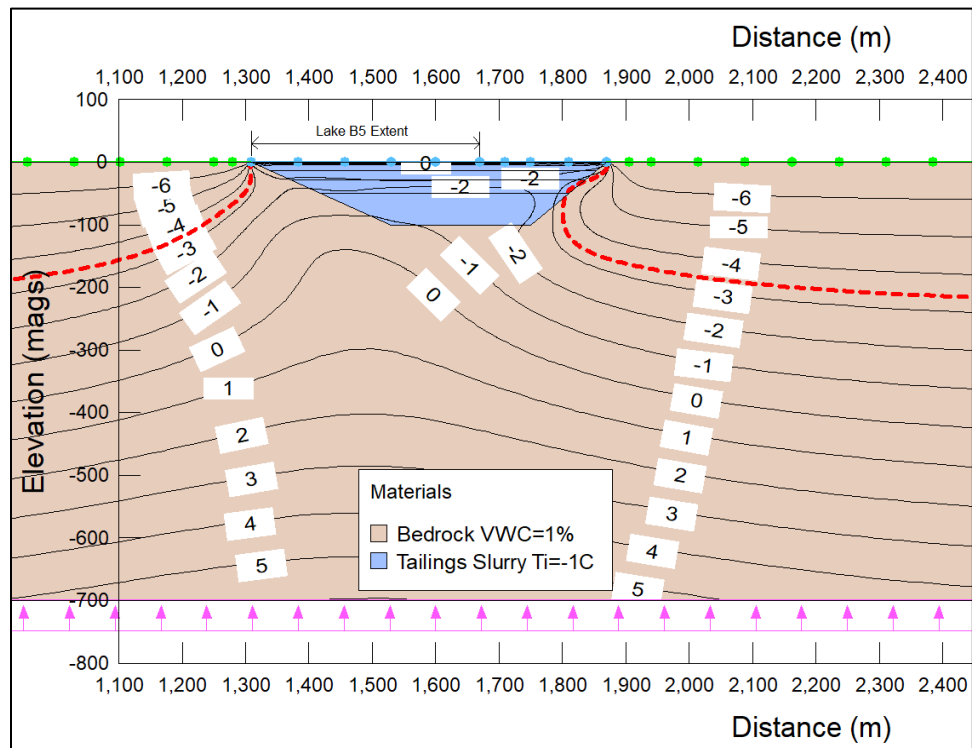
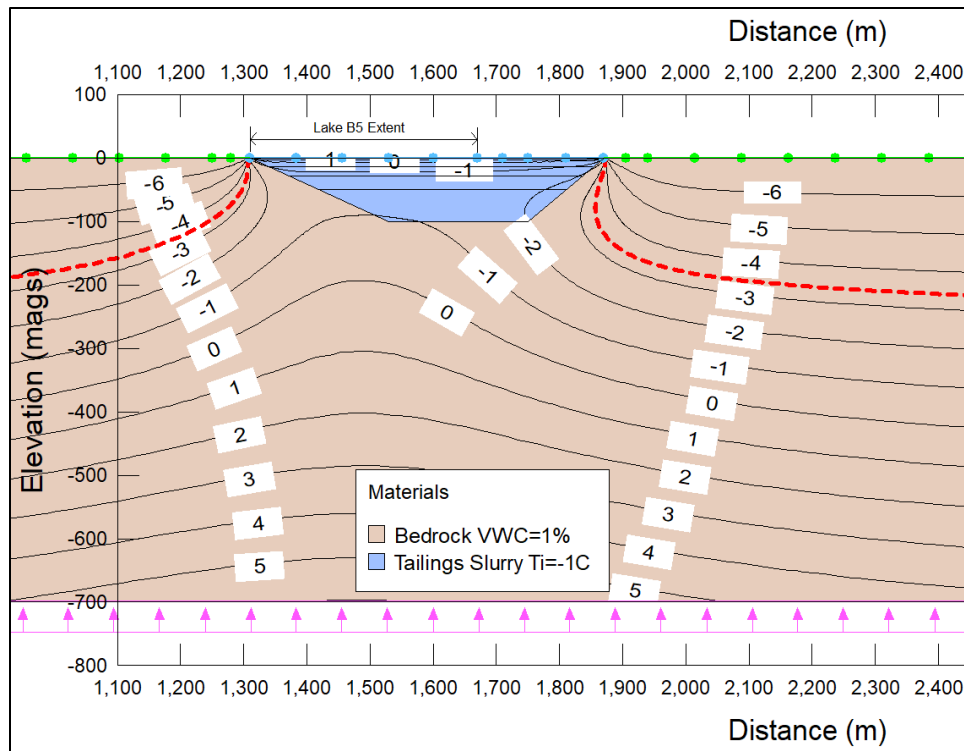
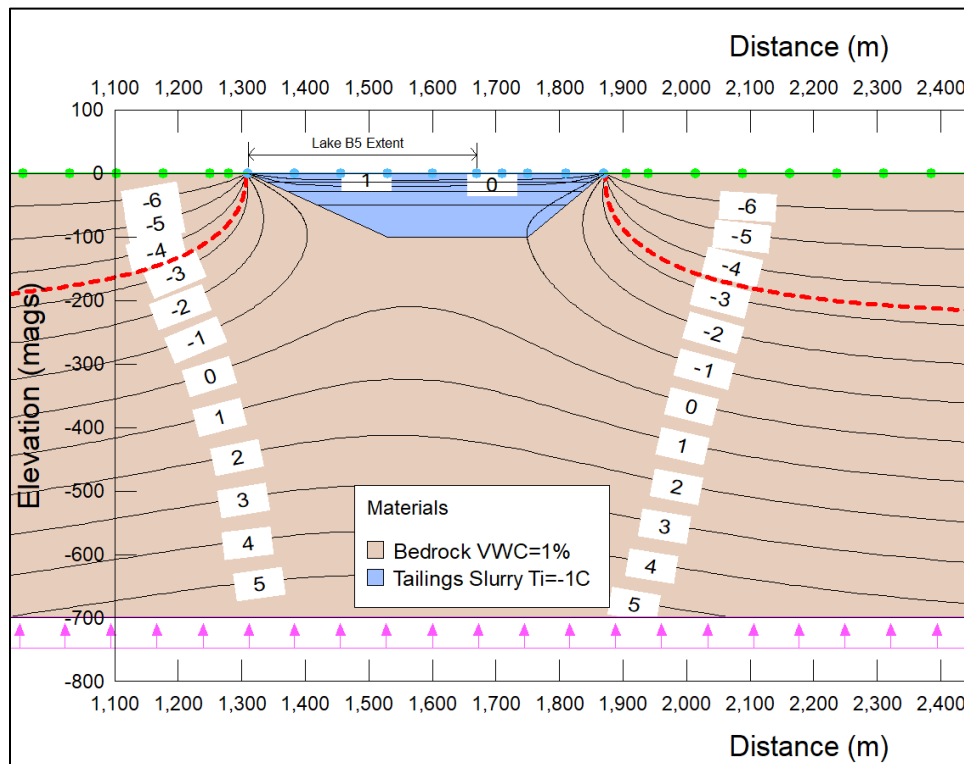


Figure 3-24: WN01 Pit, -1°C Initial Tailings Temperature, Wet Cover, 20 Years after Pit Closure



**Figure 3-25: WN01 Pit, -1°C Initial Tailings Temperature, Wet Cover, 100 Years after Pit Closure**



**Figure 3-26: WN01 Pit, -1°C Initial Tailings Temperature, Wet Cover, 1000 Years after Pit Closure**

### 3.7 ***Uncertainties and Limitations***

The intent of the thermal modelling effort and results reported herein was to provide insight regarding the subsurface thermal response to in-pit tailings deposition for pits developed in permafrost away from existing taliks, and for pits developed adjacent to or within existing open taliks beneath lakes at the Meliadine Project area. However, it is important to acknowledge that there are several uncertainties and associated limitations inherent this effort, which is true of any modelling exercise.

*Accurate* delineation of taliks (*i.e.*, the frozen/unfrozen boundaries) through time in deep permafrost is not feasible because of the large number of measurement and analysis input variables that would be required, and because of the large scale of both the spatial and temporal domains. However, although it is not possible to accurately determine talik boundaries because of limitations of available subsurface data, and because of wide uncertainties of other parameters such as spatial distribution of porewater salinity and initial temperature conditions, it is possible to use thermal modelling to understand the predominant mechanisms and sensitive parameters governing talik development for in-pit tailings disposal.

To provide some sense of the types of uncertainties related to talik delineation, a few are enumerated as follows:

- The landscape in the Meliadine Project area consists of many lakes of various sizes and depths scattered across the landscape. Open taliks will exist beneath relatively large and deep lakes, and closed taliks will exist below smaller and shallower lakes. Consequently, the initial pre-development distribution of talik boundaries over the scale of the Meliadine Project area, if one could see the talik boundaries with the naked eye, would be a complex series of surfaces in three-dimensions. Given this spatial complexity and given the very limited available information regarding subsurface spatial distributions of temperature and salinity, high accuracy delineation of the existing talik boundaries is practically impossible.
- The thermal analyses have been predicated on background thermal conditions in undisturbed rock being at equilibrium. However, owing to the significant depth of permafrost, the ground thermal regime may still be responding to temperature changes induced by the last glaciation.
- The freezing point of porewater depends on porewater salinity. The salinity within the bedrock to depths of several hundred meters in the Meliadine Project area has been sampled extensively to date, however, the exact distribution of salinity within the subsurface cannot be known with certainty.

- The overall temperature of the in-pit tailings depends on operational details regarding tailings deposition that were not known at the time of the thermal modelling work reported herein. In particular, the degree to which the tailings will cool during deposition will affect the long-term thermal response of the tailings and will affect the timeframe over which the tailings can thaw when a water cover is used on the tailings. With knowledge of other operating mining assets owned by Agnico Eagle, it should be possible to assess the expected temperature evolution of slurry deposited tailings to remove some of the uncertainty regarding the amount of latent heat of fusion liberated from the tailings during deposition. This would require a separate thermal analysis study that was outside the scope of the work reported herein.

The combination of the above uncertainties means that a highly accurate prediction of talik distribution (*i.e.*, the unfrozen zones where groundwater flow can occur) itself has significant uncertainty. However, although high-accuracy prediction of talik distribution is not possible without acquisition of more data than is practical to collect, thermal analysis does provide insight regarding long-term talik development that can inform the feasibility of in-pit tailings disposal, in particular, the effects of various tailings design and operating options, and estimation of the timeframes over which open taliks may develop, thus creating a groundwater flow pathway that may otherwise have not existed.

### **3.8 Summary**

The following findings are based on the thermal analyses to delineate taliks in the Meliadine Project area:

- The development of an open talik below waterbodies (which includes pits having in-pit tailings with water cover) depends on the depth of the waterbody (which affects if the winter ice freezes to the bottom of the water column), the mean annual temperature of the bottom of the waterbody, the overall areal size of the waterbody, and the freezing point of the bedrock porewater.
- For circular-shape waterbodies, the critical radius of the waterbody above which an open talik will develop in the long-term with sub-permafrost unfrozen zone (at thermal steady-state, which may take several decades or several centuries to achieve), for waterbody bottom temperatures of +4°C and +1°C, is 240 m and 320 m, respectively, based on delineation of the talik boundary by a freezing temperature of 0°C (Figure 3-5).
- For elongated-shape waterbodies, the critical half-width of the waterbody above which an open talik will develop in the long-term, for waterbody temperatures of

+4°C and +1°C, is 120 m and 160 m, respectively, based on the delineation of the talik boundary by the 0°C isotherm (Figure 3-7).

- For roughly circular-shaped pits located well away from existing taliks beneath lakes, such as the WES05 pit, deposition of relatively unfrozen in-pit tailings that are water-covered after pit closure slowly warm the underlying permafrost, causing an open talik to develop several decades after pit closure. For the WES05 pit specifically, under these same conditions, an open talik is expected to develop about 60 years after pit closure if the freezing point of bedrock porewater is -3.4°C, which corresponds to a porewater TDS concentration of 60,000 mg/L (Figure 3-10).
- For the WES05 pit case again with relatively warm tailings deposition, but when the tailings cover is dry instead of wet, an open talik will develop after about 60 years, identically to when a wet cover is used (compare Figure 3-11 with Figure 3-10). However, when the tailings surface is not water covered, there is significantly greater heat extraction from the dry cover, causing long-term cooling of the tailings such that after about 360 years after pit closure, the open talik will transition to a closed talik that encompasses the lower portion of the pit tailings and a portion of bedrock just below the pit bottom, to a maximum depth of about 150 m below ground surface (Figure 3-13). Thereafter, the closed talik zone in the tailings and bedrock will slowly freeze and eventually, within about 1000 years after pit closure, the subsurface temperature distribution will return to its initial, pre-development state.
- The long-term development of talik below pits with in-pit tailings deposition is sensitive to the average temperature of the tailings mass in the pit at time of pit closure, and more specifically, the degree to which the final tailings mass is frozen, or unfrozen. Tailings that are not completely frozen during deposition will have much higher latent heat than tailings that are frozen during deposition. Consequently, unfrozen in-pit tailings will cool slower and thus warm bedrock beneath a pit compared to frozen tailings, and taliks will develop faster and persist longer beneath pits with unfrozen tailings.
- For the WES05 pit with frozen tailings covered with water after pit closure, thermal analysis indicated that the tailings remained frozen 60 years after pit closure except for the top few tens of meters that thaw because of the water cover (Figure 3-14 and Figure 3-15). The warming effect of the water cover causes ongoing thaw of the tailings such that an open talik develops after about 390 years after pit closure based on a bedrock porewater freezing temperature of -3.4°C (Figure 3-16). Thereafter, the open talik continues to expand because of the water cover at the tailings surface.

- For the WES05 pit with frozen tailings having a dry cover at the top of the tailings, thermal analysis showed that the frozen tailings were preserved and cooled below their initial depositional temperature through time because of the exposure to the cold arctic environmental temperatures at the at the tailings surface. Consequently, an open talik did not develop under this set of conditions (Figure 3-18).
- For elongated-shape pits that intersect open taliks, such as the WN01 pit, that are filled with relatively unfrozen tailings and are water-covered after pit closure, frost penetrates the unfrozen bedrock where it is exposed during pit excavation and tailings infill. After four years of pit excavation, the frost depth into the pit walls and floor will extend about 20 m deep if the freezing temperature of the bedrock porewater is 0°C (freshwater), and about 7 m deep if the freezing temperature is -3.4°C (porewater TDS concentration of 60,000 mg/L) (Figure 3-20). About 20 years after pit closure, the deposition of unfrozen tailings combined with water cover at the top of the tailings will eventually cause thawing of the bedrock around the pit walls and floor, thus opening the talik in the pit with the talik that existed below the lake before pit excavation started (Figure 3-22).
- For the WN01 pit with frozen tailings and water-covered tailings, the tailings will remain frozen for about 20 years, (based on a tailings porewater freezing temperature of -1.0°C, corresponding to a porewater TDS concentration of 18,000 mg/L), except at the top of the tailings where the water cover will cause thaw penetration on the order of meters (Figure 3-24). The tailings remain frozen within the lower portion of the pit for several decades thereafter (the exact time interval being dependent on the freezing temperature in the tailings) (Figure 3-25). Thereafter, the open talik as the subsurface temperatures move toward thermal equilibrium, as would occur under a lake (Figure 3-26).
- When open pits are sited in permafrost (*i.e.*, not within existing taliks), the permafrost can be best preserved when the tailings are deposited in a mostly frozen state, and when a dry tailings cover is used. However, if a dry tailings cover is not an option, then frozen tailings deposition still provides significant benefits for permafrost preservation as it will slow the time for an open talik to develop. In the very long-term (on the order of hundreds of years) however, a talik will form beneath pits having water-covered tailings.
- For pits sited where they intersect existing lakes, the pit will be excavated within talik, and the tailings would likely be water-covered after pit closure. In this case, if the tailings are deposited mostly in the frozen state, then this will lengthen the time interval before an open talik is re-established compared to if the tailings are deposited in a mostly unfrozen state.

## ***4. Groundwater Analysis***

---



**AGNICO EAGLE**



## **4. Groundwater Analysis**

---

### **4.1 Overview**

Numerous field investigations and numerical modelling studies have been undertaken at the Meliadine project to characterize the permafrost and groundwater regimes. Most recently, the findings of these programs have been summarized in the 2021 thermal and groundwater modelling reports (Golder 2021a,b) and hydrogeology existing conditions report (Golder 2021c).

The groundwater analysis reported herein has drawn upon findings from the aforementioned studies to present a conceptual model for groundwater flow from backfilled pits post-closure, after the groundwater system has recovered from mining and hydraulic gradients have re-established towards Meliadine Lake. Analytical equations were then used to estimate contact water fluxes and travel times from backfilled pits to Meliadine Lake assuming equilibrium post-closure conditions. This was followed by a simplified 2D numerical flow and transport modelling exercise on the pit with the worst seepage outcomes (large fluxes and short travel times compared to other pits). The numerical modelling exercise was used to confirm the findings mathematical analysis and evaluate the effects of dispersion on loading to Meliadine Lake. The results of numerical transport modeling were extended to specific PCOCs determined through a comparison of measured groundwater quality and tailings source terms.

### **4.2 Conceptual Model**

The following sections discuss the conceptual model of groundwater flow on which the calculations of seepage fluxes and travel times are based.

#### **4.2.1 Baseline Conditions**

The Meliadine mine is located in a zone of continuous permafrost (NRCan, 1995) which partitions the groundwater regime into shallow and deep systems. The shallow groundwater regime resides in the seasonally active layer, estimated to be one to three meters depth (Golder, 2014a), and is isolated from the deeper groundwater system by a substantial thickness of permafrost (as discussed further below). Permafrost is assumed to be essentially impermeable in groundwater modelling undertaken for this project (Golder 2021b), consistent with other published studies (Kane *et al.* 2013, Walrood *et al.* 2012, Jaquet *et al.* 2012, Lemieux *et al.* 2008).

In areas away from open taliks, permafrost depth has been simulated to be on the order 430 m (Golder 2021a). Elevated salinity in deep project groundwater (on the order of

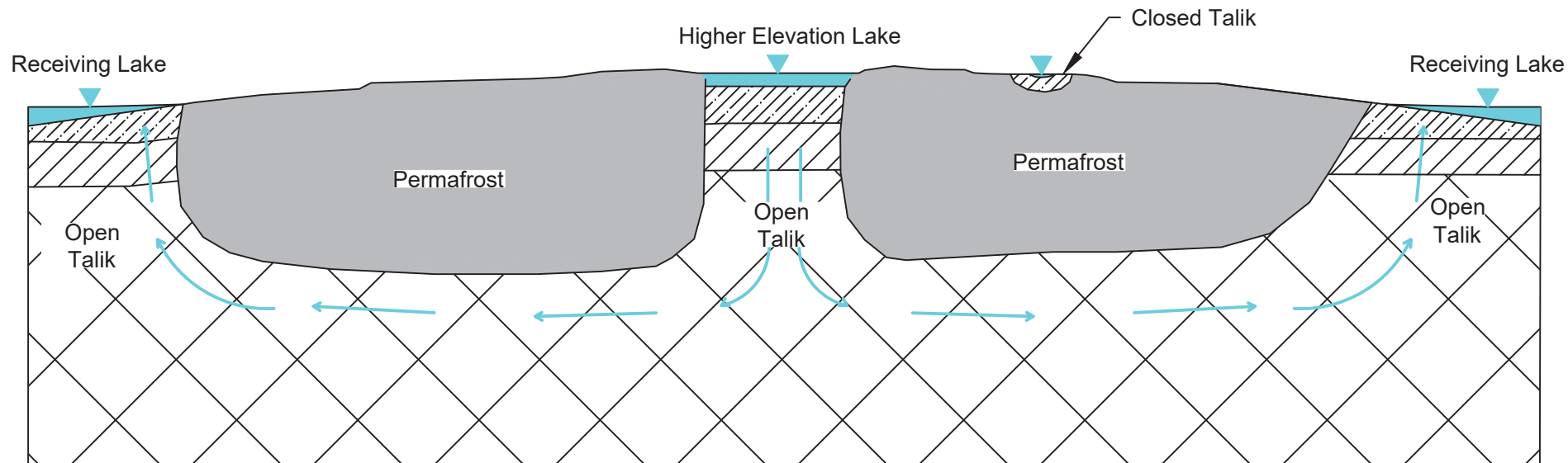
60,000 mg/L) depresses the freezing point by  $\sim 3.4^{\circ}\text{C}$  which leads the formation of a substantial cryopeg (ground that is below  $0^{\circ}\text{C}$  but remains unfrozen) (Golder 2021c). The depth to the cryopeg is estimated to be 280 to 290 m in the area of the underground developments (Golder 2021c); thus, within the permafrost zone resides a basal layer of  $\sim 150$  m thickness where unfrozen or partially frozen water exists within the bedrock.

Deep groundwater flow is driven by gentle hydraulic gradients ( $<2\%$ ) created between lakes supporting open talik formation (Figure 4-1). The regional thermal model (Golder 2021a) predicts open taliks below Meliadine Lake and lakes A6, A8, B4, B5, and B7 in the main area of the mine (Figure 1-1). Under baseline conditions, water levels in the mine area lakes supporting open taliks are 5 m to 12 m higher than that of Meliadine Lake (elevation 51.8 m asl). The mine area lakes are thus groundwater recharge areas while Meliadine Lake is inferred to be a groundwater discharge area. Groundwater flow from open taliks must travel vertically to the depth of the cryopeg, and then travel laterally until it reaches the receiving talik where it again travels upwards to discharge in the receiving waterbody (Figure 4-1).

The main geological units in the mine area are broadly grouped into Sedimentary Rock Formations and Mafic Volcanic Rock formations. Hydraulic conductivity of these units is presumed to decrease with depth, as determined through hydraulic testing and calibration of the groundwater model (Golder 2021b,c). Calibrated hydraulic conductivity values for competent bedrock and selected faults are provided in Table 4-1.

**Table 4-1:**  
**Calibrated Hydraulic Conductivity for Competent Bedrock and Selected Faults**  
**after Golder (2021b)**

Hydrostratigraphic Unit	Depth Interval (m bgs)	Hydraulic Conductivity (m/s)
<b>Competent Rock</b>		
Shallow Bedrock	0 to 60	$3 \times 10^{-7}$
Sedimentary Rock Formations	60 to 120	$3 \times 10^{-8}$
Sedimentary Rock Formations	120 to 1500	$3 \times 10^{-9}$
Mafic Volcanic Rock Formations	120 to 1500	$3 \times 10^{-10}$
<b>Faults</b>		
RM-175	0 to 1000 deep	$5 \times 10^{-8}$
WM-C	0 to 1000 deep	$2 \times 10^{-6}$
WM-B	0 to 1000 deep	$1 \times 10^{-6}$
WM-D	0 to 1000 deep	$1 \times 10^{-6}$



## LEGEND

	GW Flow		Deep Bedrock
	Permafrost		Shallow Bedrock
	Medium Bedrock		

DATE SAVED: Oct 26, 2021  
 DRAWN BY: GM  
 REVIEWED: LF  
 VERSION: 1



PROJECT: **Meliadine Extension  
In-Pit Tailings Study**

TITLE: **Conceptual Model of GW  
Flow (Baseline)**

PROJECT #: **A574-6**

FIGURE: **4-1**

The mine area is transected by numerous faults (Figure 1-1) which were simulated as zones of enhanced permeability in the numerical groundwater model (Golder 2021b). This assumption was based on findings from several field investigations where hydraulic properties (hydraulic conductivity, thickness) of these features were assessed (Golder 2021c). Groundwater is expected to flow preferentially in these enhanced permeability zones which are one to three orders of magnitude more permeable than surrounding bedrock in the area.

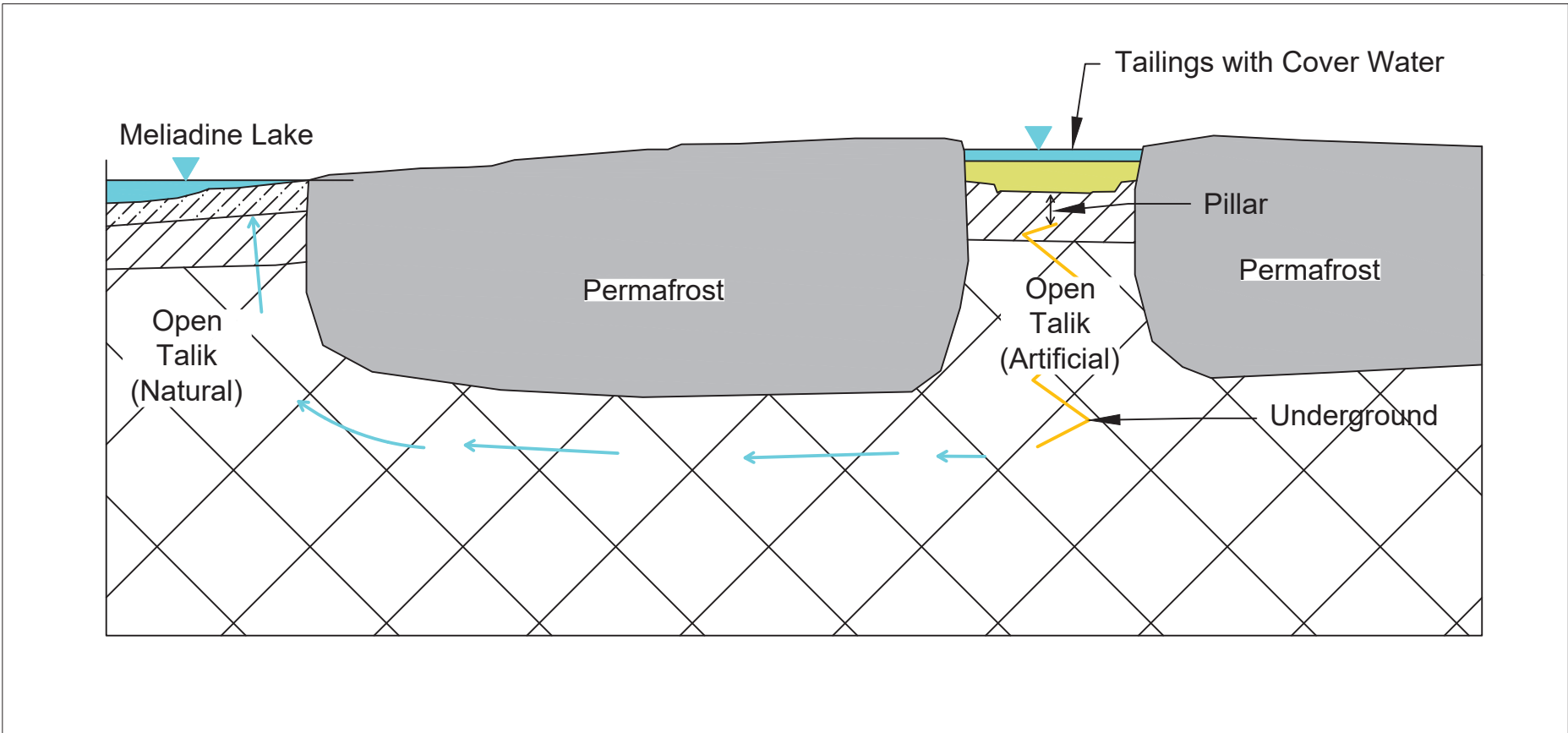
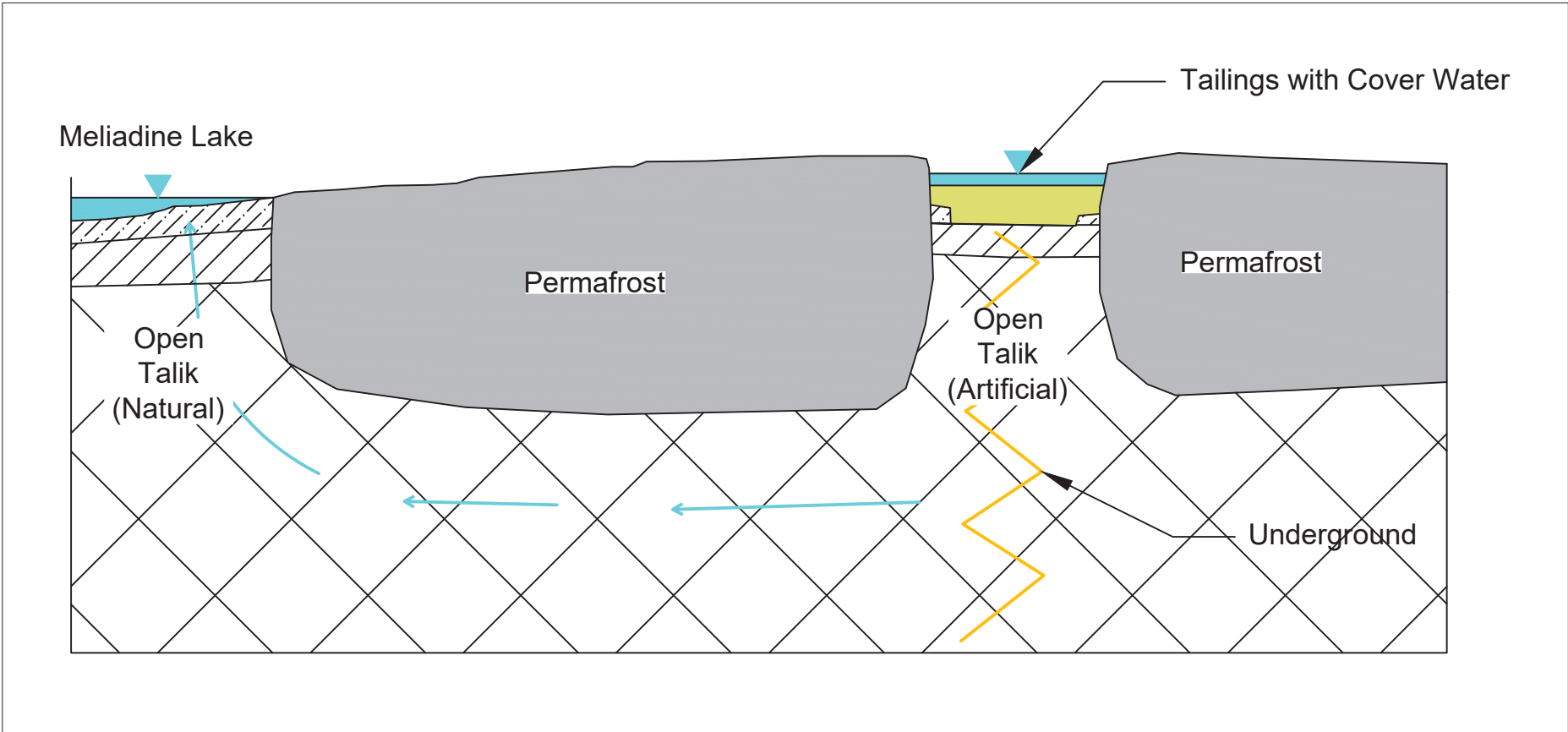
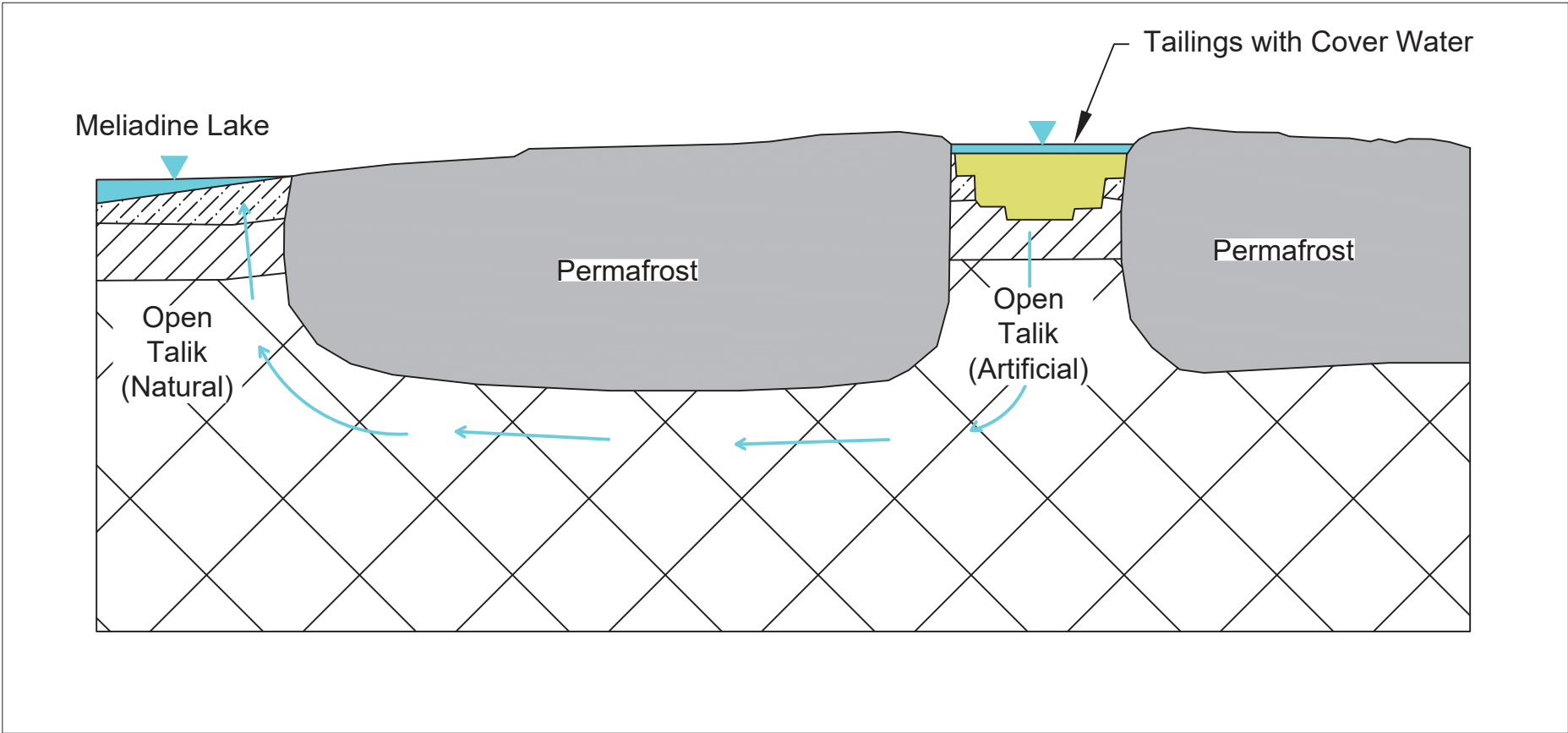
#### **4.2.2 Post-Closure Conditions**

Underground developments and pits connected to open taliks or the sub-permafrost groundwater flow system will act as a sink for groundwater flow during operations (Golder 2021b). Upon cessation of mining, groundwater levels will rebound and eventually reach a new equilibrium. Surface runoff into pits backfilled below grade is anticipated to form a water cover. The water cover on the tailings facilities drives contact water from the backfilled pits into the deeper groundwater system where it will ultimately discharge to a receiving waterbody, assumed to be Meliadine Lake based on local topography (Figure 4-2).

Generalized groundwater flowpaths for post-closure conditions are illustrated for different pit configurations in Figure 4-2 and are shown in plan view on Figure 1-1. The upper panel of Figure 4-2 illustrates the situation where there is an open pit and no associated underground workings and is applicable to WES04 and WES05 pits. Seepage from the backfilled pits first travels downward through undisturbed bedrock before traveling horizontally and then vertically upward beneath towards Meliadine Lake. In the case of WES05, two groundwater flowpaths are considered:

- i. Seepage infiltrates directly into the WM-D fault, which transects the pit, and follows a west trajectory to Meliadine Lake (Figure 1-1)
- ii. Seepage through competent bedrock in the pit infiltrates downward and northward where it is intercepted by the WM-B fault, and travels west to Meliadine Lake. (Figure 1-1).

Tailings seepage issuing from the WES04 pit follows a similar trajectory as the second WES05 flowpath above. The WES04 pit lies in competent bedrock; consequently, seepage travels downward then northward in competent rock for a short distance, where it then intercepts the WM-C fault and directed westward to Meliadine Lake.



**LEGEND**

- ← GW Flow
- Tailings
- Permafrost
- Shallow Bedrock
- Medium Bedrock
- Deep Bedrock
- Underground Workings

DATE SAVED: Oct 26, 2021

DRAWN BY: GM

REVIEWED: LF

VERSION: 1

CLIENT:

**AGNICO EAGLE**

**LORAX ENVIRONMENTAL**

PROJECT:

**Meliadine Extension In-Pit Tailings Study**

TITLE:

Conceptual Model of GW Flow (Post-Closure)

PROJECT #:

A574-6

FIGURE:

4-2

The middle panel of Figure 4-2 illustrates the geometry where underground workings are advanced below the pit with a minimal (<10 m thick) crown pillar between the two. This situation is applicable to WES01 and PUM03 pits. A single level of stopes is planned under the PUM03 pit, while the underground extends to considerable depth (~650 m below pre-mine topography) below WES01. For simplicity, it is conservatively assumed that seepage from the backfilled pit travels instantly downward through the underground workings (open developments) until it reaches competent rock whereafter it travels laterally and then upwards towards Meliadine Lake. Significant faults have not been observed to intersect PUM03 (Golder 2021c) and seepage from the backfilled pit is imagined following the shortest flowpath to Meliadine Lake (Figure 1-1).

WES01 is intersected by the RM-175 fault which is presumed to serve as one potential flowpath from this facility towards Meliadine Lake. The second potential flowpath is comprised of seepage through competent bedrock in the pit which follows a competent bedrock flowpath of similar length to Meliadine Lake.

In the case where a pillar exists between the pit bottom and underground, such as at WN01 and PUM01 pits, the tailings seepage will first need to traverse the pillar before entering the mine void from where it will migrate towards Meliadine Lake (bottom panel of Figure 4-2). PUM01 is not intersected by faults and per PUM03, seepage from the backfilled pit is imagined following the shortest flowpath to Meliadine Lake (Figure 1-1).

### 4.3 Mathematical Model

#### 4.3.1 Analytical Methods

##### 4.3.1.1 Governing Equations

Travel times from backfilled pits have been computed according to Darcy's Law for groundwater flow through a porous medium:

$$q=Ki \quad (1)$$

where  $q$  is the specified flux in ( $\text{m}^3/\text{s}/\text{m}^2$ ),  $K$  is the hydraulic conductivity ( $\text{m}/\text{s}$ ), and  $i$  is the hydraulic gradient along the flowpath. Travel times can be calculated by dividing the travel distance  $d$  by the groundwater advective velocity  $v$ . Groundwater advective velocity  $v$  is equivalent to the specific flux  $q$  divided by porosity,  $n$ :

$$v=q/n = Ki/n \quad (2)$$

The equations above describe a plug (advection) flow condition, where plume dispersion and geochemical controls are not considered.

The seepage flux from backfilled pits ( $Q$  in  $\text{m}^3/\text{d}$ ) is computed by multiplying the specific flux  $q$  by the cross-sectional area of flow ( $A$ ):

$$Q = KiA \quad (3)$$

For pits completed in competent bedrock, the hydraulic conductivity  $K$  in the equation (3) is equal to the distance-weighted harmonic mean of hydraulic conductivity computed for flow in series through a layered system (Freeze and Cherry, 1979). This harmonic mean accounts for flow through tailings and bedrock (and any fault encountered farther along the pathway).  $A$  is equal to the cross-section area of flow, taken to be the pond surface area at the backfill elevation.

When a fault directly transects the pit, an additional seepage flux is calculated which represents the tailings seepage directly into the fault. The hydraulic conductivity  $K$  used in equation (3) is the distance-weighted harmonic mean of the tailings and fault  $K$ . The cross-sectional area  $A$  is equivalent to the product of the strike length of the fault in the pit and the thickness of the fault.

#### 4.3.1.2 Parameter Values

##### *Hydraulic Conductivity*

A distance-weighted harmonic mean hydraulic conductivity of tailings backfill and bedrock was used to compute seepage fluxes and travel times (Table 4-2). Both bedrock and tailings hydraulic conductivity values were used to calculate seepage fluxes and travel times in this analysis. The bedrock values are based on calibrated hydraulic conductivity values determined in the numerical groundwater model (Golder 2021b) (Table 4-1). The tailings hydraulic conductivity is based on laboratory measurements on tailings samples from Agnico Eagle's Amaruq mine (Golder 2017). The testwork yielded tailings hydraulic conductivity values between on the order of  $1 \times 10^{-7}$  m/s (Golder 2017).

To facilitate the analysis, the hydraulic conductivity of the cryopeg was conservatively assumed to be equivalent to that of deep bedrock, thereby effectively reducing the thickness of permafrost from 430 m to 280 m. This contrasts with the numerical groundwater model (Golder 2021b), which applied a linear reduction in hydraulic conductivity from the base of the cryopeg to the base of frozen ground.

At depths beyond 120 m, the hydraulic conductivity of the Mafic Volcanic Rock Formations was simulated in the numerical groundwater model to be an order of magnitude lower than the Sedimentary Rock Formations (Table 4-1) according to the distribution of lithological zones shown in Figure 1-1 (Golder 2021b). This analysis utilized the same lithological zones for calculating travel times at depth.

**Table 4-2:  
Tailings seepage analysis parameters and results**

	Units	WES01	WES04	WES05	WN01	PUM01	PUM03
Pit Geometry							
Pit Bottom Elevation <sup>1</sup>	m asl	-10	30	-45	-65	25	-5
Tailings Backfill Elevation <sup>2</sup>	m asl	50	54	47	44	47	49
Tailings Backfill Thickness <sup>3</sup>	m	60	24	92	109	22	54
Area of Tailings Surface <sup>2</sup>	m <sup>2</sup>	76,554	9,447	80,686	166,881	29,697	41,264
Crown Pillar Thickness <sup>4</sup>	m	0	n/a	n/a	10	35	0
Depth of Underground <sup>4,5</sup>	m bgs	652	n/a	n/a	455	162	98
Post-Closure Pit Lake Elevation <sup>4</sup>	m asl	58.0	62.0	64.0	59.0	55.0	59.0
Depth of Water Cover <sup>6</sup>	m	8.0	8.0	17.0	14.6	8.0	10.2
Meliadine Lake Elevation	m asl	51.9	51.9	51.9	51.9	51.9	51.9
Flowpath Originating in Competent Bedrock							
Flowpath Length to Meliadine L. <sup>7</sup>	m	3,020	2,380	1,270	2,630	2,470	3,040
Hydraulic Gradient <sup>8</sup>	(-)	0.002	0.004	0.010	0.003	0.001	0.002
Hydraulic Conductivity <sup>9</sup>	m/s	4.8E-10	2.5E-09	2.4E-09	5.5E-10	3.2E-09	3.2E-09
Porosity <sup>10</sup>	(-)	0.001	0.001	0.001	0.001	0.001	0.001
Flowpath Originating in In-Pit Fault							
Fault Pathway		RM175	n/a	WM-D	RM175	n/a	n/a
Fault Width <sup>10</sup>	m	5	n/a	5	5	n/a	n/a
Fault Strike In Pit <sup>1,11</sup>	m	560	n/a	530	625	n/a	n/a
Flowpath Length to Meliadine L. <sup>7</sup>	m	3,020	n/a	1,980	2,630	n/a	n/a
Hydraulic Gradient <sup>8</sup>	(-)	0.002	n/a	0.006	0.003	n/a	n/a
Hydraulic Conductivity <sup>9</sup>	m/s	5.1E-08	n/a	7.3E-07	5.1E-08	n/a	n/a
Porosity <sup>10</sup>	(-)	0.001	n/a	0.001	0.001	n/a	n/a
Travel Time to Meliadine Lake							
Fastest Travel Time	years	920	7,000	14	590	18,900	12,600
Slowest Travel Time	years	96,200		1,780	56,100		
Contact Water Fluxes							
Intact Bedrock Flowpath	m <sup>3</sup> /d	0.006	0.01	0.17	0.021	0.01	0.027
Fault Flowpath	m <sup>3</sup> /d	0.025	n/a	1.07	0.038	n/a	n/a
Total Contact Water Flux	m <sup>3</sup> /d	0.032	0.009	1.24	0.060	0.011	0.027

**Notes:**

1. Golder (2021d)
2. From Lorax-generated VEAC tables (April 14, 2022) generated from Agnico Eagle (2021d)
3. Tailings backfill elevation minus pit bottom elevation
4. Agnico Eagle (2021d)
5. From Leapfrog File "Geochem\_Samples\_New.Ifview" dated June 20, 2020
6. Post-closure pit lake elevation minus tailings backfill elevation
7. Includes backfilled thickness of pit
8. Difference in head between pit lake and Meliadine Lake divided by flowpath length
9. Distance-weighted harmonic mean of values presented in Golder (2021b) and tailings hydraulic conductivity of  $1 \times 10^{-7}$  m/s (Golder 2017)
10. Golder (2021b)
11. Assumed to be the approximate long diameter of the pit



### *Porosity*

The same value of porosity was used for all faults and competent bedrock ( $n = 0.001$ ) and is consistent with the numerical groundwater model (Golder 2021b). The porosity of tailings was conservatively assumed to be the same as that of faults and competent bedrock.

### *Lake Elevations*

For this analysis, the elevation of the water cover on the tailings was assumed to be equivalent to the pit spill points of the pits. Based on the tailings elevation provided in Table 4-2, the depth of the pit lakes varies from 8 m to 17 m. Lakes of this depth would not freeze to bottom based on analytical methods (Frederking 2018) and site data. An elevation of 51.8 m asl was used for Meliadine Lake, as reported in Agnico Eagle (2021d).

### *Flowpath Length*

Groundwater flowpaths from pit areas to Meliadine Lake are illustrated on Figure 1-1 with distances provided in Table 4-2. Where a pit is situated entirely within competent ground, the flowpath represents the shortest distance to Meliadine Lake, including the depth of tailings backfill, and vertical distance down to and up from the cryopeg.

When a pit is intersected by a fault, two flowpaths were considered: one flowpath in competent rock as described above, and a second flowpath that follows the trace of the fault to Meliadine Lake. In some cases, the flowpath generated from competent sections of the pit wall first travels a short distance in competent bedrock and then deflects along a fault corridor to Meliadine Lake (Section 4.2.2).

### *Cross-sectional Area of Flow*

To compute seepage fluxes from the pits, it was assumed that the cross-sectional area of flow ( $A$ ) is the surface area of the tailings backfill. Where a permeable fault intersects a pit, the cross-sectional area of the fault was considered separately, with the cross-sectional area of the fault defined by the width and strike length provided in Table 4-2.

## **4.3.2 Analytical Results**

### *4.3.2.1 Travel Times*

Travel times for in-pit tailings seepage to Meliadine Lake are presented as a range in Table 4-2. For pits that are intersected by faults (WES05, WN01, WES01), the fastest travel time is associated with the fault flowpath, while the slowest travel time is associated with the flowpath which lies fully (or partially) in competent bedrock. For pits that not

intersected by significant faults (WES04, PUM01, and PUM03), only one travel time is reported, representing the flowpath that lies fully (or partially) in competent bedrock.

Computed travel times are highly sensitive to whether the pit is transected by a fault. Through field investigations and numerical modelling exercises, Golder (2021b,c) has estimated fault hydraulic conductivity to be between one and four orders of magnitude higher than that of deep, competent bedrock (Table 4-1). Pits transected by faults (WES05, WES01, WN01) are associated with travel times between 14 and 920 years (Table 4-2).

Pits located in competent ground (PUM01, PUM03) have travel times ranging between 12,600 and 18,900 years. The flowpath from WES04 is assumed to originate in competent ground and then follow a fault, but the resultant travel time remains very long (7,000 years).

The shortest travel time (~14 years) is associated with WES05 which is transected by the WM-D fault. The quick travel time arises from the combination of a relatively short flowpath length (~1 km), high hydraulic conductivity associated with the WM-D fault, and a relatively large hydraulic gradient created by the high pit lake spill point (Table 4-1, Table 4-2).

#### 4.3.2.2 Seepage Fluxes

Seepage losses computed for the different pit facilities are provided in Table 4-2. The total seepage fluxes for each in-pit tailings facility range from 0.01 m<sup>3</sup>/d to 1.24 m<sup>3</sup>/d, with the highest seepage flux attributed to WES05. The high seepage flux computed for WES05 is largely due to the WM-D fault flowpath (Table 4-2).

Intermediate level seepage fluxes are computed for WN01, WES01 and PUM03 pits (0.03 m<sup>3</sup>/d to 0.06 m<sup>3</sup>/d). For the WN01 and WES01 pits, most of the seepage flux travels via the RM175 fault, with seepage from the competent pit walls ultimately limited by the low mafic volcanic rock hydraulic conductivity encountered along the flowpath. For PUM03, the seepage flux is entirely within competent sedimentary rock, which is more permeable at depth than the mafic volcanic unit (Table 4-1).

PUM01 and WES04 are predicted to generate the least amount of tailings seepage of any of the proposed pits (0.01 m<sup>3</sup>/d).

#### 4.3.3 Discovery Pit Waste Rock Disposal

Deposition of waste rock in the Discovery Pit is also being considered as a waste management option. While this study has focussed on the effects of in-pit tailings storage on Meliadine Lake, the methods can also be applied to evaluate waste rock backfill effects on other receivers. In the case of Discovery Pit, the nearest downgradient receiver is lake

CH6 (Figure 1-1). This potential contamination flowpath has been evaluated here for completeness.

The analytical methods presented in the previous section are unchanged. Hydraulic parameters used in this analysis are summarized in Table 4-3 and are discussed in more detail below.

The Discovery Pit is connected to a deep underground and as such, the conceptual flowpath resembles the middle pane of Figure 4-2. The pit is in close proximity to the Pyke Fault, which is inferred to transect CH6 near its northwest margin (inset Figure 1-1). Thus, the flowpath from Discovery Pit is imagined travelling horizontally from the pit towards CH6, where it is intercepted by the fault and then moves vertically upward to CH6 along the fault trace.

**Table 4-3:**  
**Discovery in-pit waste rock seepage analysis parameters and results**

<b>Discovery Pit Geometry</b>	<b>Unit</b>	<b>Value</b>
Pit Bottom Elevation <sup>1</sup>	m asl	-75
Waste Rock Backfill Elevation <sup>2</sup>	m asl	16
Waste Rock Backfill Thickness <sup>3</sup>	m	91
Area of Waste Rock Surface <sup>4</sup>	m <sup>2</sup>	126,000
Crown Pillar Thickness <sup>5</sup>	m	0
Depth of Underground <sup>5,6</sup>	m bgs	477
Post-Closure Pit Lake Elevation <sup>5</sup>	m asl	67.0
Depth of Water Cover <sup>7</sup>	m	51.5
Meliadine Lake Elevation	m asl	63.6
<b>Flowpath Originating in Competent Bedrock</b>		
Flowpath Length to CH6 <sup>8</sup>	m	546
Hydraulic Gradient <sup>9</sup>	(-)	0.006
Hydraulic Conductivity <sup>10</sup>	m/s	9.2E-09
Porosity <sup>11</sup>	(-)	0.001
<b>Travel Time</b>		
<b>Travel Time to CH6</b>	years	300
<b>Contact Water Fluxes</b>		
Contact Water Flux	m <sup>3</sup> /d	0.63

**Notes:**

1. Golder (2021d)
2. Lorax (2022)
3. Tailings backfill elevation minus pit bottom elevation
4. From Lorax-generated VEAC tables (April 14, 2022) generated from Agnico Eagle (2021d)
5. Agnico Eagle (2021d)
6. From Leapfrog File "Geochem\_Samples\_New.Ifview" dated June 20, 2020
7. Post-closure pit lake elevation minus waste rock backfill elevation
8. Includes backfilled thickness of pit
9. Difference in head between pit lake and lake CH6 divided by flowpath length
10. Distance-weighted harmonic mean of values presented in Golder (2021b) and waste rock hydraulic conductivity of 1x10<sup>-3</sup> m/s
11. Golder (2021b)

To arrive at a distance-weighted harmonic mean hydraulic conductivity for the contaminant flowpath, and thus a seepage velocity, the following values were used:

- A hydraulic conductivity of  $1 \times 10^{-3}$  m/s was used for waste rock over a backfill distance of 91 m;
- The hydraulic conductivity of deep sedimentary rocks ( $3 \times 10^{-9}$  m/s) was used along the horizontal flowpath (~200 m) to the Pyke Fault; and,
- A hydraulic conductivity of  $4 \times 10^{-7}$  m/s (Golder 2021b) was used for the vertical flowpath (280 m) following the Pyke Fault to CH6.

Based on this parameterization of the groundwater flowpath, the contact water flux from Discovery pit is estimated to be  $0.63 \text{ m}^3/\text{d}$  and take approximately 300 years to travel to CH6. This travel time does not include the time for an open talik to form underneath the open pit. For reference, annual baseline runoff to CH6 was reported to be  $1,240,000 \text{ m}^3/\text{yr}$  in the 2014 FEIS (Agnico Eagle 2014). The volumetric seepage flux to CH6 from the Discovery pit amounts to  $<0.02\%$  of the annual runoff to the lake.

#### **4.4 Numerical Flow and Transport Model**

Numerical modelling of contaminant transport to Meliadine Lake was undertaken for the WES05 pit, which through the previous analysis was identified as the least favourable, having the highest seepage flux and shortest seepage travel time to Meliadine Lake. An arbitrary backfilled pit source concentration of 100 mg/L was used to represent a generic parameter of concern, allowing results to be scaled to tailings porewater source term concentrations. While providing transient estimates of loads to Meliadine lake, this analysis also served to check volumetric fluxes and travel times computed in the mathematical analysis.

##### **4.4.1 Modelling Methods**

Two cross-sectional groundwater flow and transport models were constructed in FEFLOW Version 7.2 (DHI, 2022), representing the flow pathways along the WM-D and WM-B faults (Figure 1-1). The models simulate the groundwater system as an equivalent porous medium. The models were constructed to closely emulate the flowpaths described in the mathematical analysis presented in Section 4.3. Annotated cross-sections of these two flowpaths, based on the conceptual model presented in the upper pane of Figure 4-2, are presented in Figure 4-3.

#### 4.4.1.1 *Model Domain*

The flow and transport model domains are shown in Figure 4-4. Both cross-sectional models cover the full representative width of the backfilled pit and extend one kilometre into Meliadine Lake (Figure 4-3, Figure 4-4).

Since the WM-D fault essentially transects the WES05 pit along its long axis (Figure 1-1), the representative pit width for the WM-D cross-section is the long axis of the pit (~530 m) (Figure 4-3). For the WM-B flowpath, the representative cross-section is the average width of the pit perpendicular to the long axis of the pit (~250 m) (Figure 4-3).

Both model domains extend to 1000 m depth. The WM-D and WM-B model domains comprise 266,896 and 174,862 triangular elements, respectively. The ground surface elevation in each model is defined on the left-hand side by the elevation of bedrock in WES05 (~70 m asl) and on the right-hand side by the elevation of Meliadine lake (51.9 m asl). Ground surface between the two areas is assumed to decrease linearly.

#### 4.4.1.2 *Model Boundary Conditions*

The following boundary conditions were applied in the numerical groundwater flow and transport models:

- A no-flow boundary was assigned to the base and left hand and right hand sides of the model domain.
- A constant head boundary condition was applied to the tailings backfill surface with an elevation head of 64 m asl. The depth of the pit lake over which this boundary was applied was 17 m. An arbitrary constant source concentration of 100 mg/L was applied in tandem with this boundary condition.
- A constant head boundary condition was applied to Meliadine Lake equivalent to 51.9 m. The depth of the lake over which this boundary was applied was 10 m. For the transport model, Meliadine Lake was assigned as an exit or Cauchy boundary, in which the mass transfer rate is naturally calculated from the flux rate based on the flow equation. This allows the groundwater mass flux to exit the model domain according to the predicted groundwater quality in the area immediately beneath the Meliadine lake.
- Elements representing frozen ground were deactivated.

#### 4.4.1.3 *Model Settings*

The flow models were run in steady-state mode assuming confined conditions (*i.e.*, operated in free surface mode). The transport models were run transiently using the steady-state flow solution. Both transport simulations used automated time-stepping. The WM-D and WM-B simulations were run for 200 years and 30,000 years, respectively.

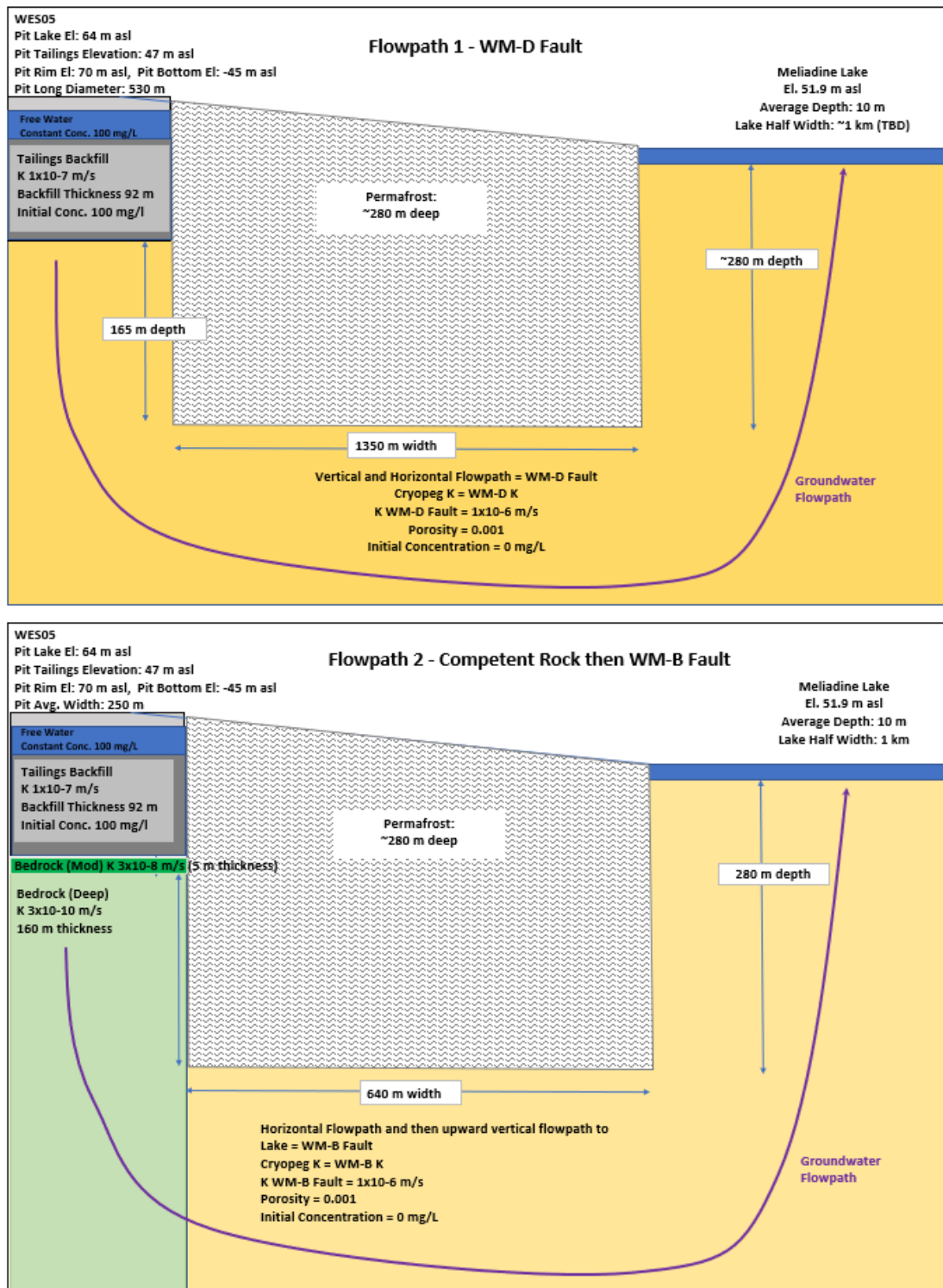
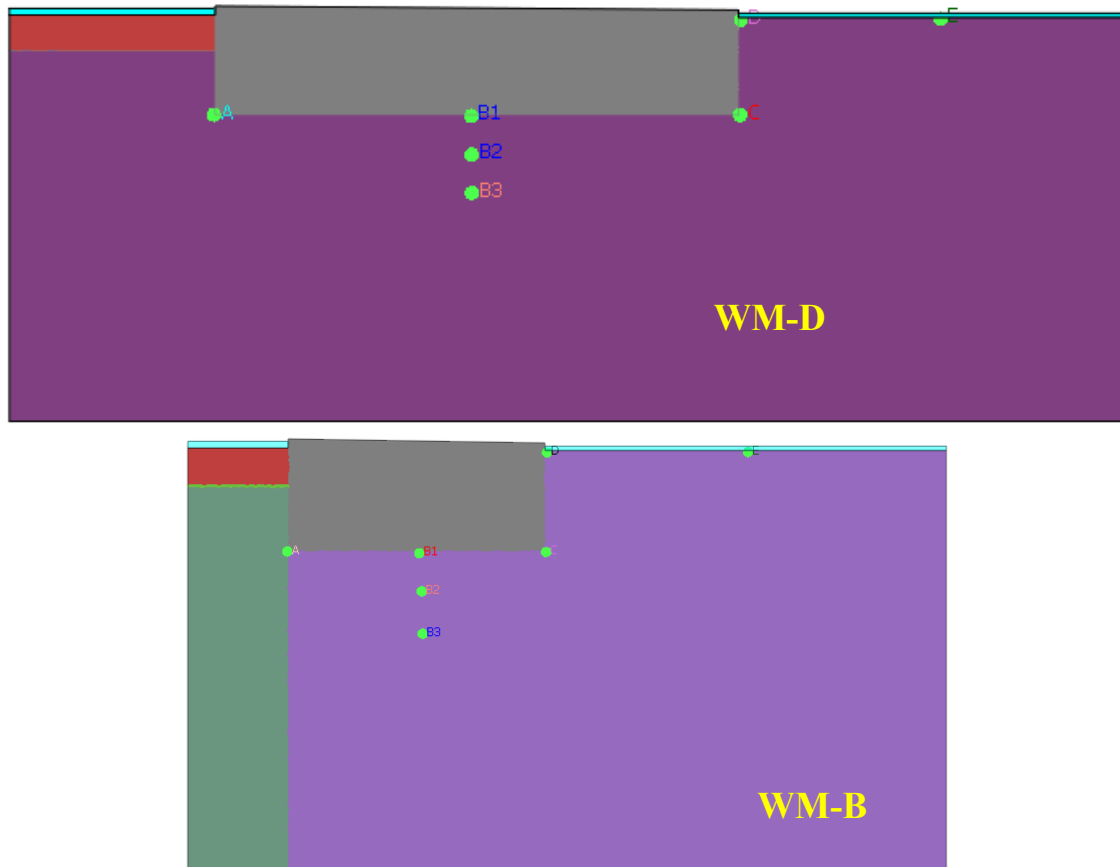


Figure 4-3: Cross-section of WES05 flowpath along WM-D (top pane) and WM-B (bottom pane) fault paths used to parameterize the 2D numerical flow and tranport models.



**Figure 4-4:** WES05 flow and transport model setup for WM-D (top pane) and WM-B (bottom pane) fault flow paths. Dots represent concentration prediction points A, B1, B2, B3, C, D and E.

#### 4.4.1.4 Model Parameterization

The hydraulic conductivity of tailings, competent rock and faults are shown on Figure 4-3

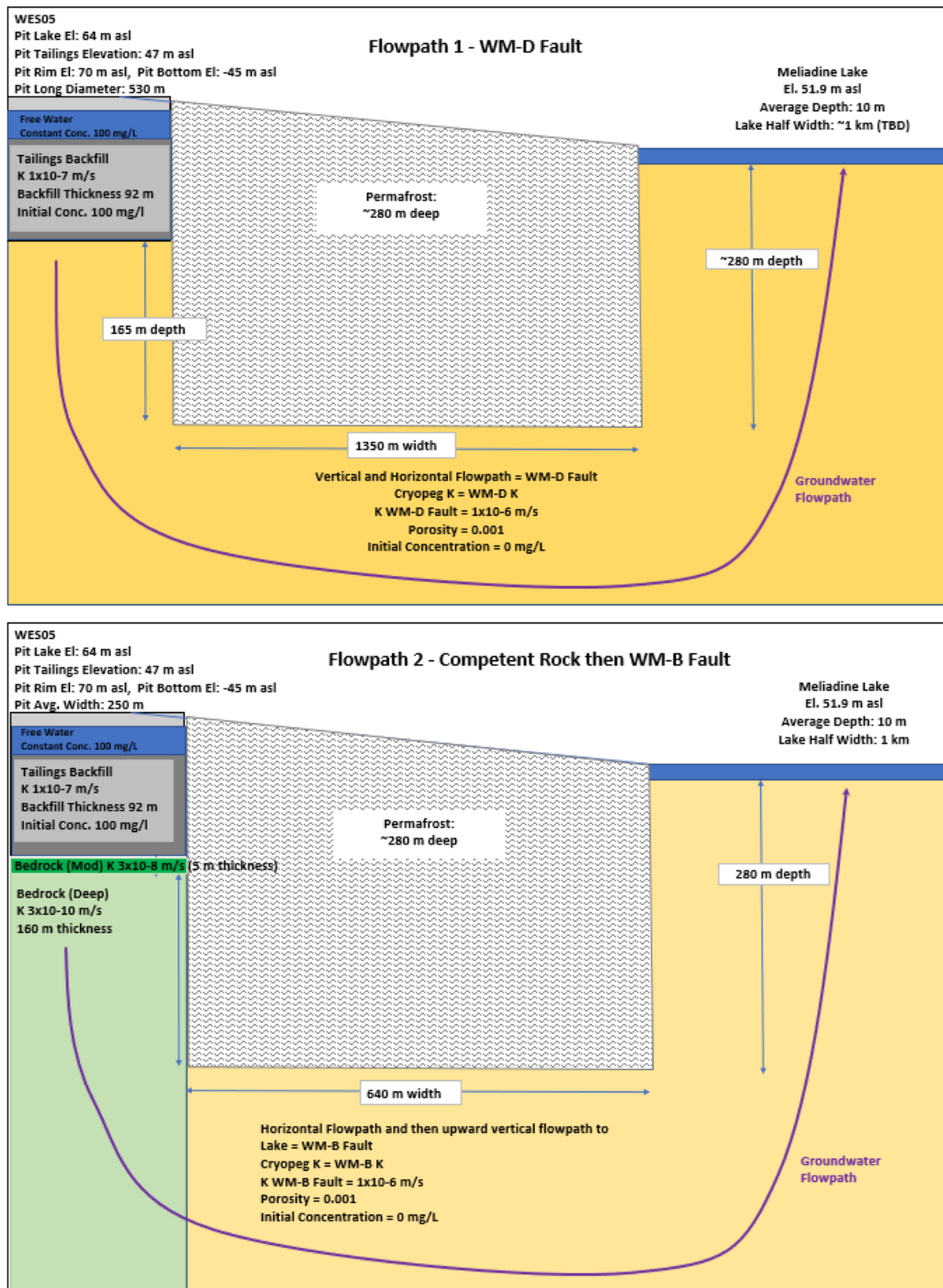




Figure 4-3 and follow values presented in Table 4-1 and Table 4-2. The model utilizes a highly simplified pit morphology, *i.e.*, a rectangle with bottom elevation equivalent to the bottom of the pit (-45 m asl). This significantly overestimates the size of the pit and volume of backfilled tailings and is highly conservative. The transport model simulates physical processes (advection and dispersion) but ignores geochemical processes (sorption/desorption, precipitation/dissolution, and degradation). The model also does not consider density effects. The transport simulations utilized the following additional transport parameters:

- A tailings effective porosity of 0.20;
- A faulted and non-faulted bedrock effective porosity of 0.001 (Table 4-2);
- Longitudinal and vertical dispersivity values of 15 m and 5 m;
- An initial concentration in the tailings backfill of 100 mg/L; and,
- A background concentration of 0 mg/L.

#### 4.4.2 Modelling Results

Key results from the WES05 flow and transport models are summarized in Table 4-4 and discussed below.

**Table 4-4:**  
**Simulated flow and transport model results for WES05 pit**

Simulated Result	Units	WM-D Flowpath	WM-B Flowpath	Total
Volumetric Flux	m <sup>3</sup> /d	1.02	0.16	1.18
Arbitrary Constant Source Concentration	mg/L	100	100	n/a
First Arrival Time in Meliadine L. (10 mg/L) <sup>1</sup>	yr	8.5	2,930	n/a
First Arrival Time in Meliadine L. (50 mg/L) <sup>1</sup>	yr	14.5	3,750	n/a
First Arrival Time of Max. Conc in Meliadine L. (98 mg/L) <sup>1</sup>	yr	25	>5,000	n/a
Steady-State Mass Flux	kg/yr	37.5	5.8	43.3

**Notes:**

n/a – not applicable

1. Does not include time for open talik to form underneath backfilled pit.

##### 4.4.2.2 Volumetric Fluxes

The model simulates a total volumetric flux entering the groundwater system from the backfilled WES05 pit of 1.18 m<sup>3</sup>/d with the breakdown by flowpath shown in Table 4-4. The fluxes computed by the flow model are nearly identical to the fluxes computed in

previous mathematical analysis (Table 4-2). This suggests that volumetric fluxes computed for other pits, which have not been simulated in a numerical model, are reasonable.

#### *4.4.2.3 Concentrations*

Concentration time series (Figure 4-5) have been extracted for several points in both model domains shown on Figure 4-4. Snapshots of contaminant plume migration over various time steps are shown for the WM-D and WM-B flowpaths in Figure 4-6 and Figure 4-7, respectively. Note that transport years discussed in the following sections do not include the time for an open talik to form underneath the backfilled pits. According to the thermal analysis presented in Section 3.5, the earliest that an open talik would form beneath the WES05 pit under a wet cover conditions is 62 years.

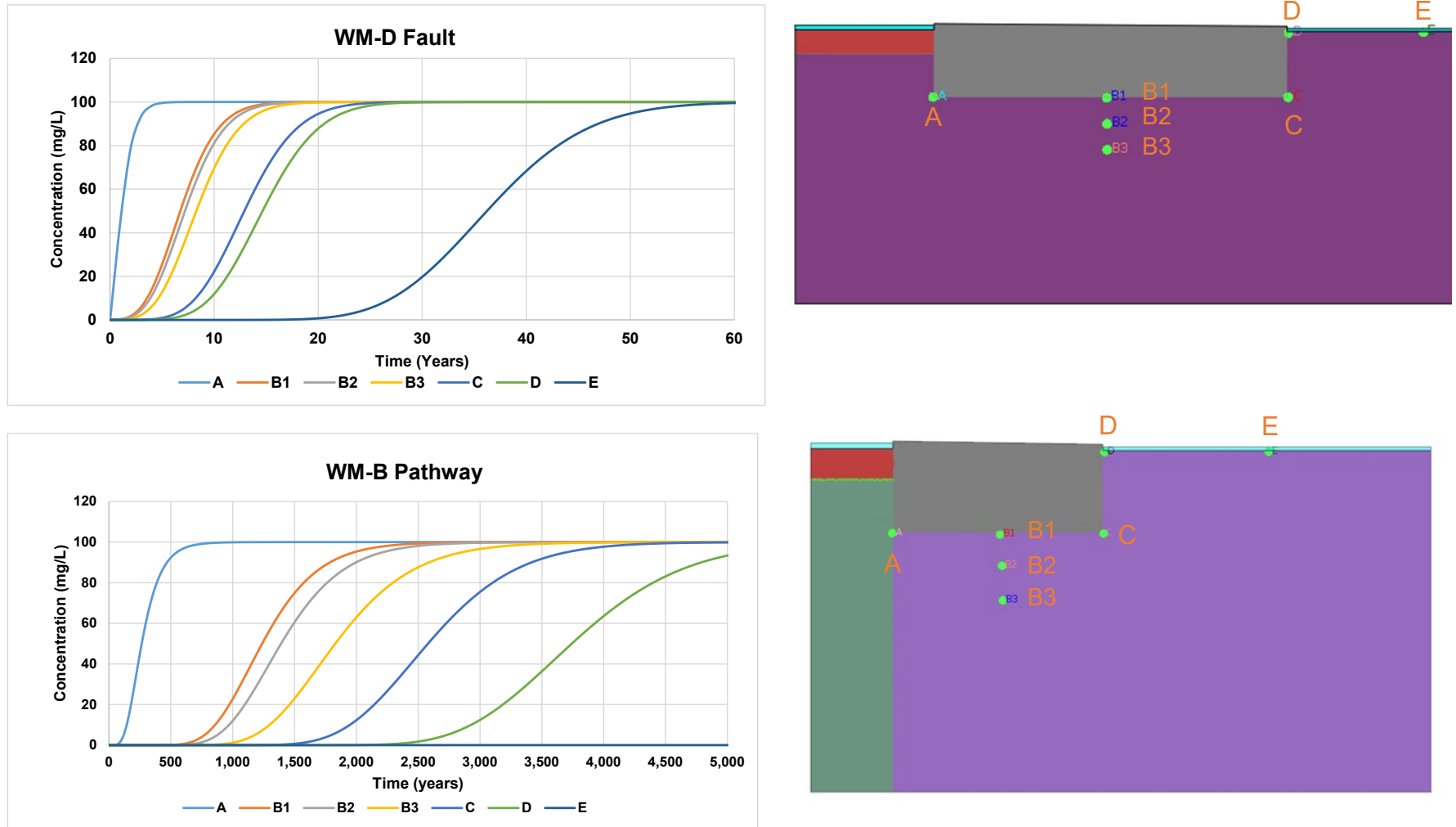
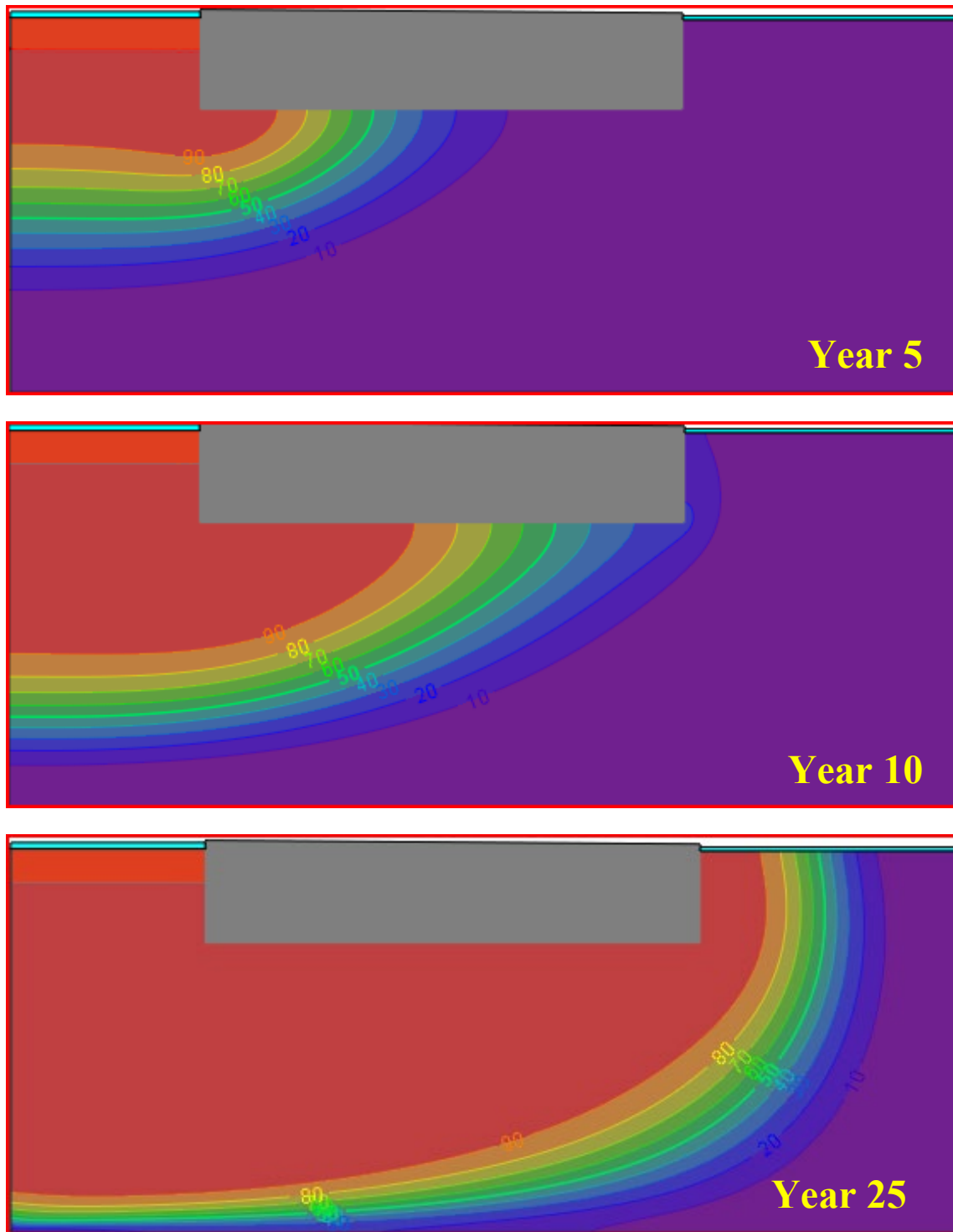
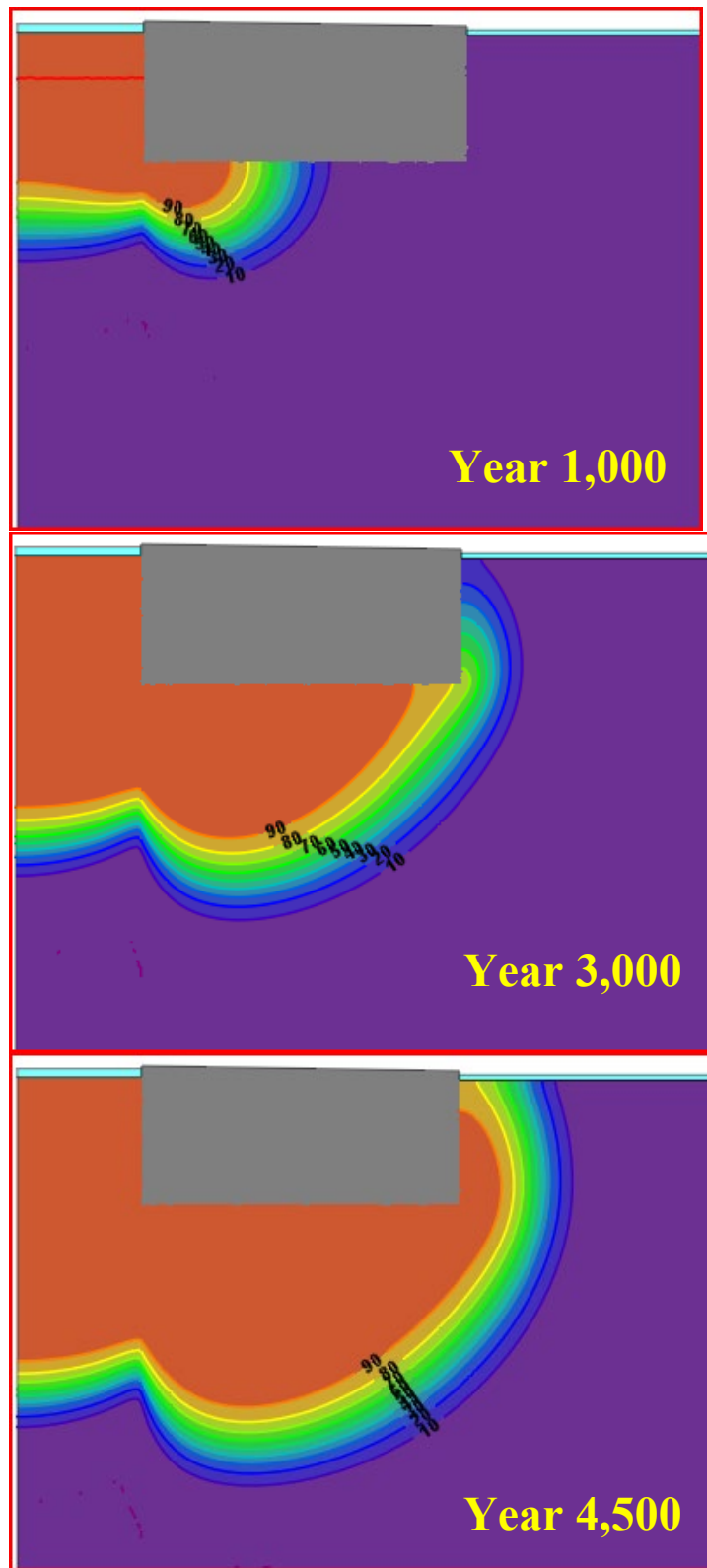


Figure 4-5: Concentration versus time for WES05 WM-D (top pane) and WM-B (bottom pane) fault flow paths. Location of prediction points shown on right hand side. Source concentration is 100 mg/L.



**Figure 4-6: Simulated concentrations for WES05 WM-D flowpath after 5, 10 and 25 years. Source concentration is 100 mg/L.**



**Figure 4-7:** Simulated concentrations for WES05 WM-B flowpath after 1,000, 3,000 and 4,500 years. Source concentration is 100 mg/L.

The plume travelling along the WM-D flowpath migrates to the bottom of permafrost within a year (Line A, upper pane of Figure 4-5). First arrival of the plume in Meliadine Lake occurs close the lateral limit of permafrost at Point D. As defined by the 10 mg/L concentration contour, first arrival of the plume occurs 8.5 years after the start of the simulation (opening of the talik). The arrival time of the 50 mg/L plume (*i.e.*, 50% of the source concentration) is 14.5 years and 25 years for the 100 mg/L plume (*i.e.*, full source concentration) (lower pane Figure 4-6). This illustrates the effect of dispersion on the plume. The arrival time of the 50% concentration is essentially consistent with arrival time computed in the mathematical analysis (14 years, Table 4-2) which only considered advective flow.

The model simulates significantly slower plume migration along the WM-B flowpath (Figure 4-7). The plume must first travel downward through competent bedrock before reaching the fault. This downward migration of the plume to the base of permafrost is predicted to take nearly 150 years, as defined by the 10 mg/L concentration at point A (line A, bottom pane Figure 4-5). First arrival of the plume in Meliadine Lake is predicted to occur after 2,900 years, as defined by the 10 mg/L concentration at point D (upper pane Figure 4-7). The arrival times for the 50 mg/L and 100 mg/L concentration in Meliadine Lake along the WM-B flowpath are 3,759 years and >5,000 years. The simulated travel times for first arrival are longer but of a similar order of magnitude than those computed by the mathematical analysis (1,780 years, Table 4-2), suggesting that relative effect of dispersivity is larger for less permeable groundwater flowpaths.

#### 4.4.2.4 Loading Rates

Loading rates from the backfilled WES05 pit and to Meliadine Lake are shown for the WM-D and WM-B flowpaths in Figure 4-8 and Figure 4-9, respectively. It takes around 100 years before the loading rate stabilizes at its maximum of 37.5 kg/yr along the WM-D flowpath (Figure 4-8). The loading rates from the WM-B flowpath is simulated to still be climbing towards its maximum level (5.8 kg/yr) at the end of the simulation (30,000 years).

Figure 4-10 illustrates the combined loading rates and cumulative loads to Meliadine Lake from both WM-D and WM-B flowpaths. Loading rates are essentially stable at 37.5 kg/yr until ~3,000 years, at which point contributions from the WM-B flowpath cause the curve to deflect upwards. Ultimately, the long-term (*i.e.*, >30,000 year) steady-state loading rate to Meliadine Lake from the backfilled WES05 pit is 43.3 kg/yr.

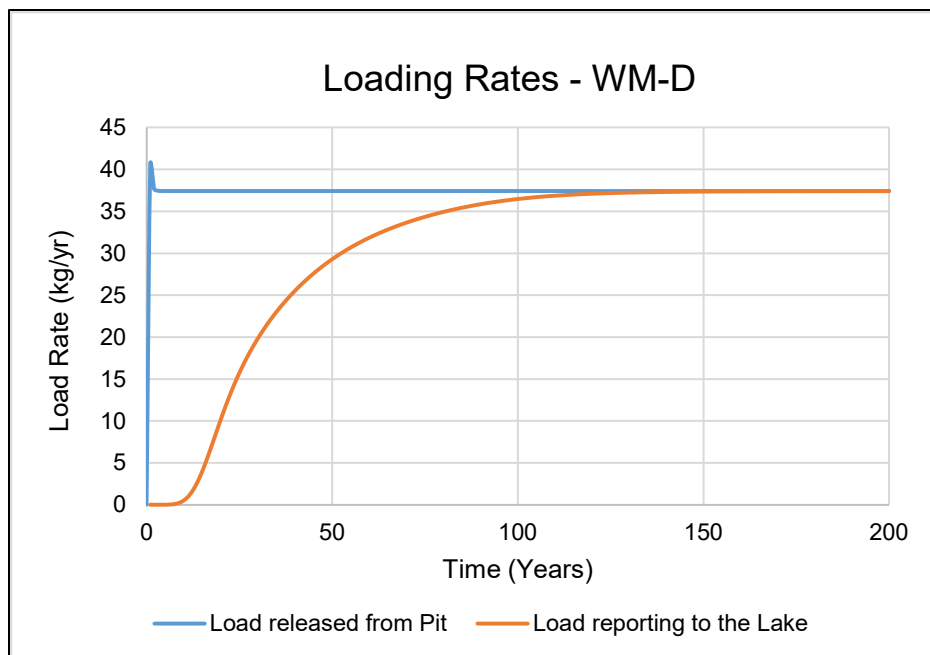


**Figure 4-8: Simulated loading rates for WM-D flowpath assuming a constant source concentration of 100 mg/L.**

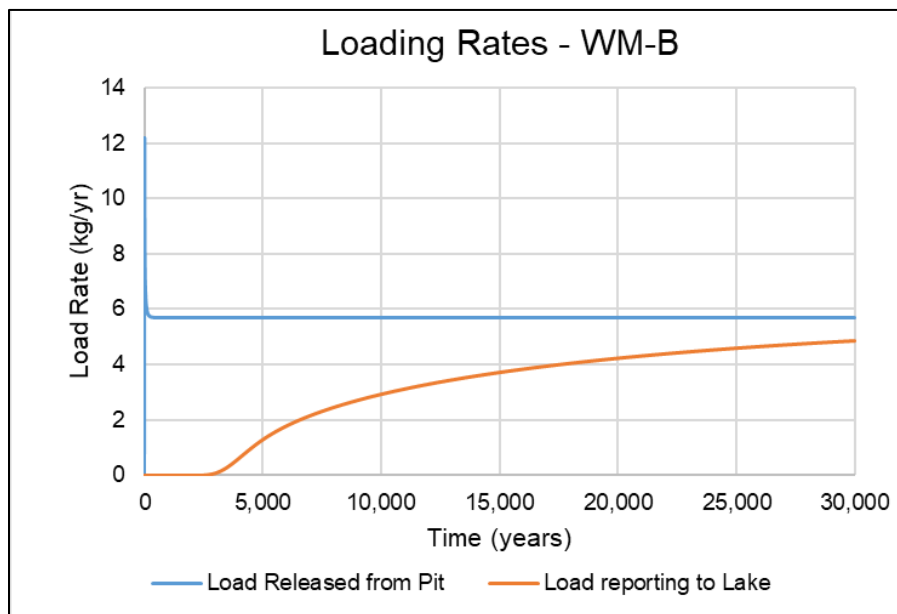


**Figure 4-9: Simulated loading rates for WM-B flowpath assuming a constant source concentration of 100 mg/L.**

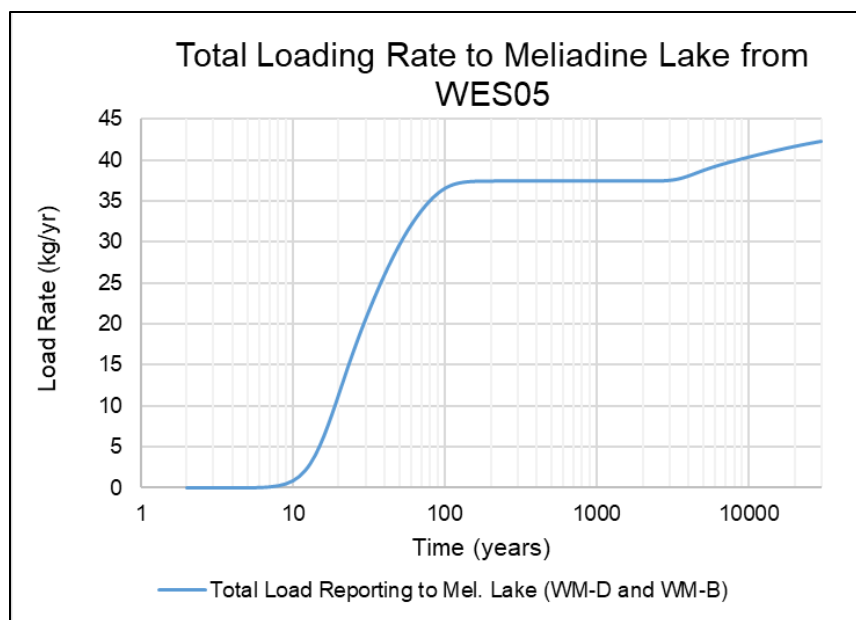


**Figure 4-10: Simulated combined loading rates and cumulative loads to Meliadine Lake from the WM-D and WM-B flowpaths assuming a constant source concentration of 100 mg/L.**

#### 4.4.3 Parameters of Concern

The results from the transport models can be applied to specific potential contaminants of concern (PCOCs) by scaling the transport simulation results for the generic 100 mg/L source term to the PCOC concentration. Estimated tailings porewater chemistry has been compared to average groundwater quality in Table 4-5 to identify PCOCs for the groundwater flowpath to Meliadine Lake.

Average groundwater quality has been computed from 2019 to 2021 samples collected from underground diamond drillhole (DDH) water intersects (Table 4-5). These samples are considered representative of non-contact groundwater (Agnico Eagle 2022). A tailings porewater source term has been derived by Lorax (2022) utilizing process water chemistry from metallurgical testing completed in support of the Meliadine 2014 FEIS (Agnico Eagle 2014), analogue data from the Meadowbank Mine, and Meliadine groundwater water chemistry.

Nine parameters in the tailings porewater source term are identified as PCOCs as they are elevated compared to groundwater concentrations: cyanide, weak acid dissociable (WAD) cyanide, fluoride, ammonia-nitrogen total phosphorous, arsenic, cobalt, copper and selenium. Concentrations of arsenic, ammonia-nitrogen, and cyanide species are at least ten times higher in the tailings porewater source term than in groundwater (Table 4-5). Most groundwater samples have below detection limit values for metals, fluoride, and to a lesser extent, total phosphorous.



**Table 4-5:  
Potential Contaminants of Concern In Tailings Seepage**

Parameters	Count Groundwater Samples 2019-2021	Groundwater Average (2019-2021) <sup>1</sup> (mg/L)	In-Pit Tailings Porewater Source Term <sup>2,3</sup> (mg/L)	In-Pit Discovery Waste Rock Porewater Source Term <sup>2,3</sup> (mg/L)
TDS	88	55,680	3,488	36.5
Chloride	88	31,193	300	8.34
Cyanide	1	0.01	<b>0.76</b>	
Cyanide (WAD)	1	0.0013	<b>0.05</b>	
Fluoride	70	0.10	0.12	0.156
Sulfate	88	3,066	1649	4.03
Ammonia Nitrogen	68	8.22	<b>85.5</b>	0.276
Total phosphorus	68	0.12	0.175	0.0035
Antimony	85	0.03	0.021	0.000239
Arsenic	85	0.01	<b>3.58</b>	0.0146
Cadmium	85	0.00057	0.00004	0.00000595
Chromium	85	0.058	0.005	0.0003
Cobalt	85	0.0114	0.0962	0.0000546
Copper	85	0.012	0.061938	0.00094
Lead	85	0.012	0.000529	0.0000797
Manganese	85	0.996	0.0248	0.00165
Nickel	85	0.06	0.00894	0.00066
Selenium	85	0.0057	0.014	0.00036
Sodium (Dissolved)	86	14,542	811	6.45
Uranium	85	0.0057	0.003633	0.000113
Zinc	85	0.29	0.0022	0.00144

**Notes:**

1. Samples collected from underground drillhole intersects between 2019 and 2021. Analyses are included in Meliadine annual monitoring reports (e.g. Agnico Eagle (2022))
2. Shading indicates source term concentration is higher than groundwater, bold indicates source term concentration is ten times higher than groundwater
3. Lorax (2022)

A source term for Discovery waste rock porewater, also developed by Lorax (2022), has been included in Table 4-5 for comparison. The waste rock porewater source term has overall lower concentrations than the tailings porewater source term with exception to fluoride. Only fluoride and arsenic are higher in the waste rock porewater source term than in groundwater. Therefore, from a geochemical loading perspective, flooded mine tailings represents a conservative case for flooded mine waste.

Potential long-term loads to Meliadine Lake from tailings backfilled into WES05 have computed for the nine PCOCs identified above for both short-term and long-term loading maxima (Table 4-6). The short-term maximum represents the load traveling along the WM-D flowpath after 100 years, while long-term maximum represents the maximum combined load from WM-D and WM-B flowpaths. These loads have been computed by scaling the numerical transport simulation results for the 100 mg/L generic source term. Since the backfilled WES05 pit represents the worst case for seepage fluxes and travel times, all other pits examined in the mathematical analysis would be expected to produce smaller loads.

The loads reported in Table 4-6 are not anticipated to result in observable changes to water quality in Meliadine Lake. For reference, annual baseline runoff to Meliadine Lake was reported to be 84,700,000 m<sup>3</sup>/yr in the 2014 FEIS (Agnico Eagle 2014). The volumetric seepage flux to Meliadine Lake from WES05 (450 m<sup>3</sup>/yr or 1.18 m<sup>3</sup>/d) amounts to 0.0005% of the annual runoff to the lake. Even with the addition of other pit volumetric seepage fluxes (50 m<sup>3</sup>/yr or 0.14 m<sup>3</sup>/d, Table 4-2), the proportion of combined pit seepage fluxes to annual runoff to the lake remains below 0.0006%.

**Table 4-6:**  
**Steady-state PCOC Groundwater Loads to Meliadine Lake from WES05**

PCOC	Source Concentration (mg/L)	Short-Term Maximum Load to Meliadine L. <sup>1</sup> (t = 100 years) (kg/yr)	Long Term Steady-State Load to Meliadine L. <sup>2</sup> (t >30,000 years) (kg/yr)
Generic Parameter <sup>1</sup>	100	37.5	43.3
Cyanide	0.76	0.29	0.33
Cyanide (WAD)	0.05	0.019	0.022
Fluoride	0.12	0.045	0.052
Ammonia Nitrogen	85.5	32.1	37.0
Total phosphorus	0.175	0.066	0.076
Arsenic	3.58	1.34	1.55
Cobalt	0.0962	0.036	0.042
Copper	0.061938	0.023	0.027
Selenium	0.014	0.005	0.006

**Notes:**

1. As simulated along the fastest (WM-D) flowpath
2. For combined WM-D and WM-B flowpaths

#### **4.5 Conservatism, Uncertainty, and Limitations**

The mathematical and numerical groundwater analyses presented herein have followed a simplified but conservative approach to provide a transparent and defensible basis on which to evaluate the suitability of different pits for tailings disposal. Typical of groundwater analyses of this scale and in this type of environment, there is uncertainty surrounding the values of key parameters:

- Bedrock and fault hydraulic conductivity values used in this analysis were based on a groundwater model calibrated to hydraulic stresses measured in and surrounding the Tiriganiaq pits and underground. Hydraulic conductivity of bedrock and faults farther afield has not been tested. Hydraulic conductivity can commonly vary over orders of magnitude.
- The porosity bedrock, tailings and faults was not constrained in the groundwater model and can also vary over orders of magnitude.
- The tailings hydraulic conductivity used both analyses is based on small-scale laboratory testing of short duration. Tailings hydraulic conductivity can vary with lateral and vertical position within the facility and is expected to decrease with depth (Smith 2020). Specific to WES05, seepage fluxes reporting along the WM-D fault flowpath are sensitive to the hydraulic conductivity of tailings since the fault is more permeable than the tailings. This is less critical for other pits as the tailings hydraulic conductivity is higher than the adjacent bedrock or fault.
- The tailings porewater source term is significantly less saline than groundwater concentrations (3,500 mg/L versus 56,000 mg/L TDS, respectively). Density effects on groundwater flow arising from contrasts in groundwater and tailings porewater salinity have not been considered but are anticipated to be small and in favor of limiting downward migration of the contaminant plume.

The seepage rates and travel times computed in both the mathematical and numerical analyses are considered conservative for several reasons:

- Faults were assumed to be laterally extensive and consistently permeable along strike.
- The cryopeg was treated as permeable as deep unfrozen bedrock. This effectively reduced the thickness of permafrost from 430 m to 280 m in the analysis, which shortened the vertical component of the groundwater flowpath from any pit to Meliadine Lake.

- Seepage that reaches flooded underground mine voids was assumed to instantaneously travel through open developments to the nearest segment of the undisturbed groundwater flowpath towards Meliadine Lake. The lateral extents of the workings were not considered.
- Both mathematical and numerical analyses assume that an open talik has formed and that the groundwater system is at steady-state, thus the travel times ignore the time for an open talik to form and for the groundwater system to achieve equilibrium conditions.

Specific to the numerical transport model simulations, the following conservative assumption applies:

- The backfilled pits are considered a constant source of contaminant loads throughout post-closure. No exhaustion of geochemical sources is applied nor mechanisms of geochemical attenuation along the flowpath implemented.

#### **4.6 Summary**

The groundwater analyses have revealed the following insights into in-pit tailings disposal at the Meliadine Mine:

- Travel times and seepage fluxes are highly sensitive to whether a pit is directly transected by a permeable fault. When the fault hydraulic conductivity exceeds tailings hydraulic conductivity, the tailings hydraulic conductivity imparts a large influence on volumetric seepage fluxes.
- The shortest travel times for pit tailings seepage, computed via the mathematical analysis, are as follows: WES05 (14 years), WN01 (590 years), WES01 (920 years), WES04 (7,000 years), PUM03 (12,600 years) and PUM01 (18,900 years).
- Total seepage fluxes for the different pit facilities, computed via the mathematical analysis, are as follows: WES05 (1.24 m<sup>3</sup>/d), WN01 (0.06 m<sup>3</sup>/d), WES01 (0.032 m<sup>3</sup>/d), PUM03 (0.027 m<sup>3</sup>/d), PUM01 (0.011 m<sup>3</sup>/d) and WES04 (0.009 m<sup>3</sup>/d).
- The 2D numerical groundwater flow and transport models constructed for the WES05 pit simulated a total seepage flux of 1.18 m<sup>3</sup>/d, essentially reproducing the seepage flux computed by the mathematical analysis (1.24 m<sup>3</sup>/d). This would suggest that volumetric fluxes computed for other pits, which have not been simulated in a numerical model, are reasonable.
- The shortest simulated travel time for WES05 seepage to Meliadine Lake is 8.5 years, as indicated by arrival of a 10 mg/L concentration at an observation point

near the shore of the lake. The arrival time of the 50 mg/L and 100 mg/L plumes at the same prediction point are 14.5 years and 25 years, respectively. This illustrates the effect of dispersion on the plume. The arrival time of the 50% concentration is essentially consistent with arrival time computed in the mathematical which only considered advective flow.

- The plume traveling along the faster (WM-D) flowpath reaches its maximum loading rate after 100 years. The load traveling the slower flowpath (WM-B) takes around 3,000 years to materialize in Meliadine Lake. The maximum combined load from both flowpaths to Meliadine Lake (43.3 kg/yr, based on a generic source concentration of 100 mg/L) is predicted occur after 30,000 years.
- A comparison of average groundwater quality to tailings porewater source term concentrations revealed nine PCOCs that are higher in tailings seepage than groundwater: cyanide, WAD cyanide, fluoride, ammonia-nitrogen total phosphorous, arsenic, cobalt, copper and selenium. Incidentally, the tailings porewater source term is has overall higher concentrations that the Discovery waste rock porewater source term with the exception of fluoride.
- Steady-state loading rates for WES05 tailings seepage for the most elevated PCOCs, scaled from the simulated results for a generic PCOC of 100 mg/L concentration, are: arsenic (1.55 kg/yr), cyanide (0.33 kg/yr), WAD cyanide (0.022 kg/yr) and ammonia-nitrogen (37 kg/yr).
- Several layers of conservatism have been incorporated in to the mathematical analysis and numerical modelling to simplify the groundwater system and contaminant transport. Results presented in this analysis are considered to be highly conservative.

## ***5. Pit Suitability for Tailings Deposition***

---



**AGNICO EAGLE**

## 5. Pit Suitability for Tailings Deposition

The groundwater analysis discussed in the previous chapter estimated seepage losses from the backfilled pits and associated travel time to Meliadine Lake. This analysis was predicated on the groundwater system having recovered from mining and open taliks having formed beneath tailings disposal facilities. Based on these assumptions, a proposed ranking of pits was developed as shown in Table 5-1.

A point total was computed for each pit based on the ratio of travel time to seepage flux. The pit with the highest point total presents the best option for tailings deposition, based solely on groundwater outcomes. Pit tailings storage volumes are presented in Table 5-1 for reference but are not incorporated into the ranking. Other operational details (*i.e.*, sequencing of pits in the mine plan, distance from mill, *etc.*) have not been considered.

According to the methods described above, PUM01 and WES04 are the pits best suited for tailings disposal in that they are predicted to generate very small amounts of seepage which will take thousands of years to arrive at Meliadine Lake. These pits, however, have the smallest tailings storage capacity (Table 5-1). PUM03 and WES01, are of intermediate ranking but can accommodate larger tailings volumes. While WN01 and WES05 offer more storage capacity than other pits considered for tailings disposal, higher seepage rates and faster travel times position these two facilities at the bottom of the ranking.

**Table 5-1:**  
**Ranking of pit suitability for tailings deposition based on groundwater outcomes.**

Pit	Tailings Backfill Volume (m <sup>3</sup> )	Total Seepage Loss (m <sup>3</sup> /d)	Fastest Travel Time <sup>1</sup> (yr)	Groundwater Point Total (Travel Time/Seepage Loss)	Groundwater Outcome Rank
PUM01	375,218	0.011	18,900	1,793,562	1
WES04	126,226	0.009	7,000	790,970	2
PUM03	1,027,283	0.027	12,600	470,147	3
WES01	2,340,568	0.032	920	28,953	4
WN01	7,162,482	0.060	590	9,881	5
WES05	2,936,368	1.24	14	11	6

**Note:**

1. Based on results of the mathematical analysis presented in Section 4.3.

The ranking of pits provided in Table 5-1 is based on backfilled pits maintaining water covers at the pit spill point and the pits subsequently forming open taliks (except WN01, which already resides within an open talik). The travel times do not include the recovery time for the groundwater system to reach a post-closure equilibrium, nor do they include the time for open taliks to form.

The ranking of these facilities is subject to change depending on how the facilities are operated and closed. Tailings deposition scenarios that promote heat loss from the tailings during operations will prolong formation of open taliks, while emplacement of dry covers could potentially prevent open taliks from forming or remaining open long term. For instance, slow tailings deposition in combination with dry cover placement on WES05 could nearly eliminate seepage from this facility thereby making it a preferred option for tailings disposal.

The rankings provided herein describe relative risk between pits and not absolute risk to the receiving environment with all other loading pathways considered (*i.e.*, surface water). Through other ongoing studies, Agnico Eagle may find that the groundwater loads associated with in-pit tailings disposal are relatively small compared to other loading pathways, and, in fact, all pits are tenable options for tailings disposal.



## **6. *Conclusions***

---



**AGNICO EAGLE**

## 6. Conclusions

---

Agnico Eagle is evaluating in-pit deposition of slurry tailings in six different open pits in support of a pre-feasibility study and permitting of the Meliadine Extension. In this study, thermal modelling was undertaken to determine effects of in-pit tailings disposal on permafrost while a groundwater analysis was conducted to quantify the magnitude of potential impacts on surface water receptors (*i.e.*, Meliadine Lake).

### 6.1 Thermal Modelling

Thermal modelling was undertaken on two proto-typical pits, WES05 and WN01, to assess the sensitivity to physical parameters to which talik development or depletion below backfilled pits are particularly sensitive. The main findings of simulations on WES05, a circular pit situated in permafrost, are summarized as follows:

- Deposition of relatively warm in-pit tailings (+1°C) in WES05 that are water-covered after pit closure slowly warm the underlying permafrost, causing an open talik (based on a -3.4°C freezing temperature, which corresponds to a bedrock groundwater TDS concentration of 60,000 mg/L) to develop about 62 years after pit closure.
- Likewise, deposition of relatively warm in-pit tailings (+1°C) in WES05 followed by dry cover placement was also predicted to form an open talik after several decades, however, the talik was predicted to close about 360 years after pit closure.
- Deposition of relatively cold in-pit tailings (-1°C) in WES05 that are water-covered after pit closure was predicted to form an open talik after about 390 years.
- Deposition of relatively cold in-pit tailings (-1°C) in WES05 that are followed by dry cover placement after pit closure was predicted to *not* form an open talik.

The main findings of simulations on WN01, an elongate pit situated in an existing open talik, are summarized as follows:

- Excavation of the WN01 pit over four years was predicted to cause frost penetration in the pit walls and floor of approximately 20 m based on a 0°C freezing temperature or approximately 7 m based on the -3.4°C freezing temperature (the latter freezing temperature corresponding to a TDS concentration of 60,000 mg/L in the bedrock groundwater). These two freezing temperatures correspond to the full spectrum of TDS concentrations in the groundwater at the Meliadine Project.

- Deposition of relatively warm tailings (+1°C) in WN01 that are water-covered after pit closure was predicted to re-open the talik within 5 years of tailings deposition based on a -1°C freezing temperature (corresponding to an anticipated tailings porewater TDS concentration of 18,000 mg/L).
- Deposition of cold in-pit tailings (-1°C) in WN01 that are water-covered after pit closure was predicted to re-open the talik within 20 years of tailings deposition based on a -1°C freezing temperature.

Overall, the findings of the thermal analysis indicate that for tailings deposited in pits sited in permafrost, the permafrost is best preserved when tailings are deposited in a mostly frozen state, and when a dry cover is used. For pits sited in existing open taliks that will be water-covered at closure, deposition of tailings in a mostly frozen state will prolong the period before an open talik is re-established.

## **6.2 Groundwater Seepage Analysis**

The groundwater analysis was undertaken in two stages to assess groundwater travel times and seepage fluxes from pits considered for tailings backfill under the presumption that the pits are water-covered upon closure and open taliks have formed. The first stage comprised a mathematical analysis using fundamental analytical solutions while the second stage comprised a simplified 2D numerical flow and transport modelling exercise for the pit with the least favorable outcomes. The main findings of the groundwater analysis are:

- The lowest seepage fluxes were calculated for PUM01 and WES04 pits (0.01 m<sup>3</sup>/d). Both the pits are located within competent ground; however, the seepage flowpath from WES04 is predicted to ultimately intercept and travel along a fault. The seepage travel time to Meliadine Lake is 18,900 years for PUM01 and 7,000 years for WES04.
- WN01, WES01 and PUM03 pits also produce a relatively low amount of seepage (0.03 m<sup>3</sup>/d to 0.06 m<sup>3</sup>/d). WN01 and WES01 pits are transected by a relatively permeable fault, RM175, which expedites seepage travel times to Meliadine Lake. Travel times along the RM175 fault to Meliadine Lake are 590 and 920 years for WN01 and WES01, respectively. PUM03 is not transected by a fault and as a result, seepage from this facility has a much longer travel time to Meliadine Lake (12,600 years).
- WES05 was estimated to generate the most (1.24 m<sup>3</sup>/d) and fastest traveling seepage (14 years) of any facility towards Meliadine Lake. WES05 is transected by highly a permeable fault (WM-D), and has a higher spill point with supports a

steeper hydraulic gradient towards Meliadine Lake. This is compounded by a shorter flowpath to Meliadine Lake than the other pits.

- The 2D numerical flow and transport simulation performed on WES05 pit confirmed the seepage rate computed via the mathematical analysis and indicated that seepage would report to Meliadine Lake in 8.5 years based on first arrival time of plume at 10% of its source concentration. The arrival time of the 50 mg/L and 100 mg/L plumes are 14.5 years and 25 years, respectively. This illustrates the effect of dispersion on the plume. The arrival time of the 50% concentration is essentially consistent with arrival time computed in the mathematical which only considered advective flow.
- Long-term steady-state loads to Meliadine Lake would amount to 43.3 kg/yr based on a generic source concentration of 100 mg/L but are not predicted to occur until after 30,000 years. A short-term steady load via the WM-B flowpath (37.5 kg/yr) is predicted to occur around 100 years.
- The tailings porewater source term was compared to average groundwater quality measured in samples collected from underground diamond drillhole water intersects. The comparison revealed that tailings porewater has higher concentrations than groundwater for the following nine parameters: cyanide, WAD cyanide, fluoride, ammonia-nitrogen total phosphorous, arsenic, cobalt, copper and selenium. Incidentally, the tailings porewater source term is has overall higher concentrations than the Discovery waste rock porewater source term with exception to fluoride.
- Long-term ( $t > 30,000$  years) steady-state loading rates for WES05 tailings seepage for the most elevated PCOCs, scaled from the simulated results for a generic PCOC of 100 mg/L concentration, are: arsenic (1.55 kg/yr), cyanide (0.33 kg/yr), WAD cyanide (0.022 mg/L) and ammonia-nitrogen (37 kg/yr).
- Based on the seepage fluxes and travel times computed for the pits in the mathematical analysis, a simplified scoring scheme was developed to rank the suitability of the pits for tailings disposal. The pit ranking in order from most suitable to least suitable for tailings storage is: PUM01, WES04, PUM03, WES01, WN01, and WES05.
- The ranking of pit suitability for tailings deposition was predicated on conservative worst-case scenario for groundwater loadings to Meliadine Lake. Depending on how these facilities are operated and closed, open talik formation under the backfilled pits could be limited or avoided altogether, essentially eliminating potential interaction between the pits and the deeper groundwater system.

## ***References***

---



**AGNICO EAGLE**

## References

---

- Andersland, O.B., and B. Ladanyi, 2004. *Frozen Ground Engineering, Second Edition*. Chichester: John Wiley & Sons.
- Agnico Eagle Mines Ltd., 2022. Meliadine Gold Mine 2021 Annual Report. April 2022.
- Agnico Eagle Mines Ltd., 2021a. Meliadine Extension Version 8 Mine Layout.
- Agnico Eagle Mines Ltd., 2021b. Meliadine borehole thermistor data. Spreadsheet filename “Model Thermistor Summary.xlsx”. Sent via email from H. Murphy (Agnico Eagle Mines Ltd.) to R. Coutts (Ardent Innovation Inc.). August 13, 2021.
- Agnico Eagle Mines Ltd., 2021c. Meliadine water quality data. Spreadsheet filename “TR291\_WATER QUALITY MONITORING\_August4and8th.xlsx”. Sent via email from H. Murphy. (Agnico Eagle Mines Ltd.) to R. Coutts (Ardent Innovation Inc.). August 18, 2021.
- Agnico Eagle Mines Ltd., 2021d. CAD Basemap filename “PLOM2021\_MEL\_ENG\_edits\_V1-Base.dwg”.
- Agnico Eagle Mines Ltd., 2019. Meadowbank Gold Project 2018 Annual Report 2018. Report submitted to Nunavut Water Board, Nunavut Impact Review Board, Fisheries and Oceans Canada, Crown-Indigenous Relations and Northern Affairs Canada and Kivalliq Inuit Association dated April 8, 2019.
- Agnico Eagle Mines Ltd., 2014. Meliadine FEIS Volume 7 Freshwater Environment Report No. Doc 314-1314280007 Ver 0. Prepared by Golder Associates for Agnico Eagle Mines Ltd. dated April 2014.
- Environment Canada. 2021. Climate normals: 1981 – 2010. [https://climate.weather.gc.ca/climate\\_normals/index\\_e.html](https://climate.weather.gc.ca/climate_normals/index_e.html)
- DHI, 2022. FEFLOW v7.2. <https://www.mikepoweredbydhi.com/products/feflow>
- Frederking, R. Predicting ice thickness for engineering applications. In Proceedings of the 24<sup>th</sup> IAHR International Symposium on Ice, Vladivostok, Russia, 2018.
- Freeze, R. A., & Cherry, J. A., 1979. *Groundwater*. Englewood Cliffs, N.J: Prentice-Hall.
- Golder, 2021a. Meliadine Extension – 2020 Thermal Assessment. Document No. 20136436-815-R-Rev2. Report submitted to Agnico Eagle Mines Ltd. December 2021.

- Golder, 2021b. Hydrogeology Modelling Report Meliadine Phase II Expansion. Document #20136436-857-R-Rev3-2300. Report submitted to Agnico Eagle Mines Ltd. December 2021.
- Golder, 2021c. Report on Summary of Existing Conditions Meliadine Extension. Document #20136436-855-R-Rev2. November 2021.
- Golder, 2021d. CAD file of 2043 Mine Layout. Filename: “2043 Year Over Site Layout.dwg” generated April 29, 2021 based on Version 8 Mine Layout.
- Golder, 2017. Whale Tail Project, Laboratory Testing on Process Plant Tailings. Document No. 001-1775467-MTA-Rev 0. Technical Memorandum submitted to Agnico Eagle Mines Ltd. December 14, 2017.
- Golder, 2014a. Volume 7.0 Freshwater Environment. Final Environmental Impact Statement (FEIS) – Meliadine Gold Project. Report by Golder Associates Ltd. Document No. 314-1314280007 Ver. 0. April 2014.
- Golder, 2014b. SD 6-1 Permafrost Thermal Regime Baseline Studies – Meliadine Gold Project, Nunavut. Report by Golder Associates submitted to Agnico Eagle Mines Ltd. Report # Doc 225-1314280007 Ver. 0. April 2014.
- Jaquet, Olivier, Namar, Rabah, Siegel, Pascal and Peter Jansson, 2012. “Groundwater flow modelling under ice sheet conditions in Greenland (Phase II)” 2012 report for Swedish Nuclear Fuel & Waste Mgt Co.
- Kane, D.L.; K. Yoshikawa and J.P. McNamara. 2013. Regional groundwater flow in an area mapped as continuous permafrost, NE Alaska (USA), *Hydrogeology Journal*, Vol. 21.
- Lorax Environmental Services Ltd, 2022. Meliadine Extension In-pit Deposition Alternative WBWQM. Prepared for Agnico Eagle Mines Ltd., by Lorax Environmental Services, December 2022.
- Lemieux, J.-M., Sudicky, E. A., Peltier, W. R. and L. Tarasov, 2008. Dynamics of groundwater recharge and seepage over the Canadian landscape during the Wisconsinian glaciation, *J. Geophys. Res.*, 113, F01011, doi:10.1029/2007JF000838.
- Teles, V., Mouche, E., Grenier, C., Regnier, D., Brulhet, J. and H. Benaberrahmane, 2008. “Modeling Permafrost Evolution and Impact on Hydrogeology at the Meuse/Haute-Marne Sedimentary Site (Northeast France) During the Last 120,000 Years.”, in *Extended Abstracts for 9<sup>th</sup> International Conference on Permafrost*, Fairbanks, AK, 2008.

- Natural Resources Canada (NRCan), 1995. Canada Permafrost Map MCR-4177. National Atlas of Canada, 5<sup>th</sup> edition. Downloaded October 19, 2021 from: [https://ftp.maps.canada.ca/pub/nrcan\\_rncan/raster/atlas\\_5\\_ed/eng/environment/land/mcr4177.pdf](https://ftp.maps.canada.ca/pub/nrcan_rncan/raster/atlas_5_ed/eng/environment/land/mcr4177.pdf)
- Smith, L., 2021. Hydrogeology and Mineral Resource Development. The Groundwater Project, Guelph, Ontario, Canada. Downloaded December 13, 2021 from: <https://gw-project.org/books/hydrogeology-and-mineral-resource-development/>
- Walvoord, M. A., Voss, C.I., and T. P. Wellman (2012), Influence of permafrost distribution on groundwater flow in the context of climate-driven permafrost thaw: Example from Yukon Flats Basin, Alaska, United States, Water Resour. Res., Vol. 48.